Supporting the UK Distribution Networks with Power Electronic End User Voltage Regulation

Gordon A. Watson

University of Strathclyde - Electrical and Electronic Engineering
Department - Doctor of Philosophy - 2015

Abstract

As time passes new technologies demanding and generating power will be increasingly connected to distribution networks. Studies found that the capacity of the network cannot support the predicted increase in demand due to current limits on the network.

To increase the capacity of the network, raising the voltage level of the system was explored. Studies indicated that raising the voltage level of the UK low voltage (LV) distribution system will significantly increase the capacity of urban distribution networks.

The difficulty with this approach is that the end-user receives an unusable voltage supply. Point of use voltage regulation (PUVR) was suggested as a possible way of resolving this difficulty. This also has the additional benefit of maintaining voltage regulation as the LV conductors can essentially be deregulated.

Results found that for PUVR to be considered viable the efficiency of the converter units in each home must be a minimum of 93.3% and the cost per unit £460-£2,100. These limits would provide on-par results with traditional network reinforcement.

An evaluation of AC-AC converter architectures was undertaken with the cost and efficiency as important selection criteria. Two system architectures were considered: the Back-to-back Inverter and the AC Chopper. After initial evaluation against the selection criteria, the AC Chopper architecture was found to be the cheaper and more efficient architecture and was investigated further.

The efficiency results from the practical experiments with the AC Chopper were found to be in line with predicted values from simulation. Efficiency values were found to be as high as 97% validating the simulation results, the voltage distortion was found to be as low as 2.5% with an input voltage distortion of 1.77% and the cost was found to be comparable to network reinforcement.

The AC Chopper with auto-transformer hybrid architecture was introduced to increase power quality however the impedance introduced by the autotransformer caused an increase of voltage distortion to 9.5% when a non-linear load was energised.

A method of controlled harmonic elimination was found to be more effective, reducing the voltage distortion from 8% to 3% at the cost of increasing current distortion.

Therefore PUVR has been demonstrated as a viable alternative to standard network reinforcement because it has the advantages of increasing capacity available without having to re-lay distribution cables. Additionally the losses, power quality and costs are within acceptable margins to be comparable, or better, than standard network reinforcement.

Declaration

This thesis is the result of the author's original research. It has been composed by the author and has not been previously submitted for examination which has led to the award of a degree.

Some of the work in the publications listed in the section titled "Normative References" has been included in this thesis. All the work in these papers is attributable to the author.

Signed: Gordon Alexander Watson

Date: 16/09/2015

Acknowledgements

I think the main lesson I have taken from my PhD is that determination is not enough. Determination is important, but it needs to be guided in the right direction and supported so that it does not collapse under its own weight.

For giving me guidance I thank my supervisor Stephen Finney, whose schedule was always unbelievably full but he always made time for his students.

For giving me support I thank my fiancée Naomi, I honestly can't imagine getting this far without you and sorry I've been so grumpy lately! For their support I would also like to thank our parents; Anna, Gordon, Roy and Sharon. It's hard to imagine better friends, never mind better parents.

To Catherine Jones, thank you for your extensive help with the papers and keeping me on track. Derrick Holliday and Charles Croser, thank you for the numerous times we've bantered about technical (and social) topics. To Lie Xu and Paul Mitcheson, thank you for taking the time to examine my thesis.

I would also like to thank Western Power Distribution in association with Power Networks Research Academy and the Engineering and Physical Sciences Research Council for providing me with the funding needed to undertake the research.

I hope that my other lessons in life come a bit easier!

List of Abbreviations

AC	Alternating Current
ADMD	After Diversity Maximum Demand
ASHP	Air Source Heat Pump
BS	British Standard
CNE	Combined Neutral and Earth
DC	Direct Current
DLH	Distribution License Holder
DNO	Distribution Network Operator
ENA	Energy Network Association
EV	Electric Vehicle
GSHP	Ground Source Heat Pump
GSR	Grid[1] Side Rectifier
HEV	Hybrid Electric Vehicle
HSI	House Side Inverter
HV	High Voltage
IGBT	Insulated Gate Bipolar Transistor
MOSFET	Metal Oxide Semiconductor Field Effect Transistor
MV	Medium Voltage
NOP	Normally Open Point
PME	Protective Multiple Earthing
PUVR	Point of Use Voltage Regulation
PV	Photo Voltaic
PWM	Pulse Width Modulation
RCD	Residual Current Device

[1] Please note that grid and network are used interchangeably throughout this thesis

SNOP	Soft Normally Open Point
THD	Total Harmonic Distortion
UK	United Kingdom
VSC	Voltage Source Converter
XLPE	Cross-linked Polyethylene

Normative References

Connor, G., C.E. Jones, and S.J. Finney,

End user voltage regulation to ease urban low-voltage distribution congestion.

Generation, Transmission & Distribution, IET, 2014. **8**(8): p. 1453-1465.

Connor, G., C.E. Jones, and S.J. Finney,

Easing Future Low Voltage Congestion with an AC Chopper Voltage Regulator.

IET Conference Proceedings, 2014, 1.11.01-1.11.01.

Table of Contents

List of Figures

List of Tables

CHAPTER 1

1. Introduction

Projected changes to how energy is used in distribution networks will place increasing demands on the capacity of electricity supply networks. Raised distribution voltages have the potential to reduce distribution losses, which is presently from 5%-6%[1], and increase capacity. However such an approach will require the use of Point of Use Regulation (PUVR) devices which will incur additional converter losses and expense.

This thesis investigates the benefits of raised distribution voltage and the potential PUVR devices suited for this application.

1. 1. UK Emissions Targets for 2020-2050

In order for the UK to meet the 2020 and 2050 greenhouse gas emissions targets set by the European Union, immediate changes are required across all energy sectors [2]. Therefore it is expected that over the next 30 years "cleaner" emerging technologies such as heat pumps [3], electric vehicles (EVs) and renewable distributed generation will be implemented in order to meet legislation. Other drivers for change in the way we use electricity are rising energy costs, concerns about security of energy supply and fossil energy reserves [4].

The National Grid Future Energy Scenarios 2014 report states that in the event of a scenario where greener technologies are adopted (low carbon life and gone green scenarios) peak demand is set to increase by 4.5-7.6GW over the next twenty years [5], this is shown in Figure 1-1.

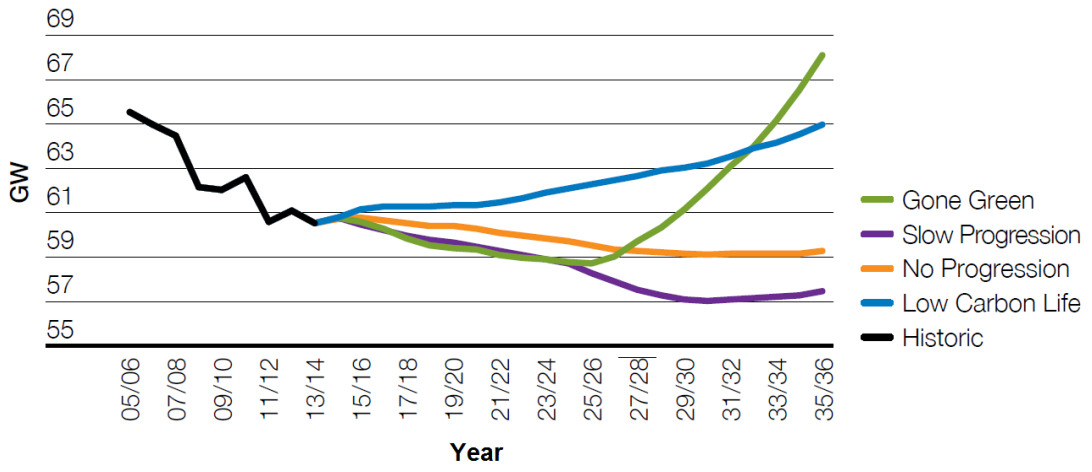

Figure 1-1 - Peak Demand until 2035 of various Future Energy scenarios [5]

If the existing urban low-voltage distribution infrastructure is left unchanged, it is unlikely to provide sufficient capacity for this predicted increase in demand particularly in urban areas where conventional reinforcement is also limited by space restrictions. PUVR is a potential solution to this problem. The concept of PUVR is to set the line-to-line voltage in the three-phase distribution cabling to be higher than the standard $415V_{AC}$ line therefore less current is required for a constant load, effectively increasing the current capacity.

At present, the insulation limit of low voltage (LV) cables used in the UK is at least $1.2kV_{AC}$ line [6]. Therefore it is clear that the distribution cabling is underutilised, but in order to make the power usable when it reaches the customer it must be transformed or converted down to $230V_{AC}$ phase. Another issue caused by increasing distributed generation is the difficulty in regulating voltage [7]. PUVR solves this issue by regulating the voltage at the end user.

PUVR would require the replacement of the LV substation transformer in order to increase the voltage of the LV distribution system to $600V_{AC}$ three-phase, however substation transformer replacement may be necessary as part of system upgrades to future proof the network and allow full bi-directional power flow. For more information on this subject please see Section 2. 1. 2.

1. 2. Future Trends

Climate change targets are the primary cause for changing the way we use electricity. This section will elaborate on this change and how it will affect our present distribution infrastructure. It also discusses PUVR as a solution.

1. 2. 1. Distributed Generation

The connection of distributed generation on the distribution grid close to the point of use reduces transmission losses and helps to meet local power demand [8]. During periods of off-peak demand where there is a significant reduction in the local load, local distributed generation can contribute to voltage rise. This can lead to the voltage exceeding acceptable standards [8]. This is further discussed in Section 1.2.2.
In addition to voltage rise, the reverse current limit of the distribution transformers may be exceeded [9]. This is further discussed in Section 1.2.3.

1. 2. 2. Voltage Rise

The voltage drop as current flows through a conductor is dependent on the impedance of the conductor [10]. Consider a street of houses in an urban distribution system, it is not possible to ensure each house receives 230 V_{AC} due to the voltage drop therefore it is acceptable for the voltage to fluctuate within the limits of 230 V_{AC} + 10−6% [11]. PUVR can be used to overcome this problem of fluctuating voltage by deregulating the voltage on the incoming AC cables and then regulating at the end user, resulting in each house on the distribution network receiving exactly 230 V_{AC}.

1. 2. 3. Reverse Current Limit

The present grid infrastructure was designed for unidirectional power flow from large scale generation through high voltage (HV) transmission networks and then gradually stepping down voltage through the distribution system to the consumer/load [12].

With the introduction of distributed generation to the grid it is now conceivable that power will flow in both directions. This is not what the infrastructure was designed for and may lead to problems. For example the design of some on load tap changers is such that reverse power flow may not be possible or is restricted [13]. In some extended rural networks, transformer taps may be set to maximum voltage in order to ensure that the furthest consumer receives a satisfactory voltage. In these cases embedded generation can lead to operation outside of voltage limits in reverse power flow conditions [9].

1. 2. 4. Electric Vehicles

Personal transport accounts for 13% of the UK's emissions. One possible way of reducing this is the introduction of EVs and Hybrid Electric Vehicles (HEVs) [14]. Due to economic and range factors with EVs [15] the present car market share is very low, 2,600 (0.01% of cars in the UK) for EVs and 102,300 (0.36% of cars in the UK) for HEVs [16, 17]. However, by 2030 it is predicted that market penetration of EVs and HEVs will increase to a maximum of 5.8 million EVs and 14.8 million HEVs [16, 18]. As a percentage of today's car population of 28.4 million cars [17] this is equivalent to 20.4% EVs and 52.1% HEVs.

Widespread charging of EVs will increase the electricity demand on the low-voltage infrastructure by 1.4-19 kW of instantaneous power at each end-user [4] depending on the charging power level. It is worth noting that public EV charging stations have a higher power level of 50-120kW. What power level is used is dependent on the charging strategy used. If an uncoordinated strategy is used it is suggested that power level 1 (1.4kW-1.9kW) is used, as the EV would be charged at times of peak load [4].

Uncoordinated charging is estimated to increase the UK peak load by 17.9% at 10% EV market penetration and 35.8% at 20% EV market penetration [19]. PUVR would increase the capacity available for this extra load and would also assist in the charging speed of the EV with the possibility of a >415V charging socket [20, 21].

Another solution is to use a coordinated charging strategy to optimize the charging time of the EV. This would utilize charging power level 2 (4kW-19.2kW) and would charge the EV during times of off-peak loading. It follows that there is no effect on the peak load and therefore generation capacity does not need to increase. Another coordinated charging strategy is the daytime charging of EVs using distributed generation.

If the clean energy generated by solar photo voltaics systems (PVs) is curtailed due to voltage rise from lack of demand then EVs could be charged from this normally curtailed clean energy source [22]. However there are many management, control and social challenges to overcome in implementing coordinated charging strategies [4].

A similar concept to PUVR has been explored in Sweden in preparation for the increased loading cause by EVs [20]. Whilst not directly applicable due to the differences in conductor distances and end user voltage, it found that future EVs with large batteries will require network reinforcement and that this could be achieved by operating a separate 1kV LV network.

1. 2. 5. Electric Heating

Much the same as the EV the number of electric boilers is expected to increase in the UK due to the drive for cleaner energy technologies. Approximately 1,000 ground source heat pumps (GSHP) were installed in the UK in 2005/2006. This increased to 3,000 installations in 2007 and this trend is expected to continue [23]. Air source heat pumps (ASHP) are another type of electric boiler but these are far less common in the UK [23].

The effect of a GSHP at each loading point would be substantial. The typical power rating of a GSHP ranges from 8-14kW [23]. It would also very likely be used around peak times due to the demand profile for space heating and hot water. Considering the effect a 2kW EV charger at each end user had on the peak demand increase, see Section 1. 2. 4. , an 8-14kW increase in demand from each end-user presents a challenge to future network capabilities.

1. 2. 6. Future Trends in Cost

Rising demand for copper on the international market has led to an associated increase in cost [24]. In contrast, the cost of semi-conductor devices has historically decreased due to a high pace of technological advancement and more efficient bulk manufacturing processes driving down the cost per unit [25].

If both these trends continue in the future then, from a cost viewpoint, using a semiconductor based solution over a copper replacement solution will become more attractive.

1. 2. 7. Conversion or Transformation

The introduction of PUVR would reduce the reliance of the distribution network on transformers to regulate voltage levels.

The use of power electronics in the LV network is advantageous over transformers for this purpose as the implementation of the modulated switching control around power electronics is easier to implement than control of a tap changing transformer.

Modern power electronics are almost as efficient as traditional transformers in addition to having a smaller form factor [26, 27]. Power electronics can also be more cost efficient. It is expected that a power electronic converter would cost half as much as an equivalent transformer [28-31].

1. 3. Possible Solutions and Chosen Research Area

It has been established in Section 1. 2. that personal transport and heating is becoming increasingly electrified in the UK and that this will affect the load profile of homes, potentially increasing the daily peak demand.

A number of solutions exist to increase the capacity of the LV network to meet this new demand. This section will explain what the available solutions are; and what the benefits and drawbacks are in using a particular solution.

1. 3. 1. Cable Replacement

Network reinforcement is a possible way to resolve the need for extra capacity. To replace the conductors in the LV distribution network, it is necessary to remove the present cable in the ground by digging. The new conductor with a higher current limit, or current carrying capacity, can then be installed. This would increase the capacity of the LV distribution network. This method is intrinsically reliable as the network has always operated in this fashion.

However this leaves many issues unresolved. All the conductors must be replaced; this will be a significant cost and will affect the customer directly. The reverse current issue means that a replacement transformer may also be required.

The voltage rise issue caused by distributed generation would still be a problem which could only be solved by curtailment, daily manipulation of LV and MV tap changers, limiting the amount of PV allowed to be installed on the network or implementing a second solution such as demand side management. Therefore this solution does not solve all the problems the future network will experience.

1. 3. 2. Low Voltage DC Distribution

Utilising DC instead of AC in the present LV conductors increases the intrinsic power capacity. This is achieved by the higher voltage rating permissible by DC [32]. Using DC also removes power quality problems due to reactive power draw and harmonics and will increase efficiency by removing conversion stages [32, 33]. However using DC in distribution network is a radical solution and there are many problems that must be addressed before it becomes feasible.

The primary problem with DC distribution is that there are many research areas that are still in infancy and must be explored before a serious consideration of implementation can begin. These areas of research are [34]:

- Power electronic converters
- Losses of the system
- System protection and electrical safety
- Converter control electronics and algorithms

- Converter filtering
- DC cable phenomena
- Overall control of the system
- Smart grid functionalities (if applicable)

This solution would also be an expensive one, the system proposed in [32] will require an inversion stage at each end-user and it would require a rectification stage after the local transformer. It also leaves the reverse current issue unresolved which may require the replacement of the local transformer, see Section 1. 2. 3.

1. 3. 3. Demand Side Management/Smart Metering

Smart metering allows the end user to observe and control their use of electricity. By offering cheaper electricity at times of the day with less demand and vice versa, the user peak demands can be lessened/modified. Thereby avoiding problems with future capacity congestion [35].

The problem with this approach is including the customer in the electricity delivery process. Successful projects to date have involved collaborative communities already invested in their energy infrastructure [36]. It is unknown how this change will affect the wider community.

A second problem is that not all loads can be deferred in this way. Whilst an EV is an example of a load that can be easily deferred and is widely discussed [4, 16, 19, 37-39] electrification of the heat sector is not as widely discussed and is of larger concern. Heat can be deferred for a reasonable amount of time dependant on the how well the house in question is insulated. However it can not be deferred to a different time of day like EVs and will be a larger source of demand in the future than EVs, see Section 1. 2. 5.

There are solutions to this in the form of electric storage heaters, however these heaters are inflexible and bulky[40].

As the demand side management system tries to match local generation with local demand by shifting the demand, it may have fewer problems with curtailment of distributed resources and the reverse current limit of the local transformer. This would have to be analysed in a case by case basis. This solution has the advantage over network reinforcement in that the conductors do not require replacement.

Another issue with demand side management is the increasing percentage of renewables in the UK generation mix [5]. It is logical to assume that solar farms will consistently generate during the day and that the generation of wind farms will be random. Hypothetically the customer consistently matching load with this instability in generation is considered unlikely. Overall this may lead to further complications for the customer, which is undesirable.

1. 3. 4. Battery Installations at Substations

By placing energy storage (in the form of batteries) at the local transformer, the battery can absorb the excess energy generated by local renewables when demand is low and then, when demand is high, use the stored energy to supply the peak demand. This essentially shifts the generation instead of the demand [41]. However this solution would need to be used in conjunction with network reinforcement, as the conductors will not have the current capacity to carry the future current demand.

This solution will solve all of the issues, the capacity will be fixed with network reinforcement, distributed generation does not need to be curtailed or limited as the battery can store the excess energy and there will be little to no reverse current through the transformer as reverse current is stored in the battery[41].

However, commercial batteries are new to this role and power level, there are many unknowns about certification, operation and reliability [41]. They also have a high operating cost and are presently not economically justifiable, however technological progress is being made in this area [42] .

Another concept is the use of EV batteries as local energy storage [42]. This is a very elegant solution that may address almost all the issues, as if the storage can supply to the household then there is an additional power source not utilising the conductor. The charging and discharging of the battery could be intelligently controlled to regulate voltage.

However EV battery storage would not be available during the day as this is the primary time of use and this would be the prime generation time for local PV. There are also many legislative factors that have to be resolved before implementation. Primary of which is, there is no incentive for the EV owner to participate in local energy balancing markets, especially when increased cycling of the battery will decrease its lifetime [42].

1. 3. 5. Reactive Compensation using Distributed Generation

PV generation connected to the LV distribution network under normal circumstances generates active power. However it is also possible for the PV inverters to contribute reactive power. Using reactive power generation it possible to control the voltage locally [43]. This solution corrects the voltage regulation problems cause by increased distributed generation on the grid. However, the problem with this solution is that the resistance to reactance ratio (R/X) of the LV distribution network is very high, therefore reactive power export does not have as great an effect on the voltage [43]. Therefore the amount of reactive power required to change the voltage causes so much loss in real power generation that it negates the generation gains made by having distributed PV generation [43].

Another problem with this solution is that it does not fully prepare the LV distribution system for future loads and therefore network reinforcement would be required. This solution does not solve the reverse current issue and the local transformer may require replacement, see Section 1. 2. 3. In order to supply or draw reactive power the PV inverter must be over-rated or reduce its active power output. This will come at additional cost (or loss of revenue) some models of inverters may not have this functionality. There is no driver for any customer to replace their PV inverter if this is the case.

There are also many regulatory problems in implementing this solution, as reactive power export is a service that supports network infrastructure, there is no incentive for the generation owner to participate.

1. 3. 6. Soft Normally Open Points (SNOPs)

By utilising normally open points (NOPs) in the MV distribution system, two separate distribution networks can be connected; this operation is normally reserved for emergencies. However by controlling the power flow through NOPs with power electronics, creating a Soft Normally Open Point (SNOP), it is possible to share the burden of an electrically stressed distribution network with another distribution network [44].
This has been demonstrated theoretically as a viable way of maintaining voltage regulation and allowing the expansion of PV on the distribution network [44]. SNOPs have the capability of balancing the power network branches; this could potentially mitigate the need for network reinforcement but would need to be considered on a case-by-case basis.
This solution would also address the issue of reverse current limits on local transformers it would be possible to redirect the reverse current to a section of the network with greater demand or less limitations on power flow.

1. 4. Contribution

In terms of novelty of the research undertaken, the following contributions can be identified:

- Creation of a load flow simulation of a representative part of the UK distribution network
- Identification of the key factors against implementation of PUVR and targets that PUVR must meet to become a valid alternative
- Identification of the most suitable converter architecture for this application through simulation work

- Design and build of prototype converter architecture for validation of simulated results
- Control software of microcontroller which implements a semi-soft switching strategy with PI control to regulate the output voltage
- Testing of prototype with various loads that could be used in a UK household
- Testing of a new half-converter, half-transformer prototype with various loads that could be used in a UK household
- Revaluation of financial figures based on the new converter architecture
- Simulation of a control strategy to eliminate low order harmonic content from the end user voltage and current

1. 5. Validation

The load flow simulation work presented in this thesis is based on data gained from industry partners.

The ac-ac converter architectures presented in this thesis was modelled using MATLAB Simulink and PLECs, following accepted methods for power electronic and controller model development.

These models were then validated by hand calculation and the construction of a prototype hardware platform which was tested in the same states as the model.

1. 6. Thesis Outline

Chapter 1. introduced the thesis and the issues that are considered and the changes that are predicted to UK LV distribution networks.

This Chapter has also considered the consequences of these changes, possible solutions to these consequences are stated and then the choice of research area.

Chapter 2. describes all the necessary technical knowledge for all subsequent Chapters. This includes regulations of the UK low voltage distribution grid, information on any power electronic architectures referred to in the main text and details of how these architectures operate. Finally any other ancillary information is included necessary for the understanding of the thesis.

Chapter 3. describes the present distribution system, using a simulated network based on a representative area of the UK LV network, and applies to it the worst case scenario for future grid conditions i.e. greater demands at peak times.

Chapter 4. then proceeds to describe the effect of using voltage regulation at the end-user under the previously established worse-case conditions. This forms an opinion on whether voltage regulation at the end-user is a valid hypothesis to enhance the LV distribution network using power electronics and some of the conditions for validity are formed. A cost comparison is made between standard network reinforcement and using end-user voltage regulation with off-the-shelf power electronics for the same representative area of the UK LV network.

This Chapter completes the formation of an opinion on whether the low voltage regulation at the end-user is a valid hypothesis to enhance the LV distribution network and some of the conditions for validity are found.

Chapter 5. describes the presently available power electronics architectures that are available to perform the voltage regulation and the advantages and disadvantages of each. This Chapter considers the available architectures with against the previously defined important conditions for validity before coming to recommendation on architecture choice and all validity conditions for point of use voltage regulation to be a viable alternative to conductor replacement.

Chapter 6. describes the practical implementation of the previously recommended voltage regulator architecture and is used for validation of the results in Chapter 5. This Chapter has an extensive methodology thoroughly explaining the challenges in implementing the architecture and how these can be overcome. The Chapter continues to introduce a new architecture based on the previous architecture that should improve some performance aspects of the original architecture. This new architecture is also practically tested and the results given before a recommendation is provided on which architecture to use.

Chapter 7. provides an updated cost-benefit analysis based on the previous results from Section 4. 1. 2. 3. The updated results consider the recommended architecture against a previously considered important condition for PUVR validity.

Chapter 8. focuses on control improvements possible for the recommended architecture and how these improvements increase the validity of the architecture for PUVR.

Chapter 9. will provide a conclusion on the research to date, stating the conclusions found from each Chapter and what these conclusions mean as a whole.

CHAPTER 2

2. The UK Grid and Power Electronic Converters

In order for the Chapters in the main text to be understood first the technical details of the subject areas must be explored. The technical details will be state-of-the-art so that the novelty of any future work is recognised.

2. 1. Regulations of the UK Distribution Network

In order to correctly implement a system on the LV distribution network the specifications, regulations and recommended practices of the said network must first be understood. This can be achieved through examination of the UK distribution code, Energy Networks Association (ENA) documents and relevant British Standards. This section of the literature review will explore these documents in order to specify the electrical conditions of the LV distribution network.

2. 1. 1. Conductors Used in the UK Distribution Network

It is important to discover the limits of the present LV distribution infrastructure. By discovering the limits of the conductors, in particular the voltage limits, it becomes possible to enhance the LV infrastructure without greatly altering it.

2. 1. 1. 1. Voltage Limits

The first step is identifying the cables recommended for use in the low-voltage distribution system. Information on the design of low voltage distribution systems is available from the ENA. This information is placed in documents which are engineering recommendations and therefore are not strictly regulated; however this thesis assumes that most UK networks follow these recommendations as engineering best practice. The document entitled G81 - Part 1: Design and Planning [45] includes specification of the conductors used in LV distribution networks in Section 7.7. The following is an excerpt from this document:

"7.7 Low voltage underground cable network
a. The low voltage underground cable network shall be of CNE construction utilising the standard sizes of cable employed by the Host DLH as specified in Appendix B.
b. The network shall be earthed using the PME system in accordance with ER G12/3.
c. The voltage drop on the low voltage underground cable network between the substation LV busbars and all extremities of the network shall not exceed the limits specified in Appendix B. This voltage drop shall be calculated assuming that all customers are taking their design ADMD with allowance for unbalance and diversity. Host DLH-specific design ADMDs for different classes of customer are listed in Appendix B."[45]

Where CNE refers to Combined Neutral and Earth, DLH refers to Distribution License Holder, PME refers to Protective Multiple Earthing and ADMD refers to After Diversity Maximum Demand. From this document it is known that each Distribution Network Operator (DNO) sets its own standard with reference to distribution level conductors and that the earthing scheme employed in the UK is PME.

While each DNO is able to determine which conductor they wish to use, making it difficult to define a specification of insulation limit, the conductors used will always be to British Standards. Therefore the next step is to examine notable British Standard publications.

The first publication that was examined is BS EN 60228:2005 which classifies the conductors generally used in fixed installations, such as distribution cables, as solid or stranded conductors. The cables used for distribution systems and how they are selected is described in BS EN 7870-1:2011 entitled "LV and MV polymeric insulated cables for use by distribution and generation utilities" where Annex A provides a guide to cable selection. The following excerpt is taken from section A.2.1.

"*A.2.1 General*

The cables specified in BS 7870-3 and BS 7870-4 are designed to be installed in air (indoors and/or outdoors), or may be buried directly in free draining soil or in ducts or in special backfills. Cables specified in BS 7870-3 and BS 7870-4 are not specifically designed for use:

a) as self supporting cables;

b) as submarine cables;

c) where subsidence is likely, unless special precautions are taken to minimize damage;

d) where any exposure to excessive heat is involved."[46]

Therefore the cables specified in BS 7870-3 and BS 7870-4 contain the necessary technical details to which the DNOs conform. The relevant standard of these two is BS 7870-3 as BS 7870-4 refers to conductors used in the 33kV section of the distribution network.

BS 7870-3, part 3 of the standard entitled "LV and MV polymeric insulated cables for use by distribution and generation utilities" has the sub heading "Part 3: Specification for distribution cables of rated voltage 0.6/1kV Section 3.50: XLPE insulated, copper wire waveform or helical concentric cables with solid aluminium conductors, having low emission of smoke and corrosive gases when affected by fire" [6].

Section 3 of this document entitled "Voltage designation", refers to the voltages of these cables as U_o=0.6kV, U=1kV and U_m=1.2kV [6]. Where U_o is the rated voltage between any conductor and armour or earth, U is the rated voltage between phase conductors and U_m is the maximum voltage between phase conductors [46]. Therefore from these publications we can surmise that conductors used in the LV distribution system have a voltage rating of $600V_{AC}$ single phase up to an absolute maximum of $692.8V_{AC}$. The present line voltage of $415V_{AC}$ leaves a large amount of headroom available for to increase the power rating of the conductors and lower the copper losses in the cables.

2. 1. 1. 2. Current Limits

The current limit varies with the type of conductor, but typical ratings are 155–415 A (taken from industry average conductor size). The higher the current and current rating of the cable, the higher the cost of the cable.

Typical industry cost for a length of copper underground cable, of area 16 mm^2, is 0.71 £/m (costing information received from industry partners) and has a current limit of 111A while a 35 mm^2 copper cable costs 1.29 £/m and has a current limit of 178 A. Therefore there is a clear trade-off between line cost and its current (and hence capacity) limitations.

2. 1. 2. Transformers in the UK Distribution Network

A full understanding of the transformers used in the UK LV distribution network is necessary in order to properly inform the main text.

As with the cable conductors, engineering recommendations from the ENA and the relevant British Standards have been reviewed to give a comprehensive understanding of distribution transformers.

From Section 7.9 of the G81 the following excerpt is a quote pertaining to the design of distribution network transformers.

"7.9 Substations

a. The HV/LV distribution substation(s) shall utilise the standard sizes of transformer employed by the Host DLH as specified in Appendix B.

b. Transformer sizing shall be based on the aggregated ADMDs for all customers fed from the substation and the permissible cyclic rating of the transformer as specified in Appendix B, and minimising lifetime cost criteria as set out in 7.5 above.

c. The substation location shall take into account access and environmental factors such as: noise pollution, flooding risk and vandalism. (See also ESQCRs and associated DTI Guidance).

Early discussion is required between the Applicant and the Host DNO over the substation ESQCR risk assessment and the proposed design features which take account of this.
d. Substation earthing shall be such as to prevent danger from rise of potential during system earth faults and shall take account of touch potentials, step potentials and transferred potentials. See ENATS 41-24 for further information."[45]

This informs that, as with the conductors, the choice of transformer is at the DNO's discretion; it however advises that any design choice shall be efficient, coordinated with other equipment and economical, from [45] Section 7.5. It also informs that the transformer shall be suitably earthed and that transformer rating should be chosen based on the after diversity maximum demand from all consumers.
It is also worth noting that, in urban areas that are heavily populated, logically due to space constraints installing the transformer so as not to cause any problems with access or environmental factors such as noise pollution may become increasingly difficult.
The relevant British Standards concerning LV distribution transformers is BS EN 50464-1:2007+A1:2012 which is entitled "Three-phase oil-immersed distribution transformers 50Hz, from 50kVA to 2500kVA with highest voltage for equipment not exceeding 36kV - Part 1: General requirements"[47].
In Section 3.2 of this standard, the following excerpt is shown which describes the highest voltage possible on the transformer.

"3.2 Highest voltages for equipment for windings
Insulation levels and dielectric tests shall be in accordance with the requirements of EN 60076-3.
The values of the highest voltage for equipment are
− for the high-voltage winding:
3,6 kV– 7,2 kV – 12 kV – 17,5 kV – 24 kV – 36 kV,
− for the low-voltage winding:
1,1 kV."[47]

Therefore the low-voltage side of the transformer which has a rated voltage of 400V-433V [47], is capable of more than double the voltage at which it nominally operates. However this is also a section in the standard which refers to the maximum tapping, an excerpt follows:

"*The HV winding can be provided with tapping. The preferred tapping ranges are ± 2,5 % or ± 2 x 2,5 % unless otherwise specified ,but in any case maximum taps shall not exceed 7 positions and the total maximum range shall not exceed 15 %.*
The tapping range has to be specified by the purchaser or by agreement between manufacturer and purchaser.
These taps shall be connected to an off-circuit tapping switch."[47]

Therefore even if the distribution transformer is capable of higher voltages than $415V_{AC}$ line, with the present equipment the maximum possible voltage output from the tap-changer is 415V+15% which is 477.25V.

2. 1. 3. Protection of the UK Distribution Network

A full understanding of any protection systems utilised in the UK LV distribution network is necessary in order to properly inform the main text. As with the cable conductors and transformers engineering recommendations from the ENA and the relevant British Standards have been reviewed to give a comprehensive understanding of LV protection systems. From the G81 Engineering Recommendations document, the following excerpt is taken:

"The protection of LV feeder circuits shall meet the following requirements:

• Feeder circuits supplying more than one customer shall be protected by fuses to BS88 part 5.

• LV supply cables to single customers shall be protected by fuses or circuit breakers, dependent on supply capacity and customer's protection.

• Fuses must provide short-circuit protection for the whole length of the circuit up to the service cut out. Phase to neutral fault clearance time shall be as stated by the Host DLH in Appendix B.

• Fuse ratings must allow for the cyclic overload rating of the circuit.

• For discrimination, the minimum pre-arcing I^2t of a feeder circuit fuse must exceed maximum total I^2t of any individual fuse downstream.

• Excess current protection shall be provided at the point of supply.

• LV fuses shall be sized to ensure discrimination with the transformer HV protection in accordance with ENATS 12-08."[45]

This informs that one of the relevant British Standards is BS88 part 5 which is further discussed in this Section. It also states that clearance times are determined by the DNO and that the fuses shall be placed at the point of supply and shall be adequately sized to provide protection from overcurrent yet small enough that any fault can be discriminated correctly.

BS 88-1: 2007+A2:2014 and BS EN 60269-1:2007+A2:2014 is a merged standard entitled "Low-voltage fuses - Part 1: General requirements" which focuses on the general specification of low voltage fuses. From Section 5.2 of this standard entitled "Rated voltage" standardised voltage ratings of household fuses can be found.

From the Standard the voltage rating of the fuses in the LV distribution system varies considerably. Therefore in any system where the LV distribution system voltage is changed, the fuses of the households supplied by that distribution system would require checking to ensure that fuses of the correct rating are installed [48].

The relevant British Standard for circuit breakers used in the LV distribution system is BS EN 60898-1:2003+A13:2012 entitled "Electrical accessories - Circuit breakers for overcurrent protection for household and similar installations - Part 1:Circuit-breakers for a.c. operation."[49] An excerpt from the relevant section of the standard entitled "Rated quantities," follows:

"5.2.1.1.Rated operational voltage (Ue)

The rated operational voltage (hereinafter referred to as rated voltage)of a circuit-breaker is the value of voltage, assigned by the manufacturer, to which its performance (particularly the short-circuit performance)is referred. NOTE The same circuit-breaker may be assigned a number of rated voltages and associated rated short-circuit capacities.

5.2.1.2 Rated insulation voltage (Ui)

The rated insulation voltage of a circuit-breaker is the value of voltage, assigned by the manufacturer, to which dielectric test voltages and creepage distances are referred.

Unless otherwise stated, the rated insulation voltage is the value of the maximum rated voltage of the circuit-breaker. In no case shall the maximum rated voltage exceed the rated insulation voltage."[49]

Therefore the voltage limit of any household switchgear is dependent on the manufacturer specifications. This means that, as with fuses, the circuit breakers of a LV distribution system with a modified voltage level must be checked and if necessary, replaced. However it is also stated in Section 5.3.1. of this standard that the preferred rated value of single phase voltage is 230V[49]. Therefore it is considered likely that in a distribution system with a modified voltage level all household switchgear would require replacement.

The relevant British standard for Residual Current Devices (RCDs) used in the LV distribution system is BS EN 61008-1:2012+A2:2013 entitled "Residual current operated circuit-breakers without integral overcurrent protection for household and similar used (RCCBs) - Part 1:General rules."[50] An excerpt from the relevant section of the standard entitled "Rated quantities and other characteristics," follows:

"5.2.1.1. Rated operational voltage (Ue)

The rated operational voltage (hereafter referred to as "rated voltage") of an RCCB is the value of voltage, assigned by the manufacturer, to which its performance is referred.

NOTE The same RCCB may be assigned a number of rated voltages.

5.2.1.2 Rated insulation voltage (Ui)

The rated insulation voltage of an RCCB is the value of voltage, assigned by the manufacturer, to which dielectric test voltages and creepage distances are referred.

Unless otherwise stated, the rated insulation voltage is the value of the maximum rated voltage of the RCCB. In no case shall the maximum rated voltage exceed the rated insulation voltage."[50]

Therefore the voltage limit of any household RCD is dependent on the manufacturer specifications. This means that, as with fuses and circuit breakers the RCDs of a LV distribution system with a modified voltage level must be checked and if necessary, replaced. However it is also stated in Section 5.3.1. of this standard that the preferred rated value of single phase voltage is 230V [50].Therefore it is considered likely that in a distribution system with a modified voltage level any RCDs installed within any of the households would require replacement.

2. 1. 4. Power Quality of the UK Distribution Network

A full understanding of the necessary power quality of any power delivered in the UK LV distribution network is necessary in order to properly inform the main text. As with the cable conductors, transformers and protection systems engineering recommendations from the ENA and the relevant British Standards have been reviewed to give a comprehensive understanding of delivering power to the end-users at sufficient power quality.

The relevant ENA engineering recommendation for harmonic limits in the UK is G5/4-1 entitled "Planning Levels For Harmonic Voltage Distortion And The Connection Of Non-Linear Equipment To Transmission Systems And Distribution Networks In The United Kingdom."[51] Section 4 entitled "System Planning Levels for Harmonic Distortion," of this engineering recommendation contains two tables which summarises the allowable harmonic voltage in the grid. These are shown in Table 2-1 and Table **2-2**, where PCC is the Point of Common Coupling and THD is the Total Harmonic Distortion.

Table 2-1: Summary of THD Planning Levels [51]

System Voltage at the PCC	**THD Limit**
400V	5%
6.6,11 and 20kV	4%
22kV to 400kV	3%

Table 2-2: Planning Levels for Harmonic Voltages in 400V Systems [51]

Odd harmonics (Non-multiple of 3)		Odd harmonics (Multiple of 3)		Even harmonics	
Order "h"	**Harmonic voltage (%)**	**Order "h"**	**Harmonic voltage (%)**	**Order "h"**	**Harmonic voltage (%)**
5	4	3	4	2	1.6
7	4	9	1.2	4	1
11	3	15	0.3	6	0.5
13	2.5	21	0.2	8	0.4
17	1.6	>21	0.2	10	0.4
19	1.2			12	0.2
23	1.2			>12	0.2
25	0.7				
>25	0.2+ 0.5(25/h)				

It can be observed that the maximum recommended THD of voltage is equal to 5% and there are many criteria for maximum harmonic content at individual frequencies.

For current harmonics, Section 6.2 of the document entitled "Customer's Non-linear Equipment having an Aggregate Load or Rated Current less than or equal to 16A per phase," states that the harmonic emissions of any equipment or plant of a single consumer rated less than or equal to 16A may be connected without further consideration [51].

The relevant British Standard in this case is BS EN 50160:2010 entitled "Voltage characteristics of electricity supplied by public electricity networks,"[52]

In order to correctly understand the specification given, the definition of voltage harmonics must be given. Section 3.6 of this Standard defines the harmonic voltage as a sinusoidal voltage with frequency each to an integer multiple of the fundamental frequency of the supply voltage [52]. Numerically harmonics are defined either by each individual harmonics relative amplitude (u_h) or it is defined as Total Harmonic Distortion (THD) which accounts for all the individual harmonics relative magnitude, up to a set limit, the THD of a waveform can be calculated using Equation 1[52].

1
$$THD = \sqrt{\sum_{h=2}^{40} (u_h)^2}$$

Now that the method of defining harmonic distortion has been established the limits placed on the LV distribution system can be understood. An excerpt from BS EN 50160:2010 follows:

"4.2.5. Harmonic voltage

Under normal operating conditions, during each period of one week, 95 % of the 10 min mean r.m.s. values of each individual harmonic voltage shall be less than or equal to the values given in Table 1.Resonances may cause higher voltages for an individual harmonic. Moreover, the THD of the supply voltage (including all harmonics up to the order 40) shall be less than or equal to 8 %.

NOTE The limitation to order 40 is conventional.

4.2.6. Interharmonic voltages

The level of interharmonics is increasing due to the development of frequency converters and similar control equipment. Levels are under consideration, pending more experience.

In certain cases interharmonics, even at low levels, give rise to flicker (see 4.2.3.2), or cause interference in ripple control systems."

From this excerpt it is understood that the maximum voltage THD is 8% and that THD is measured up to the 40th harmonic of the 50Hz fundamental (or 2kHz) and that there is no specific definition for allowable levels of interharmonics (harmonics that are not integer multiples of the fundamental frequency). Interharmonics can be generated by power electronics switching at a speed that is a non-integer multiple of the fundamental frequency as well as other sources. Table 2-3 taken from BS EN 50160:2010 describes the limits of individual harmonics on the LV distribution network.

Table 2-3: Values of individual harmonic voltages at the supply terminals for orders up to 25 given in percent of the fundamental voltage u_1

Odd harmonics (Non-multiple of 3)		**Odd harmonics (Multiple of 3)**		**Even harmonics**	
Order "h"	**Harmonic voltage (%)**	**Order "h"**	**Harmonic voltage (%)**	**Order "h"**	**Harmonic voltage (%)**
5	6	3	5	2	2
7	5	9	1.5	4	1
11	3.5	15	0.5	6…24	0.5
13	3	21	0.5		
17	2				
19	1.5				
23	1.5				
25	1.5				
>25	1.5				
NOTE No values are given for harmonics of order higher than 25, as they are usually small, but largely unpredictable due to resonance effects.					

2. 2. Semiconductors

In order to understand the content of the thesis it is necessary to understand the operation of several semi-conductor devices that are used in the power electronic converters. In particular, due to the content of the thesis, it is important to focus on the loss mechanisms involved with each of the devices used in the main text.

2. 2. 1. IGBTs

The electrical symbol for a negative-positive-negative type Insulated Gate Bipolar Transistors (IGBTs) is shown in Figure 2-1. The IGBT is an electrically controlled solid-state switch.

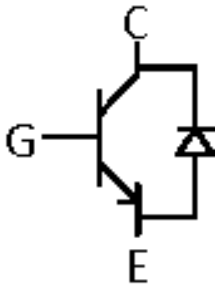

Figure 2-1: IGBT Electrical Symbol

Where the diode operation is dependent on the current direction, IGBT operation is dependent on the voltage applied to the Gate pin, shown in Figure 2-1 as “G”. If switched on by a high voltage at the gate (10V-15V) current is able to flow from the collector “C” to the emitter “E”; this is not instantaneous however and there is a time period when the device is between states.

For device turn-on this is simply known as the turn-on time. During the on-state, a small voltage is produced across the device and, as with the diode, this is known as the forward voltage. Current can always flow from the emitter to the collector through the intrinsic diode in the device. When the device is switched off flow of current through the device ends, though not instantaneously. The time taken for the device to change states from fully on to fully off is known as the turn-off time. The IGBT will continue to block unless the voltage breakdown limit of the device is exceeded; this should not occur in normal operation [53].

2. 2. 2. MOSFETs

The electrical symbol for a negative-positive-negative type Metal Oxide Silicon Field Effect Transistors (MOSFETs) is shown in Figure 2-2. As with the IGBT the MOSFET is an electrically controlled solid state switch.

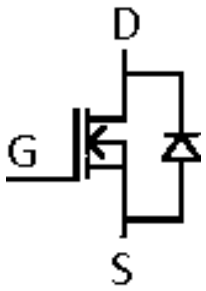

Figure 2-2: MOSFET Electrical Symbol

As with the IGBT operation is dependent on the voltage applied to the Gate pin, shown in Figure 2-2 as “G”. If switched on by a high voltage at the gate, current is able to flow from the drain “D” to the source “S”.

As with the IGBT there is a time period when the device is between states when switching on or off; this produces delays known as the turn on time and turn off time respectively. During the on-state, as with the diode and IGBT, the MOSFET is subject to a forward voltage.

Current can always flow from the source to the drain through the intrinsic diode in the device; it is also worth noting that the intrinsic diode is optional. When the device is switched off flow of current through the device ends. The MOSFET will continue to block unless the voltage breakdown limit of the device is exceeded, this should not occur in normal operation [53].

2. 2. 3. Conduction Loss

From the previous sections on Diodes, IGBTs and MOSFETs it has been established that all three devices are subject to a forward voltage when fully on. This forward voltage drop results in power being dissipated in the device and lost as heat; this is known as conduction loss.

Figure 2-3 shows the conduction loss in line with device operation and this loss can be calculated via Equation 2 [53].

2
$$P_{ON} = V_{ON} \times I_{ON} \times \frac{t_{ON}}{T}$$

Where T is the period of switching and t_{ON} is the on-time of this period, therefore the on-time divided by the period effectively represents the duty cycle of the control signal [53].

An effect of the possible increase in temperature is the lowered reliability of devices; the failure rate for semi-conductors doubles for each 10°C-15°C temperature rise above 50°C [53]. This can be mitigated by good thermal design but in any case it is prudent to keep semi-conductor losses as low as possible.

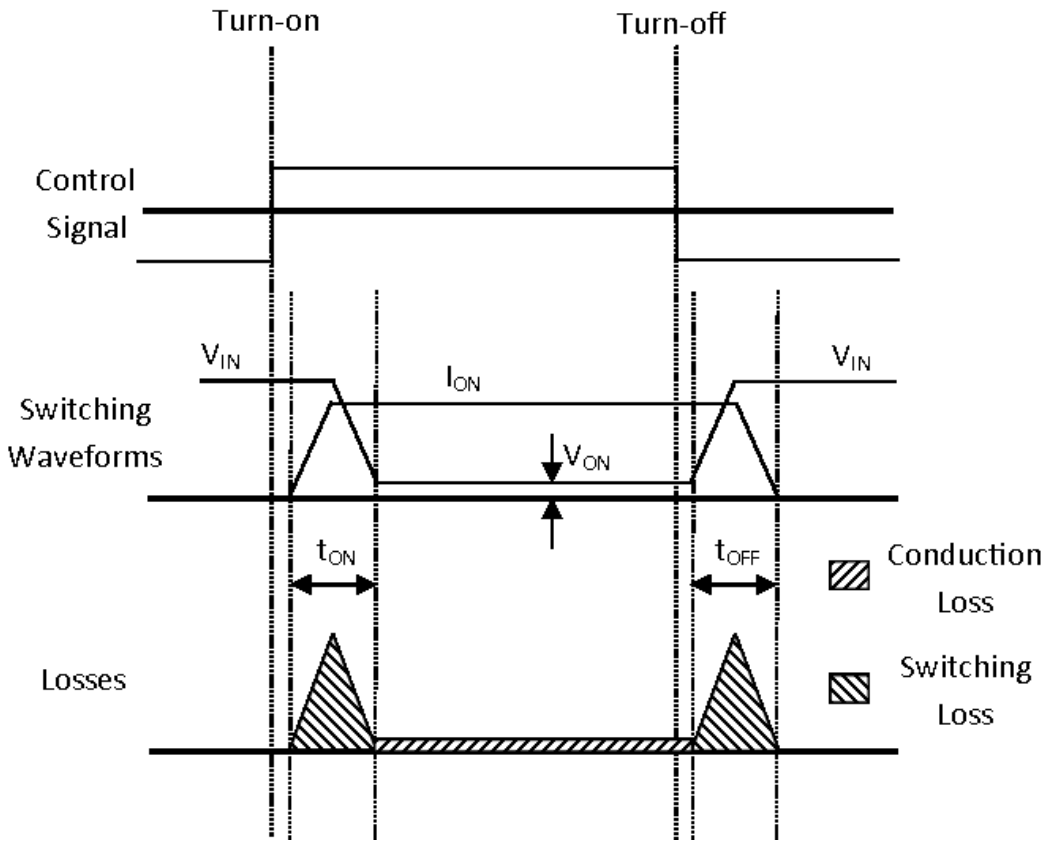

Figure 2-3: Losses in switching semi-conductor devices

2. 2. 4. Switching Loss

From the previous sections on IGBTs and MOSFETs it has been established that the transition between states on and off is not instantaneous and this results in delays known as turn-on time and turn-off time.

These transitional states of voltage and current result in power being dissipated in the device and lost as heat; this is known as switching loss. Figure 2-3 shows the conduction loss in line with device operation and this loss can be calculated via Equation 3 [53].

3 $$P_S = \frac{1}{2} \times V_{IN} \times I_{ON} \times f_S \times (t_{ON} + t_{OFF})$$

As with the conduction loss, the power loss generated by the switching is converted to waste heat in the semi-conductor; the junction temperature will affect the turn-on and turn-off times. This again makes the switching loss difficult to accurately calculate and simulate.

As with the conduction losses the increased junction temperature can severely affect semi-conductor lifetime. This is fully described in Section 2. 2. 3.

2. 2. 5. Reverse Recovery Loss

If a diode becomes forward biased its switch on can be considered ideal, as the diode turns on very fast [53]. However when a diode becomes reverse-biased current is able to travel in the reverse direction for a small amount of time known as the reverse recovery time. This results in a small power loss due to time spent in a transitional state and as with the switching losses, it can also lead to voltage spikes in inductive circuits [53].

With fast-recovery type diodes the reverse recovery time becomes very small in the order of microseconds [53]. Therefore this loss is considered negligible in loss calculations in the main text.

2. 2. 6. Device Comparison

With the MOSFET and IGBT seemingly fulfilling the same purpose the need to explain the operation of both may seem odd. However each semi-conductor has its own advantages over the other device. The MOSFET has very high switching speed but can only be used in low power converters.

The IGBT has a reasonably fast switching speed and can be used in medium power converters. This is summarised in Table 2-4 [53].

Table 2-4: Summary of Device Comparison

Electrical Property of Device	IGBT	MOSFET
Maximum Breakdown Voltage (kV)	2	1
Maximum Current Output (A)	500	100
Maximum Switching Frequency (kHz)	100	1,000

2. 3. The Back-to-back Inverter

Using the semi-conductors discussed in Section 2. 2. converter architectures can be developed. The relevant converter type is this case is an AC-AC converter architecture. The two most prevalent AC-AC converter architectures are discussed in this section, the back-to-back inverter is one of these [54].

2. 3. 1. Circuit Architecture

A circuit diagram of the back-to-back inverter is shown in Figure 2-4. This circuit diagram also shows the separate distinct stages of the back-to-back inverter which will be elaborated upon in this section.

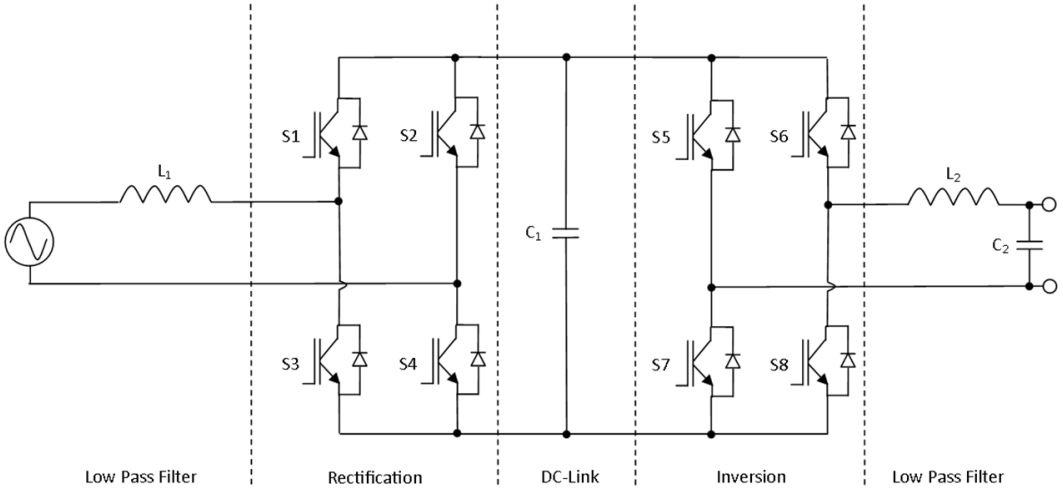

Figure 2-4: Back-to-back Inverter Circuit Diagram

2. 3. 2. Low Pass Filtering

From Figure 2-4 it can be observed that there are two low pass filters in the back-to-back inverter. These filters exist to smooth the harmonics generated by the switching semiconductors and reduce them to within acceptable standards. For more information on harmonics see Section 2. 1. 4. The first filter which consists of a single inductance L_1 also serves as a reactance, *X*, to draw power from the grid to the rectification stage of the back-to-back inverter.

2. 3. 2. 1. Supply of Power

Equation 4 is used to describe the transmission of real power between two sources linked by a series inductance [53].

4
$$P = \frac{V_1 \times V_2}{X} \times \sin(\delta_1 - \delta_2)$$

Where V_1 is the voltage of the primary source at angle δ_1, V_2 is the voltage of the secondary source at angle δ_2 and X is the reactance of the inductance i.e. L multiplied by the angular frequency ω.

Therefore from Equation 4 we can state that the real power transfer between the grid and the back-to-back inverter rectification stage is dependent on the phase difference between the two and the power draw to the rectification stage can be controlled.

2. 3. 2. 2. DC-Link Capacitor

The output DC voltage of rectified AC is subject to ripple at a frequency of twice the line frequency[53], in the UK this would be equal to 100Hz. In order for the output of the rectifier to be considered DC this frequency component must be filtered. This is achieved via the DC-link capacitor which acts as a low pass filter with cut-off frequency below 100Hz.

As the DC-link capacitor has a very low cut-off frequency, it has a high value of capacitance. See Section 2. 3. 2. 3. for a detailed description. This results in a very large time-constant element between the rectifier stage and the inverter stage of the back-to-back converter architecture. This decouples the instantaneous energy from the stages allowing harmonic and reactive power mitigation.

Increasing the size of the DC-link capacitor will decrease the voltage ripple on the DC section of the topology, therefore maximising the size of the DC-link capacitor is prudent as this will increase the lifetime of the component [53, 55]. Equation 5 is used to calculate the voltage ripple for a full-bridge converter [56]

5
$$V_{ripple} = \frac{V_{peak}}{2 \times R_{load} \times C_1} \times T$$

Where T is the switching period, V_{peak} is the highest voltage point of the ripple voltage, R_{load} is the load resistance and V_{ripple} is the ripple in the DC voltage.

2. 3. 2. 3. First Order Filter

Switching semiconductors introduced harmonics to the input current, output voltage and output current in the form of multiples of the switching frequency. To reduce this distortion, the output voltage and current must be filtered in order to meet acceptable power quality standards, for more information on these standards see Section 2. 1. 4. Therefore an inductive 1st order filter was designed.

The open-loop transfer function for the first order filter is given in Equation 6 and the cut-off frequency can be calculated using Equation 7.

6

$$\frac{V_{out}}{V_{in}} = \frac{R}{R + sL}$$

7

$$\omega_n = \frac{R}{L}$$

2. 3. 2. 4. Second Order Filter

The transfer function of the inductive and capacitive second order low pass filter shown in Figure 2-5 is given in Equation 8. In order to tune this filter to give the desired response, the transfer function in Equation 8 was manipulated to have the form of a standard second order transfer function as shown in Equation 9. By comparison of Equation 8 with Equation 9 the values for the inductance and capacitance for a given cut-off frequency can be calculated, using Equations 10 and 11.

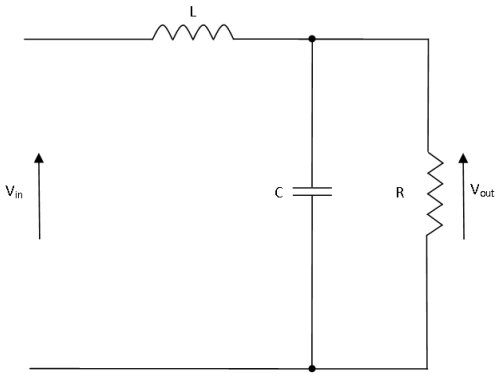

Figure 2-5: Second Order Low Pass Filter Circuit Diagram

8

$$\frac{V_{out}}{V_{in}} = \frac{\dfrac{\dfrac{R}{sC}}{R + \dfrac{1}{sC}}}{\dfrac{\dfrac{R}{sC}}{R + \dfrac{1}{sC}} + sL}$$

9

$$\frac{V_{out}}{V_{in}} = \frac{\omega_n^2}{s^2 + 2\omega_n \xi s + \omega_n^2}$$

10

$$\omega_n = \sqrt{\frac{1}{LC}}$$

11

$$2\omega_n \xi = \frac{1}{RC}$$

2. 3. 3. Rectification

The input stage rectifier of the back-to-back inverter shown in Figure 2-4 is technically known as a VSC full-bridge bidirectional boost converter [57]. This means that power can flow in both directions for an appropriate application. This is important as bi-directional power flow is becoming increasingly relevant in the UK LV distribution system, see Section 1. 2. The full bridge version is used in order to half the ripple on the DC output, and therefore the size of DC-link capacitor can be reduced, see Section 2. 3. 2. 2. The rectifier not only converts from AC to DC but also "boosts" the DC voltage to a controlled value across the DC-link capacitor [57].

2. 3. 4. Inverter

The output inverter shown in Figure 2-4 is identical to the rectification stage but in reverse, and therefore technically the converter "bucks" rather than "boosts" and also converts the DC voltage to AC.

2. 3. 5. Control

Where the inverter and rectifier are very similar technically, their control systems are very different.

2. 3. 5. 1. Inverter Control

If left uncontrolled V_{out} will vary with load; this is not desired in most cases. To control the output voltage, a feedback loop can be placed in the system which measures the V_{out}, compares with a set point and passes the resultant difference to a PI controller. This information is then utilised to control the switching of the inverter semiconductors and changes the modulation index of the H bridge dependant on what is required.

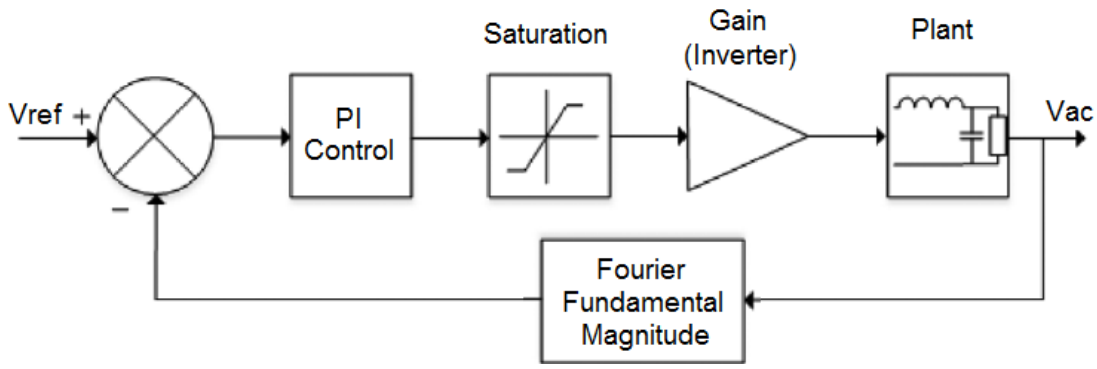

Figure 2-6: Control of the Inversion Stage

2. 3. 5. 2. Rectifier Control

In order to control the power flow into the rectifier, an additional control loop is required as shown in Figure 2-7.

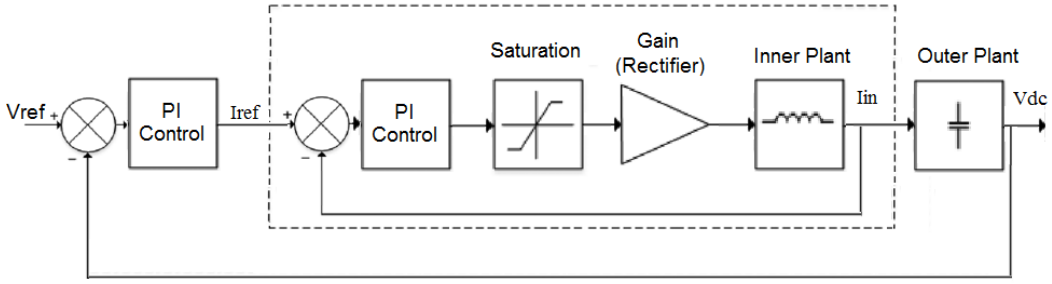

Figure 2-7: Control of the Rectification Stage

The power flow from the grid to the back-to-back inverter is controlled via two classic cascaded control loops, where the outer control loop regulates the DC link voltage and the inner loop regulates the current flowing from the grid through the rectifier.

In order for the controller to work correctly, the speed of the inner and outer loop PI controllers must be set to an order of magnitude apart. This allows the two control loops to be decoupled and hence operate independently of each other [58, 59]. Therefore the outer control loop was treated as a standard second order control loop.

2. 3. 5. 3. Modulation

In order for the H-bridge of the inverter stage to generate a sine wave at the desired magnitude and frequency the correct control signals must be sent to the H-bridge. This is achieved through a comparison of the reference sine wave, the reference wave being at the desired magnitude and frequency, to a triangular carrier wave with frequency of the desired semi-conductor switching frequency.

In the comparison of the two signals, if the reference sine is greater in magnitude than the triangular wave then the output square wave is positive i.e. S5 and S8 of Figure 2-4 are switched on to allow positive current flow. If the reference sine is lesser in magnitude than the triangular wave then the output square wave is negative i.e. S6 and S7 of Figure 2-4 are switched on to allow negative current flow.

This is known as bipolar voltage switching and an example of this operation is shown in Figure 2-8, although please note that the switching frequency of the example is very low in order to clearly demonstrate the switching operations and normally would be much faster.

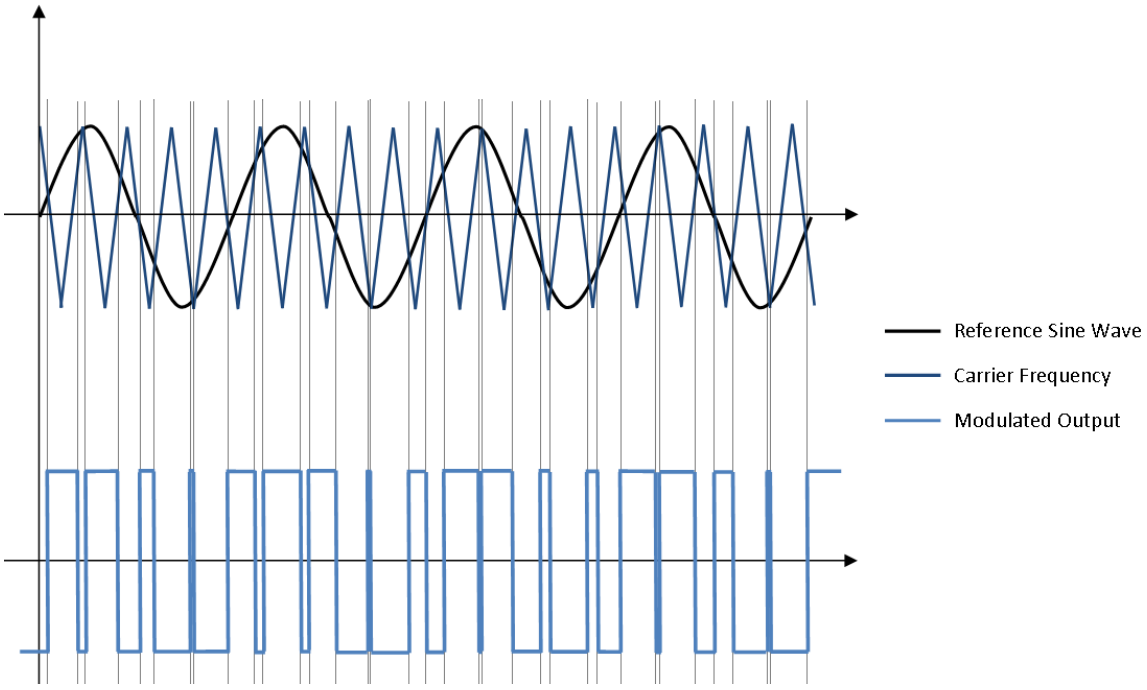

Figure 2-8: Bipolar Voltage Switching

It can therefore be observed from Figure 2-8 that a reduction in the amplitude of the reference sine wave when compared with the carrier signal will result in a modified square wave sent to the H-bridge which will decrease the actual output sine wave.

This ratio of signals is known as the modulation index, *m*, and controls the amplitude of the output sine wave from the H-bridge. As the modulation index is a ratio Figure 2-8 has no axis markings as they would be redundant [53].

2. 3. 5. 4. Deadbands/Blanking Time

In the previous section it can be seen that the control signals sent to the semiconductors in Figure 2-8 instantaneously change from on to off. However it has already been established in Section 2. 2. 4. that in reality semiconductors are presently not able to change states quickly enough as to be considered instantaneous. Therefore an additional delay must be added to the control signals that allow for the devices to change state otherwise a "shoot-through" condition will occur which may damage the semiconductors [53].

This will cause additional low order harmonic voltage distortion around the current zero-crossing of the back-to-back inverter [53]. However this is considered to be negligible in magnitude considering the turn-on and turn-off time of the semi-conductors, see Section 2. 2. 1.

2. 3. 6. Snubbers

Quickly switching on/off (i.e. high rate of change of current) a semiconductor with stray inductance intrinsic to the device severs power flow of stored energy. This energy is dissipated in the device as a voltage overshoot across the device potentially causing damage or stress [60].

This can be alleviated via use of snubber circuits which allow a free-wheeling path for extremely high frequency current transients.

Decoupling capacitors provide this path and they are placed across the relevant device. A series resistor is also placed in series with the discharge capacitance in order to provide damping and absorb the power dissipation of the transient in lieu of the semiconductor [60].

The sizes of the components can be estimated by use of Equations 12 and 13, where C_{SN} is the snubber capacitance, L_S is the stray inductance, I_R is the rated current, V_{PK} is the peak/overshoot of voltage, V_R is the rated voltage and f_{SW} is the switching frequency. The power lost in the snubber resistor is given by Equation 14 [60].

12
$$C_{SN} = \frac{L_S \times {I_R}^2}{(V_{PK} - V_R)^2}$$

13
$$R_{SN} = \frac{1}{(6 \times C_{SN} \times f_{SW})}$$

14
$$P_R = \frac{1}{2} \times C_{SN} \times ({V_{PK}}^2 - {V_R}^2) \times f_{SW}$$

2. 4. The Matrix Converter

Another method of AC to AC conversion is to convert directly without the intermediate DC stage. This can be achieved via the use of a matrix converter.

2. 4. 1. Circuit Architecture

If the matrix converter has a single phase source and load, two bi-directional cells are required. The matrix converter architecture in this case is shown in Figure 2-9 and is known, and will be henceforth referred to, as the AC Chopper. Figure 2-9 shows the distinct stages of the circuit architecture which will be described in this section.

2. 4. 2. Low Pass Filtering

The AC Chopper has two low pass filters placed before and after the bidirectional cells as shown in Figure 2-9. These filters are placed to remove harmonic content from the voltage and current. The operation of the second order low pass filters has been described previously in Section 2. 3. 2. 4.

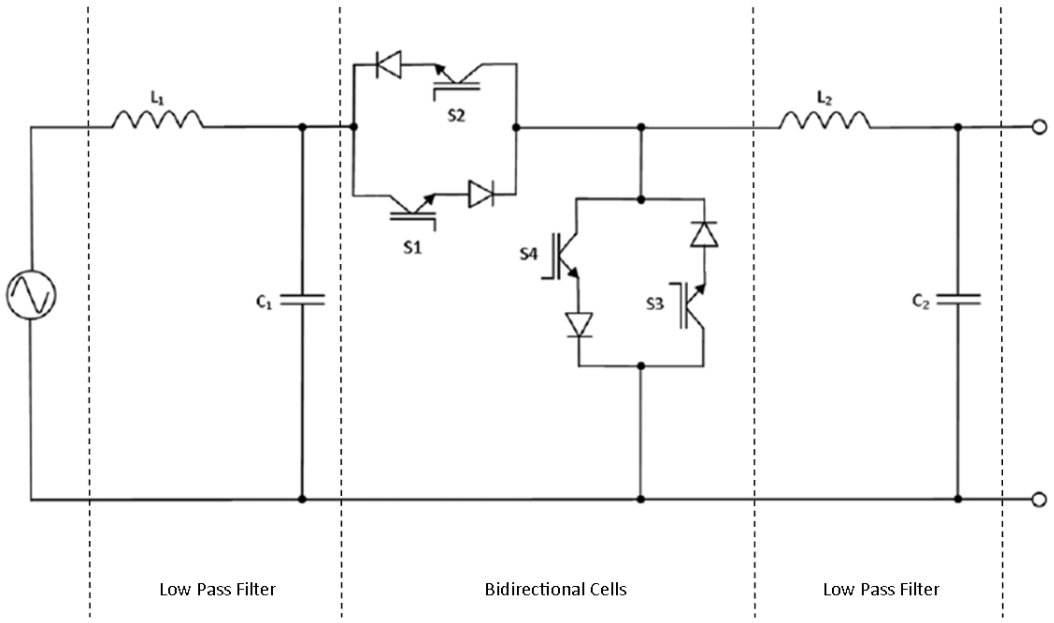

Figure 2-9: AC Chopper Circuit Diagram

2. 4. 3. Bi-directional Switches

A matrix converter architecture is comprised of an *m* by *n* array of bi-directional switches, where *m* is the same as the number of phases of the voltage source and *n* is the same as the number of phases of the load. Using the semi-conductors described in Section 2. 2. a bi-directional switch can be created the variations of bi-directional cells are shown in Figure 2-10[61].

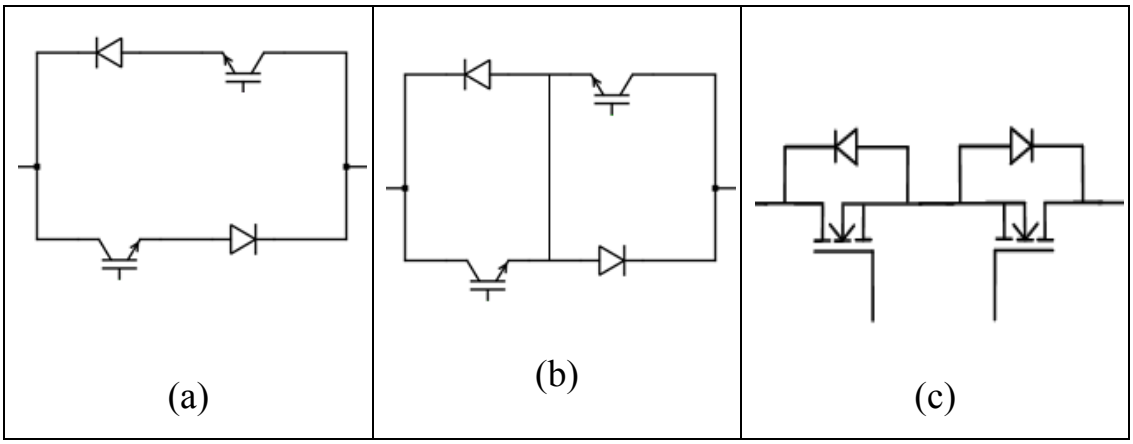

Figure 2-10: Bi-directional cells made with uni-directional semi-conductors (a) bi-directional cell using IGBTs and diodes, (b) bi-directional cell using IGBT and diodes with optional common emitter bridge arm (improves transient performance), (c) bi-directional cell using MOSFETs.

Using these bi-directional cells the amplitude of an incoming AC waveform can be directly "chopped" similar to simple DC PWM, providing a drop in average magnitude of the sine wave, this process is shown pictorially in Figure 2-11.

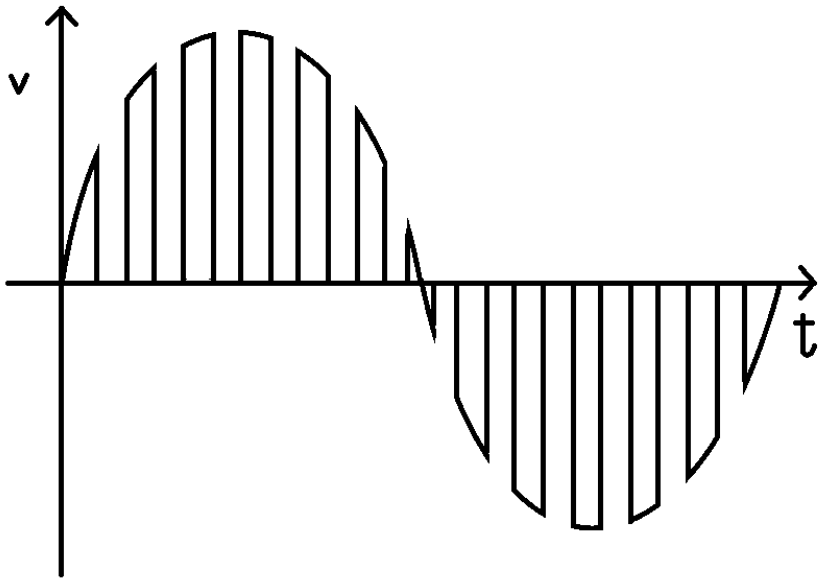

Figure 2-11: Chopped AC Voltage Waveform

Activation of switches S1 and S2 will connect the load to the source voltage, whilst activation of S4 and S3 will apply zero voltages to the load. Modulation of these states allows the load voltages to be controlled as shown in Figure 2-12 and fully described in Section 2. 4. 4. 1.

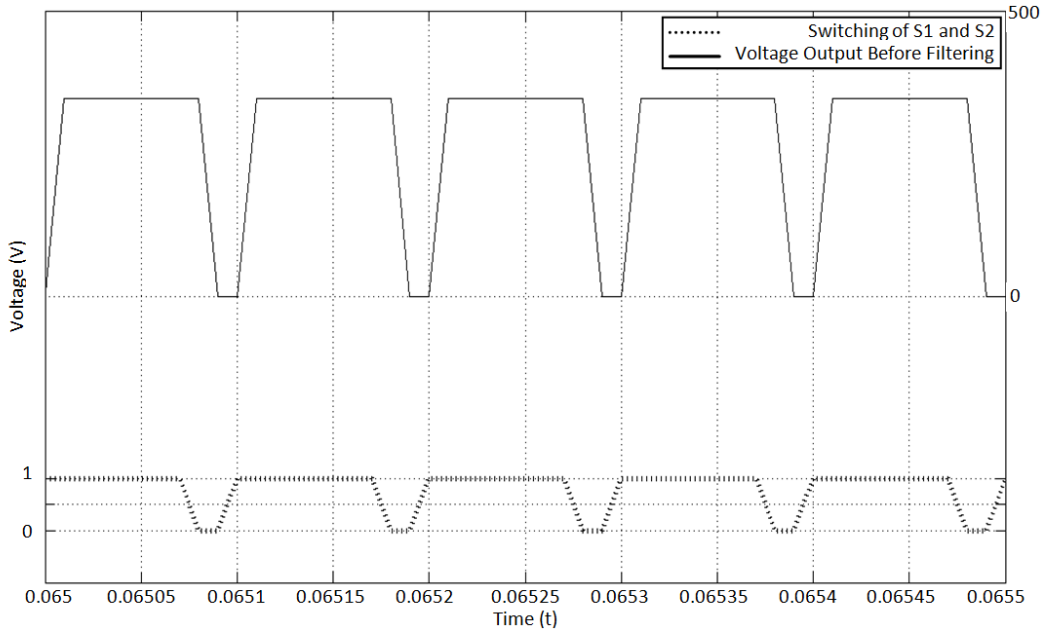

Figure 2-12: Switching Waveforms of AC Chopper Showing the Input Signals to S1 and S2 and the Resultant Chopper Output

Once filtered, the resultant waveform is of the same frequency but of reduced amplitude that is directly proportional to the duty cycle of the chopped waveform. Note that for a three phase matrix converter it is also possible to vary the frequency however this comes at the cost of a reduction in possible output voltage magnitude of 50-87% [61]. Although, it is possible to overcome this limitation with advanced modulation methods which implements a "fictitious DC-link"[61].

2. 4. 4. Control

If left uncontrolled or open loop controlled, the output voltage will vary with changes in input voltage and normally this is undesired. With a negative feedback closed loop control the output voltage may be set to a particular reference value that is maintained even when the input voltage is altered. Negative feedback closed loop control was previously described in Section 2. 3. 5. 1.

2. 4. 4. 1. Modulation

In order to generate the control signals for the AC Chopper a DC value of desired magnitude must be compared to a triangular waveform with frequency of the desired semiconductor switching frequency.
In the comparison of the two signals, if the reference DC line is greater in magnitude than the triangular wave then the output square wave is positive i.e. S1 and S2 of Figure 2-9 are switched on to allow bi-directional current flow.

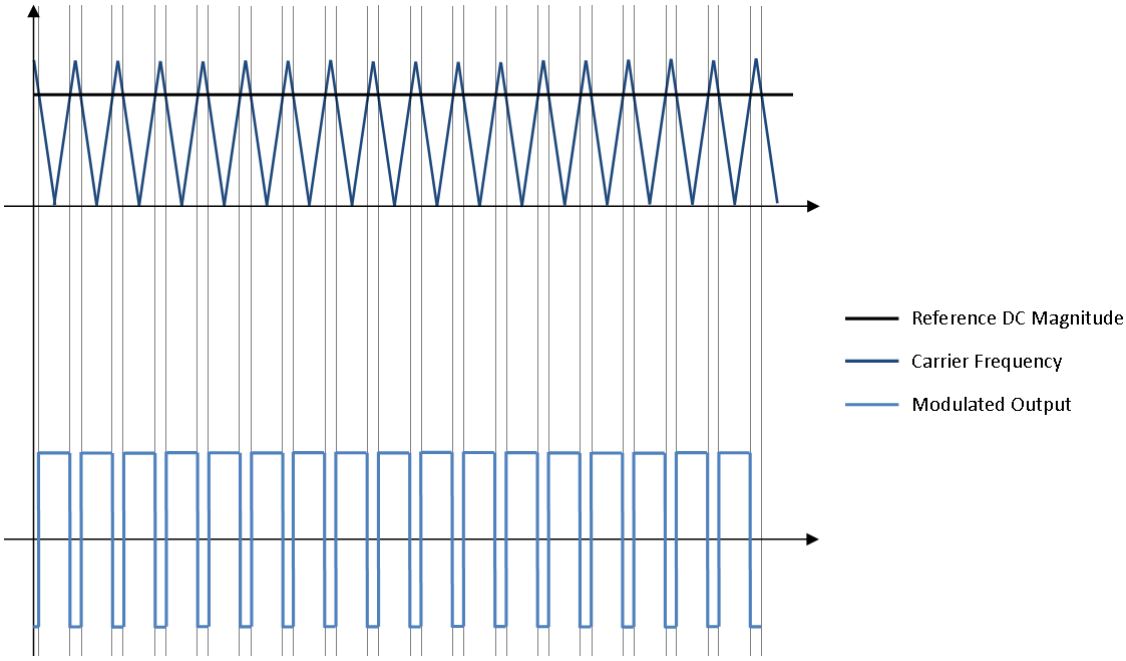

Figure 2-13: Voltage PWM

If the DC line is lesser in magnitude than the triangular wave then the output square wave is negative i.e. S3 and S5 of Figure 2-9 are switched on to cease current flow.

This is an example of a common pulse-width modulation signal used to vary the magnitude of the input voltage and an example of this operation is shown in Figure 2-13, although please note that the switching frequency of the example is very low in order to clearly demonstrate the switching operations and normally would be much faster.

It can be observed from Figure 2-13 that a reduction in the amplitude of the reference DC line when compared with the carrier signal will result in a modified square wave sent to the H-bridge which will decrease the actual output sine wave. This ratio of signals is known as the modulation index, *m*, and controls the amplitude of the output sine wave from the AC Chopper. As the modulation index is a ratio Figure 2-13 has no axis markings as they would be redundant.

2. 4. 4. 2. Deadbands/Blanking time

The importance in allowing deadbands in control and the consequences of this has been previously described in Section 2. 3. 5. 4.

2. 4. 4. 3. Semi-Soft Switching

There are two methods to control the four semi-conductors that are within the bi-directional switch cells shown in Figure 2-9, hard-switching and semi-soft switching. Hard-switching is the more traditional method of commutation that consists of waiting until the semi-conductors are fully switched off utilising deadbands before switching on the next semi-conductor [61].

Another method of commutation is semi-soft switching which, instead of waiting until all switches are off, transitions certain semi-conductions while some switches are still on. A popular method of achieving this is the four step commutation method shown in Figure 2-14 [61]. This method transitions the semi-conductors that are not conducting in the present current direction first, this provides a free-wheeling path for trapped energies caused by stray inductance and parasitic capacitance [61], see Section 2. 3. 6. for more information on these subjects.

According to the present research [61] this is the preferred method of commutation as the switching losses are reduced by 50% [61].

Another semi-soft switching technique is also possible, the two step commutation method. This method switches off the semi-conductors that are not conducting in the present current direction for the duration of time spent in the relevant current direction. This results in lower losses as no unnecessary switching occurs, however this method also reduces the amount of current paths available resulting in less robust operation unless an advanced control scheme is employed which involves the use of intelligent gate driver circuits [61].

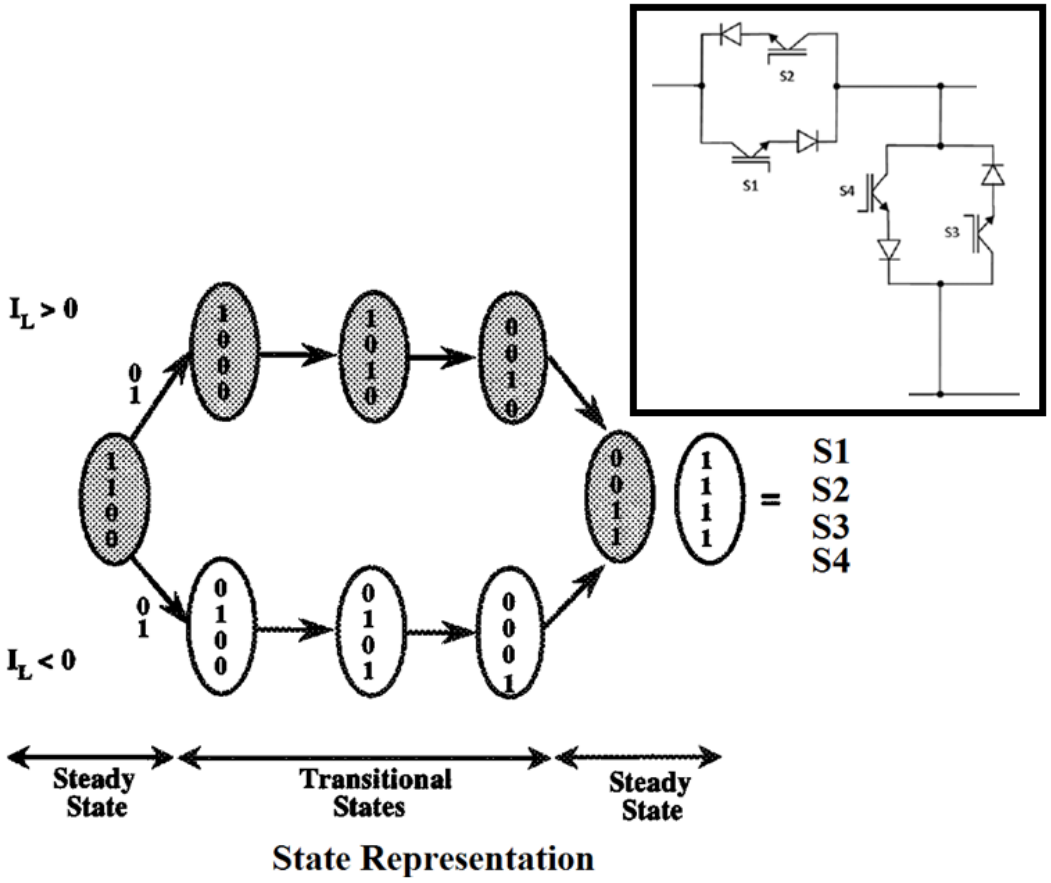

Figure 2-14: Semi-soft switching 4 step commutation method [61], see Figure 2-9 to observe switch designations S1-S4

A prerequisite of using any of these semi-soft commutation techniques is the knowledge of the present current direction.

2. 4. 4. 4. Zero Crossing Detection Methods

As established in the previous section, the method of commutation if using a semi-soft commutation strategy requires information on the direction of current. The simplest way to do this is to measure the input current to the bi-directional switches directly and use this measurement to inform control circuitry.

According to the present research this method is not recommended at high power levels due to the difficultly in reliably measuring low current values when large ranges of current are possible in high power applications [61].

Other methods of zero crossing detection exist for high-power applications exist which use a dead-zone around the current zero in which no current flows and the switching method is reconfigured. Another method employs driver level intelligence so that each semi-conductor detects the correct current direction independently [62].

2. 4. 5. Snubbers

The importance of including snubbers in semiconductor based circuitry and the consequences of this has been previously described in Section 2. 3. 6.

2. 5. Power Distribution

In order to correctly understand the main text, mechanisms of the low voltage distribution system must be described in order to inform later work.

2. 5. 1. AC Conductor Losses

There are several losses that occur when transmitting AC power via conductors. Conductor current losses, dielectric losses and sheath losses. In the distribution system by far the most prevalent loss is the conductor current loss [63], this is described by Equation 15. Where n is the number of cores, I is the current through the cables and R is the resistance of the core [63].

15 $$P_C = n \times I^2 \times R$$

2. 5. 2. Types of Electrical Load

As time has passed more complex devices are being powered by electricity from the UK distribution system. It is important to understand the effect these loads will have on the voltage and current.

2. 5. 2. 1. Unity Power Factor Linear

A unity power factor load is the type in which the voltage and current waveforms are not phase displaced and a linear load is one in which the voltage across it varies linearly with current through it. These types of load generally represent heating elements which are resistive in nature. A good example of a large household unity power factor linear load is an electric shower which can typically be 10kW in rating.

2. 5. 2. 2. Non-Unity Power Factor Linear

A non-unity power factor load is the type in which the voltage and current waveforms are phase displaced. These types of load generally represent household machines which contain inductive as well as resistive elements. A good example of a large household non-unity power factor linear load is an electric shower which can typically be 1kW in rating and have power factors as low as 0.75 lagging [64].

2. 5. 2. 3. Non-Linear

A non-linear load is one in which the voltage magnitude across it does not vary linearly with current magnitude through it. These types of load generally represent loads with semi-conductors converting the AC signal into whatever is appropriate. A good example of a large household non-linear load is a microwave which is provided DC power by an uncontrolled rectification stage, they are generally 1kW in rating [65].

CHAPTER 3

3. Load Flow of the UK Urban Distribution Network

The first step taken in the research was to consider the UK LV distribution system as it is presently. An accurate representation of the UK LV distribution system would be modelled using data from industry partners. Once established, the effects of future technologies on the LV distribution grid could be explored.

3. 1. Power flow Analysis of a UK LV Network

The software PowerWorld Simulator was used to model a representative section of the UK urban distribution network shown in Figure 3-1. The model considered two cases; the first case is the present network and its associated load, the second case is a future scenario with an estimation of the worst possible future load.

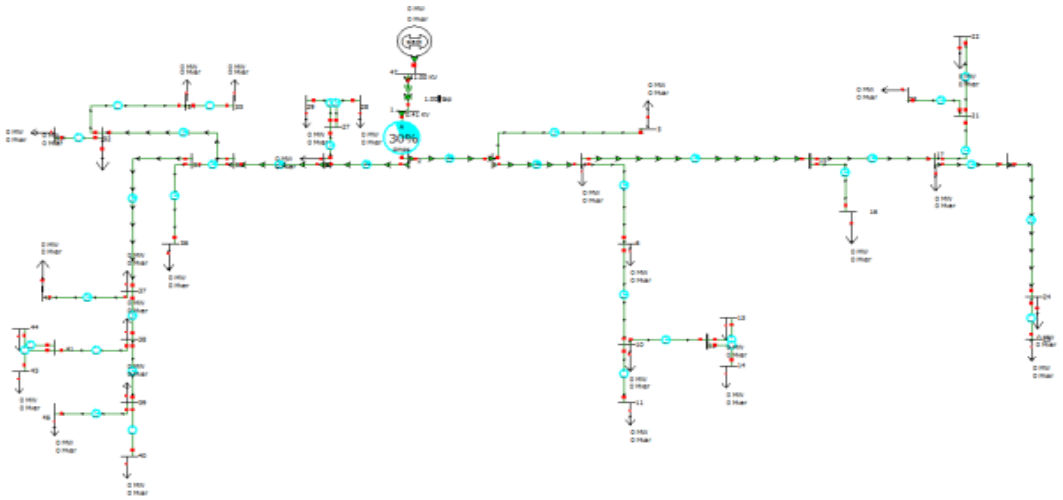

Figure 3-1: Representative Section of the UK Distribution Network

3. 1. 1. 415V LV Network

3. 1. 1. 1. Methodology

In the simulation studies carried out, the cables were modelled using typical parameters of cables used in urban distribution networks. A section of the low-voltage distribution system was modelled using PowerWorld simulator in order to study the current limits.

This model was based on real data for a representative section of the UK distribution network: it was created from a diagram received from industry partners that specified the length and type of each cable.

A separate document which specified resistance and reactance per length and cable type was then used to calculate the total resistance and reactance for each line. The characteristics of each cable could then be entered into PowerWorld simulator; the data for each cable is presented in Appendix A - PowerWorld Cable Data.

The model enabled the study of current losses in the distribution system because of current levels, hence enabling the current limits of the low-voltage distribution system to be studied. In these simulations, it is assumed that each end user is a three bedroom house consuming 1 kW per household this corresponds to the maximum average demand for each house during early evening in winter in the UK [66].

Since demand is not easy to predict and has a random element it was expected that the demand pattern would be short spikes in demand occurring randomly over long periods of smaller base demand. The present low voltage cabling was designed for this demand pattern (see Figure 3-2).

This random element is not possible to simulate in PowerWorld simulator however when all of the random demands are amalgamated the overall demand of an area will generally be consistent with an assumed average demand across all feeders.

As a result all spike and base demands were averaged in order to be useable with PowerWorld, this also means that conductors carrying fewer amalgamated results will be a less accurate representation of what the demand actually looks like i.e. the conductors further away from the transformer have less accurate results than conductors closer to the transformer.

3. 1. 1. 2. Results

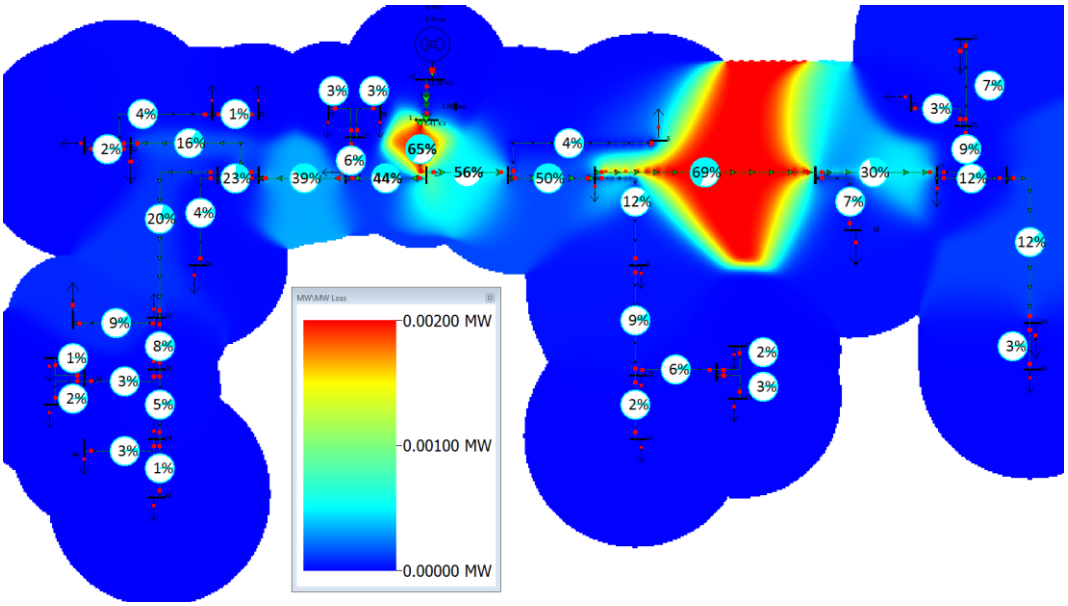

Figure 3-2: Model of the Present LV Distribution System with Present Loading

Figure 3-2 shows the results of this study. By inspection of Figure 3-2 it can be seen that the main feeder is at 65% of its current capacity and that other feeder conductors range from 20% loaded to 69%. Figure 3-2also shows that the current losses presently range from 1kW-2kW on the main feeders. This simulation result indicates that a further 120kVA could be drawn from the distribution network before the current limit of the main feeder reached 100% capacity. From the used assumptions this is the equivalent of 124 more houses.

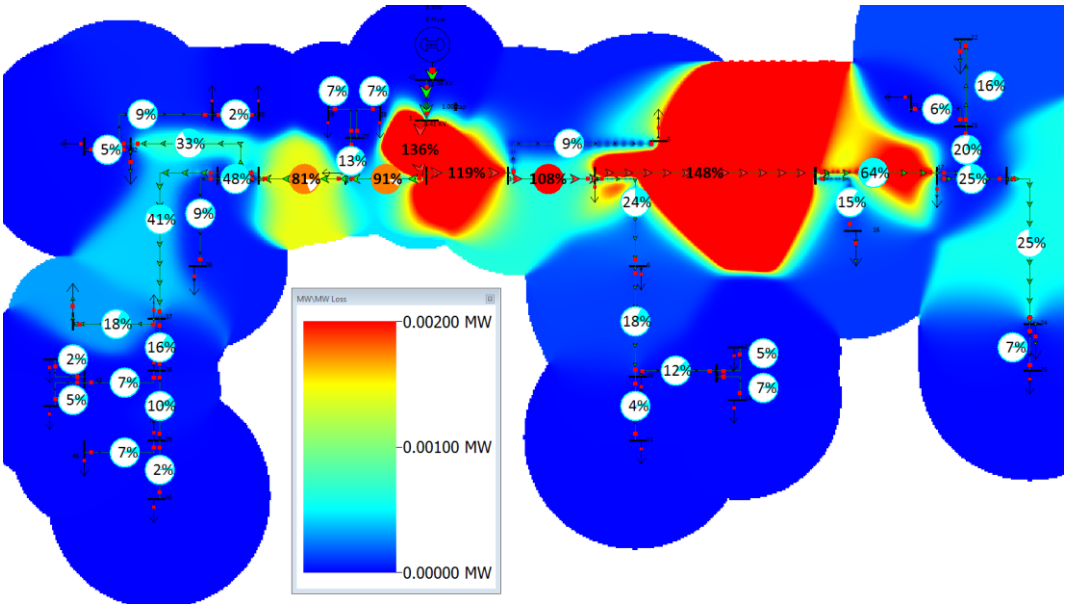

Figure 3-3: Model of the Present LV Distribution System with Future Loading

If EVs or heat pump boilers were introduced to each household in the present system, as discussed in Section 1. 2. , it would more than double average household load [3, 4, 67]. The effect of doubling the average load at each household to 2 kW is shown in Figure 3-3.

It can be observed from Figure 3-3 that the main feeder is 136% loaded and three secondary feeders are also past their insulation limit and the loading of the secondary feeders ranges from 81%-148%. Figure 3-3 also shows that the current losses are consistently higher than those presented in Figure 3-2.

3. 1. 1. 3. Discussion

The results presented indicate that the capacity of the network cannot support the increased load due to current limits on the network. Therefore to increase the capacity of the network, increasing the voltage level of the system must be considered as the conductors of the UK LV distribution system were found to have an underutilised insulation limit in Section 2. 1. 1. 1.

3. 1. 2. 600V LV network

3. 1. 2. 1. Methodology

The same simulation was used as produced in Section 3. 1. 1. in order to produced consistent results. The 415V LV network results are used as a control to demonstrate the result of changing the voltage level clearly.

3. 1. 2. 2. Results

As discussed in Section 2. 1. 1. the cables used in low-voltage distribution have a maximum line voltage limit, based on the insulation, of 1.2 kV_{AC} or a maximum phase voltage limit of 690V_{AC} .

The effect of increasing the voltage on the distribution network is shown in Figure 3-4 and Figure 3-5. Figure 3-4 has a network voltage level of 600V_{AC} line, while in Figure 3-5 the voltage level is increased further to 1kV_{AC} line. Although setting the network voltage at 1kV_{AC} line would provide the most effective capacity increase, it is only being shown here as a comparison. It is not a viable option as it is too close to the cable insulation limit of 1.2kV_{AC} line. Upon discussion with a WPD representative it was discovered that, in reality, it is possible the cable insulation limit will be below 1.2kV_{AC} line because of factors such as weak sections due to jointing, tolerances, degradation and bends/twists in the cabling [68].

From Figure 3-4, it can be observed that the main feeder is now 86% utilised under the previously established future load conditions of average demand, constant 2kW per household. Other secondary feeders range from 52%-96% loaded. Figure 3-4 also shows that the current losses have decrease from 1kW-2kW on the main feeders in Figure 3-2 to 0.25kW-1.5kW.

This is a decrease from 136% loading on the primary feeder and 81%-148% loaded on the secondary feeders from the results presented in Figure 3-3. This means that no cables need to be replaced and a further 24 houses could be placed on the system.

This is an increase of 200 kVA in available capacity compared to the present system shown in Figure 3-2.

Figure 3-5 shows a further decrease from 136% utilisation of the primary feeder and 81%-148% utilisation of the secondary feeders to 51% utilisation of the primary feeder and 31%-54% utilisation of the secondary feeders. Figure 3-5 also shows that the current losses have decrease from 1kW-2kW on the main feeders in Figure 3-2 to 0.01kW-0.25kW. From the estimated average loading values used a further 84 houses could be placed on this system. This is an increase of 500 kVA in available capacity compared to the present system Figure 3-2.

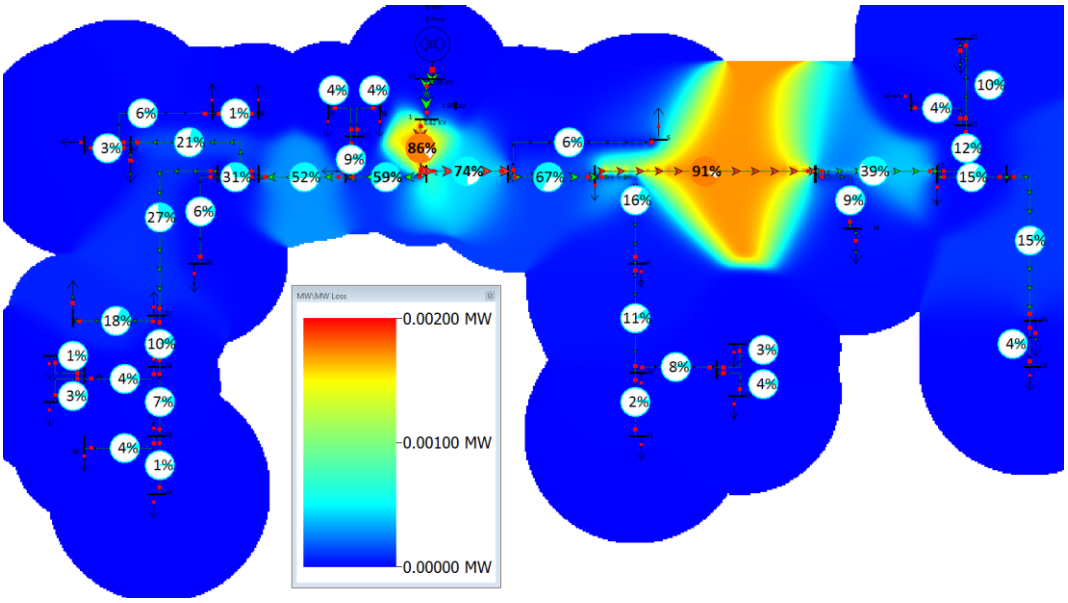

Figure 3-4: Model of a 600V$_{AC}$ line LV Distribution System with Future Loading

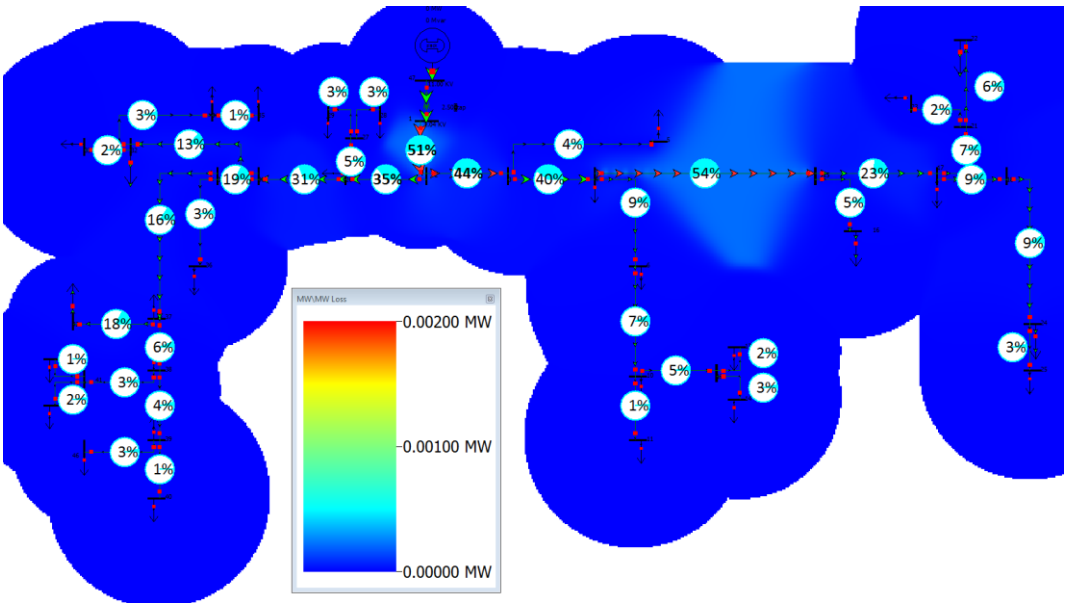

Figure 3-5: Model of a 1kV$_{AC}$ line LV Distribution System with Future Loading

3. 1. 2. 3. Discussion

Therefore these studies indicate that increasing the voltage level of the UK LV distribution system will significantly increase the load capacity of urban distribution networks. The difficulty with this approach is that the end-user receives an unusable voltage supply incompatible with any household equipment. A novel way of achieving this would be using Point of Use Voltage Regulation (PUVR) [69, 70] .

3. 2. Chapter Summary

It was found that the capacity of the network cannot support the predicted increase in load due to current limits on the network. This increase in load would be synonymous with a heat pump boiler or electric vehicle at every household.

To increase the capacity of the network, increasing the voltage level of the system was explored; this is possible due to the conductors of the UK LV distribution system were found to have an underutilised insulation limit.

These studies have indicated that increasing the voltage level of the UK LV distribution system will significantly increase the load capacity of urban distribution networks.

Another benefit of this approach is that the voltage over the converter can vary as the voltage is regulated at the end-user therefore

The difficulty with this approach is that the end-user receives an unusable voltage supply incompatible with any household equipment. Point of Use Voltage Regulation (PUVR) is a possible way of solving this difficulty.

CHAPTER 4

4. Point of Use Voltage Regulation

The concept consists of deregulating the LV distribution network and allowing the voltage level to output from the LV transformer at $600V_{AC}$ line. A compact power electronic converter would then regulate the voltage to $230V_{AC}$ phase at the end-user. A comparison of the present distribution layout and PUVR is shown in Figure 4-1 and Figure 4-2. Another option would be to regulate voltage at the equipment level, however this would incur additional difficulties as the voltage limit of household wiring is lower than three-phase distribution cables and a large legislative change would have to take place which some household electrical equipment manufacturers may not agree to. Therefore regulating at the point of entry to the household is considered most appropriate.

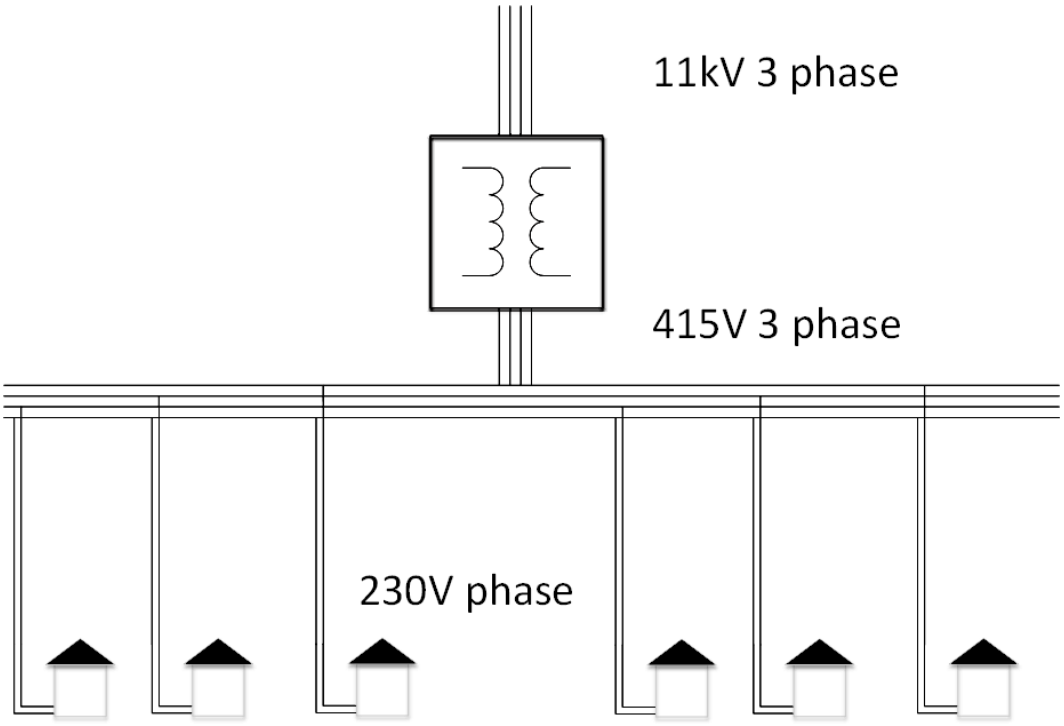

Figure 4-1: Present UK LV distribution layout

In order to assess the viability of PUVR two important issues in implementation have been considered; how the introduction of a power electronics converter affects the losses and how it affects the cost.

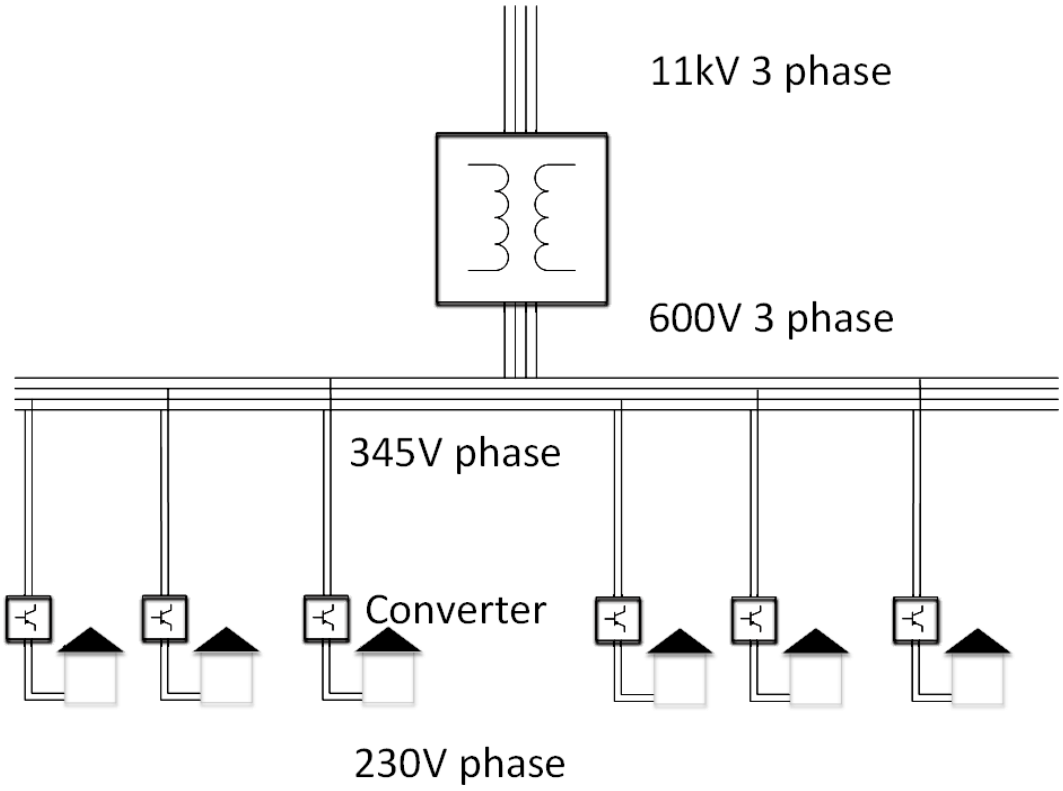

Figure 4-2: Proposed UK LV distribution layout with PUVR

4. 1. Losses of a PUVR Distribution System

In Chapter 3. increasing the voltage of the UK LV distribution has been shown to be an effective means of increasing the capacity available. This can be achieved via PUVR, however in order to assess whether this approach is realistic the first step would be to consider the losses introduced by the converter and evaluate this keeping in mind that the current losses of the cable are reduced due to the increase in voltage.

4. 1. 1. Cable loss

There are many losses in the LV conductor however the dominant loss value is caused by current losses; this was previously described in Section 2. 5. 1.

4. 1. 1. 1. Methodology

The current losses of the cables were calculated using the load flow simulator PowerWorld. The simulations were created using real world cable data and an assumed constant average load of 1-2kW per consumer, dependant on scenario.

The loss on each cable was then exported to excel where the total loss was calculated for each scenario using Equation 16.

16

$$P_{LOSS\%} = \frac{\sum P_{LOSS}}{S_{IN}} \times 100$$

4. 1. 1. 2. Results

From the heat maps in Section 3. 1. it is clear that increasing the voltage of the LV distribution system lowers the current losses present in the cabling due to the lower current levels in the network.

Table 4-1 summarises the different current losses for the urban distribution network considered in Chapter 3. operating at different voltage levels.

Table 4-1: Conductor Current Losses as a Percentage of Total Input Power

	415V 1kW Average Load (Figure 3-2)	415V 2kW Average Load (Figure 3-3)	600V 2kW Average Load (Figure 3-4)	1kV 2kW Average Load (Figure 3-5)
Cable Loss (%)	3.1	6.74	1.26	0.16

The present urban distribution network, drawing the maximum average from all loads simultaneously, loses 3.1% of its transmitted power as heat in the cabling. At the estimated future maximum average load, 6.74% of the power transmitted is lost. Transmission of power at 600V decreases this loss at maximum load to 1.26% and transmission at 1kV furthers this decrease to 0.16%.

4. 1. 1. 3. Discussion

From the results shown in Table 4-1 it is clear that the current losses of the UK LV distribution system is are not significant and this is in line with expectations [71]. However these losses more than double under future loading conditions, due to the losses being directly proportional to the square of current, see Section 2. 5. 1. for further detail.

Increasing the voltage by $175V_{AC}$ decreases this loss by 5.5%, increasing the voltage by $575V_{AC}$ decreases this loss by 6.6%. Therefore it is clear that the optimal voltage is $600V_{AC}$ line as the additional voltage does not decrease the loss as significantly and increasing the voltage to $1kV_{AC}$ line increases the risk of damaging the conductors [68].

4. 1. 2. Converter loss

When using PUVR, the voltage level must be stepped down at the end-user. In the case of the urban network, this would take place at each house connected to the distribution network. This voltage conversion will not be 100% efficient, and therefore extra losses will be introduced to the network.

4. 1. 2. 1. Methodology

Using presently available information, a high level evaluation of the converter losses can be estimated. A best and worst case was considered; where the best case would be a single efficient conversion stage and the worst case would be two inefficient conversion stages.
With this in mind the best case considered was 2%, [54, 72] and the worst case considered was an inefficient conversion of 4% [54] with two conversions which would therefore give an 8% conversion loss.

4. 1. 2. 2. Results

The effect of the addition of the estimated converter losses are shown in Table 4-2. It was found that the lowest loss in a 1kV PUVR system with a highly efficient conversion stage would be 2.15% and that the highest loss is a 600kV PUVR system with a less efficient conversion stage would be 9.26%.

Table 4-2: Total Loss in a PUVR system, see Figure 3-4 and Figure 3-5 for PUVR 600V_{AC} line scenario and PUVR 1kV_{AC} line scenario respectively

	PUVR 600V Best Case	PUVR 600V Worst Case	PUVR 1kV Best Case	PUVR 1kV Worst Case
Cable Loss (%) (Table 4-1)	1.26	1.26	0.16	0.16
Converter Loss (%)	+2	+8	+2	+8
Total Loss (%)	3.26	9.26	2.16	8.16

4. 1. 2. 3. Discussion

To be considered on-par with the present LV distribution architecture, from Section 4. 1. 1. Table 4-1, the target for the total loss which would make a PUVR based architecture viable is 3.1%-6.7%. Therefore from the results shown it is clear that a converter of 92% efficiency is outside this target and not viable for use with PUVR.

According to these criteria, the absolute minimum efficiency to be considered viable in terms of efficiency is 93.3%. This level of efficiency should be possible with high quality modern power electronic converters [54].

4. 1. 3. Summary

The studies carried out have strongly indicated that PUVR would be effective in easing congestion of low voltage urban distribution systems by increasing capacity of the network without exceeding current/current limits of the cables.

A potential disadvantage of implementing PUVR using power electronic converters is that conversion losses are introduced to the system. However, the results shown in Table 4-1 and Table 4-2 have shown that this additional loss is compensated for by the lower losses in the conductors due to the lower current levels so far as the efficiency of the conversion stage is above 93.3%.

4. 2. Cost-Benefit Analysis of a PUVR Distribution System

Section 3. 1. established that increasing the voltage level of the LV distribution network is a viable way in increasing the capacity and Section 4. 1. established the lowest possible loss limit to be considered on par with the presently used distribution method. Another important issue that affects the viability of PUVR is cost and this section will focus on this aspect, with particular reference being made to the cost of the business as usual case i.e. network reinforcement by conductor replacement.

4. 2. 1. Methodology

The costs of transformer and cable replacement including excavation and reformation were taken from the Scottish and Southern Energy (SSE) 2012 Statements, Methodology, Charges and Connection document [73]. Using this document and a diagram gained from industry partners which specified cable length and type an estimation of the cost of replacing the distribution cables was made.

The SSE document states a particular maximum and minimum charge for laying LV cable in three classes of current rating 95mm^2, 95-185mm^2 and >185mm^2. This cable sizing was taken into account when estimating the conductor replacement costs for the representative section of the network. The total distance of the network from the provided diagrams is approximately equal to 1.7km and the calculated cost per meter was found to be between £100/m-£280/m.

Please note that these figures estimate supply and installation of the conductors only and does not account for such factors as traffic management, project management e.t.c.

The cost of the converters was estimated using the cost of present off-the-shelf converter units [74, 75].

A transformer replacement was considered for the cable replacement method as it is possible that the breaching the reverse current limit with future high distributed generation penetrations would trigger network reinforcement i.e. transformer replacement in any case. More information on this issue is described in Section 1. 2. 3. However in order to consider a worst case scenario a replacement was not deemed necessary for this study.

4. 2. 2. Results

It was found that, at present, the PUVR method has a greater cost and that a 20kW converter would need to cost £460-£2,100 (worst case and best case respectively) to be equivalent to replacing the cables.

4. 2. 3. Discussion

The costing for these converters was for 220 individual units and it is expected that the price would reduce significantly if ordered in bulk. It is also expected that when PUVR is taken into consideration semi-conductor costs would be lower than they are at present as the cost of semi-conductor devices decreases over time [76].

Table 4-3: Cost-Benefit Analysis

Proposed Method	Cost of Transformer Replacement (£1,000)		Cost of Cable Replacement (£1,000)		Cost of Converters (£1,000)		Total Cost (£1,000)	
	Min	Max	Min	Max	Min	Max	Min	Max
PUVR Method	13.8	69.2	-	-	622	1,336	635.8	1,405
Cable Replacement Method	-	-	169.7	476.6	-	-	169.7	476.6

4. 2. 4. Summary

It was found that using off-the-shelf inverter units, PUVR is not as cost-effective as network reinforcement i.e. replacing the LV distribution cables. It is expected, however, that future decreases in semi-conductor costs and bulk orders will bring the cost to a comparable level with the cable replacement method.

4. 3. Chapter Summary

Issues of cost and efficiency were investigated in this section. Results found that for PUVR to be considered viable the efficiency of the converter units in each home must have a maximum lower limit of 93.3% efficiency and the cost per unit must inexpensive and estimated to be between £460-£2100. These limits at the very least provided on-par results with traditional network reinforcement.

Therefore an evaluation of AC-AC converter architectures can be undertaken with these limits as important selection criteria.

CHAPTER 5

5. An Evaluation of Converter Architectures

Increasing the voltage of the distribution network was established in Chapter 3. to be a viable method of increasing the capacity of the LV network. Chapter 4. then established that if a power electronic converter was used to buck the network voltage to a usable $230V_{AC}$ phase, the converter must be cost effective and highly efficient. This Chapter will evaluate two converter architectures in detail according to these criteria the back-to-back inverter and the AC chopper.

5. 1. Methodology

In order to evaluate the two topologies a design of both topologies was undertaken. Design parameters were simply to receive a $345V_{AC}$ phase voltage and convert this to a $230V_{AC}$ phase voltage with identical frequency. Section 5.2 and 5.3 describe the design process for the AC chopper and back-to-back inverter respectively.

Once designed, the two topologies were simulated using Matlab Simulink and a comparison made which forms the basis of an evaluation that determines the more suitable topology for use with PUVR.

5. 2. AC Chopper

The AC Chopper, which is a variant of the matrix converter architecture, is described in detail in Section 2. 4. This section will use the information described to design an AC Chopper circuit.

5. 2. 1. Design

The sections to be designed for the AC Chopper are the input and output filters and the switching frequency.

5. 2. 1. 1. First Order Low Pass Filter Design

The cut-off frequency of the filter was chosen to be 75Hz as this is between the fundamental and second harmonic frequencies ensuring the 3rd harmonic is filtered.

This is represented in angular frequency by ω_n=471rads^{-1} and using an average household load of R=53Ω (taken from the earlier 3 bedroom household consumption average of 1kW as described in Section 3. 1. 1. 1.) using Equation 7 the value for L was calculated to be 112.5mH.

A filter with this cut-off frequency is able to filter the high frequency harmonics of the switching and additionally filter lower frequency harmonics due to non-linear loading, which typically are at odd multiples of the fundamental [77].

5. 2. 1. 2. Second Order Low Pass Filter Design

Using Equations 9 and 10 with values R=53Ω, ω_n=471rads^{-1} and ξ=1 using the values for L and C were calculated to be: L=225mH and C=20μF.

The second order filter was found to have improved performance as, post cut-off frequency, the first order filter has a slope of 19.2dB/decade and the second order filter has a slope of 37.3dB/decade.

5. 2. 1. 3. Switching Frequency against Harmonic Distortion

In order to optimise the size of the filter an analysis of harmonic distortion and switching frequency for varying filter sizes was carried out. The focus was to minimise harmonic content caused by the introduction of the AC Chopper whilst also trying to minimise filter size. A higher switching frequency will increase the frequency of the harmonics, therefore the size of the filter can decrease [77].

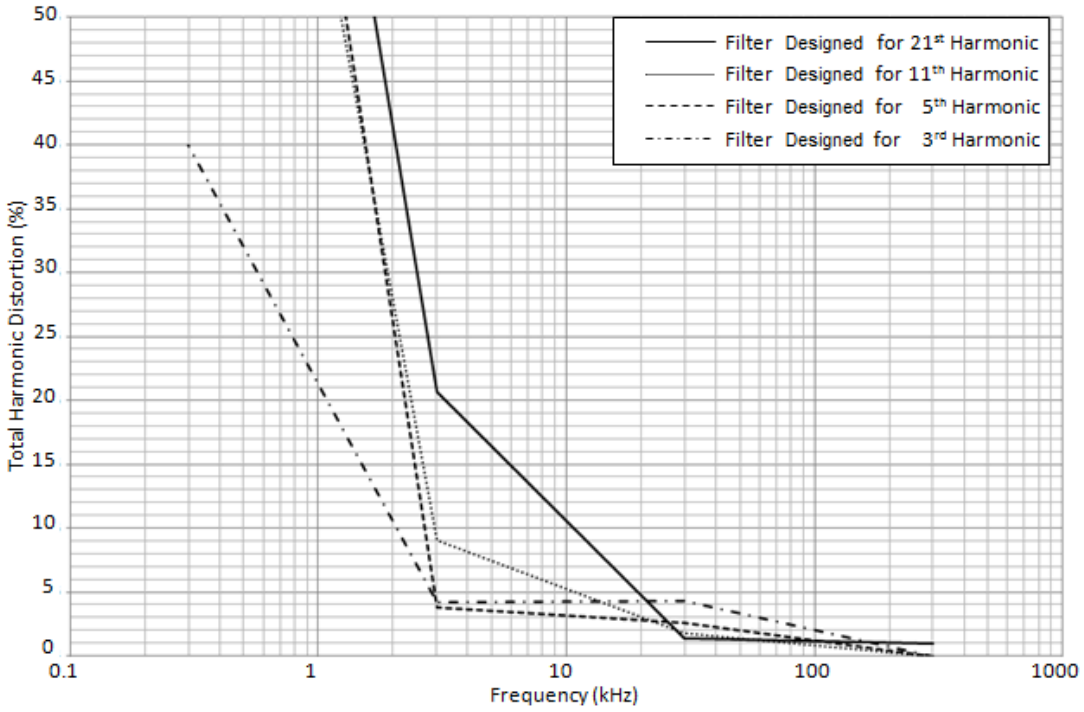

Figure 5-1: THD of Voltage/Current Output for Increasing Switching Frequency for Various Filters (Note that there are 4 data points per filter design)

5. 2. 2. Results

Figure 5-2 shows the initial design of the AC Chopper operating at 10kHz switching frequency and with a first order filter. The final output is a controlled 230V AC waveform at 50Hz shown in Figure 5-3, the output shown is phase-shifted which is the result of filtering.

Figure 5-3 demonstrates the steady state operation of the AC Chopper it is clear that the circuit successfully lowers a voltage of 346V to 230V. A phase shift of 32° between the waveforms can also be observed; this is due to the inductance in the low pass filter. This phase shift is not detrimental to the operation of the circuit.

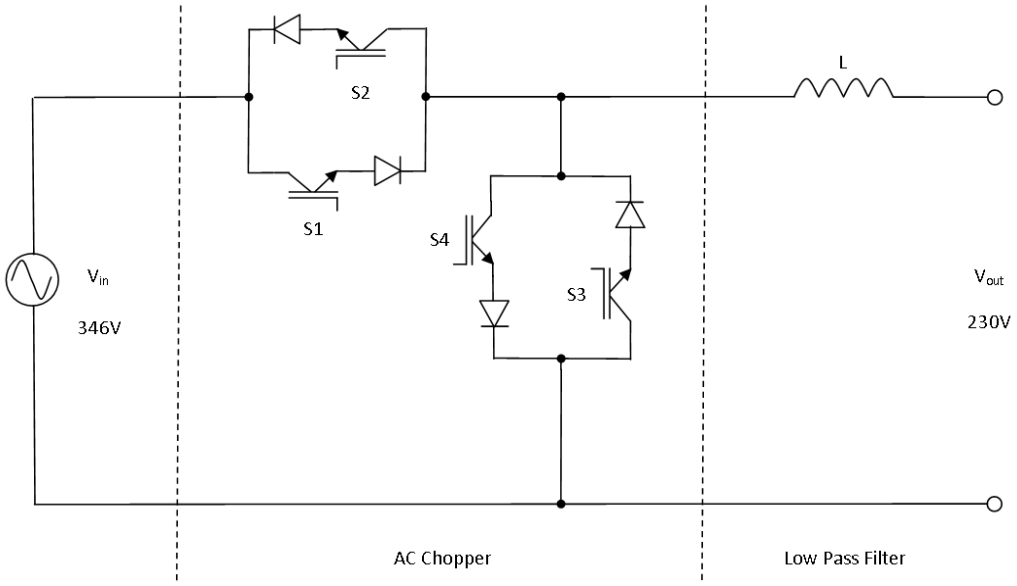

Figure 5-2: Initial Design of AC Chopper, 10kHz Switching Frequency and First Order Low Pass Filter

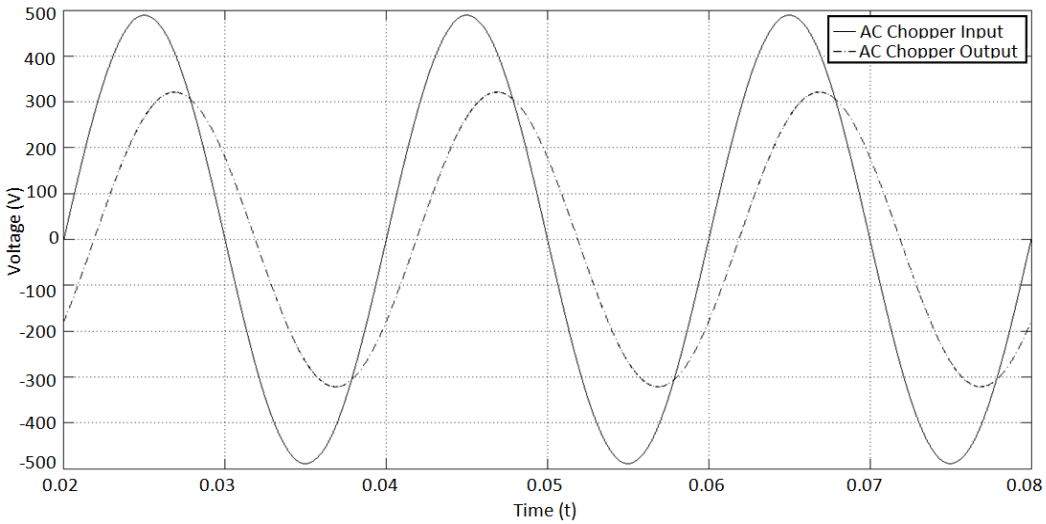

Figure 5-3: Input and Output Voltage Waveforms of Initial AC Chopper Design, Output Phase Shifted by 32°

5. 2. 3. Discussion

While the initial design has been demonstrated as acceptable, it is clear that improvements can be made. A capacitor was added to the design to increase the order of the filter; therefore increasing the response time of the filter and decreasing the magnitude of any passed higher frequencies, see Section 5. 2. 1. 2. Second order filters are also recommended for use in matrix converter circuits [78]. For these reasons second order filters are the design choice for output filter.

A second filter was also found to be required at the input in order to limit the current harmonics injected back into the grid [61].

From the results shown in Figure 5-1 a second order filter designed to filter out the 21st harmonic of the fundamental combined with a switching frequency of 33kHz was chosen.

This allows the use of a small filter without the distortion becoming greater than 5% within the thresholds defined in Section 2. 1. 4. The new value of L_1/L_2 was calculated to be 2mH and the new value of C_1/C_2 is 0.6μF.

It is worth noting that the filters were initially sized to filter low multiples of fundamental frequency, this focus later changed to only filter multiples of high frequency switching harmonics as the filter design while suitable for simulation was found to be unrealistic in practice.

5. 2. 4. Summary

An AC Chopper design has been produced which has two low pass filters of size L_1/L_2 equal to 2mH, C_1/C_2 equal to 0.6μF and a switching speed equal to 30kHz.

5. 3. Back-to-back Inverter

The back-to-back inverter is described in detail in Section 2. 3. This section will use the information described to design a back-to-back inverter.

5. 3. 1. Design

The first step of the design is to determine a suitable switching frequency. Once this has been determined the filters can be sized to appropriately determine a cut-off frequency that limits the generated harmonics.

5. 3. 1. 1. Switching Frequency and Output Filter

In order, to give more comparable results the same switching frequency and filter values of the AC Chopper were used for the back-to-back inverter. These sizes were determined in Section 5. 2. 1.

5. 3. 1. 2. Input Inductance

Where V_1 is the voltage of the primary source at angle δ_1 ($346V_{rms}$), V_2 is the voltage of the secondary source at angle δ_2 ($425V_{rms}$) and X is the reactance of the inductance L (0.02H) multiplied by the angular frequency (100π). Therefore from Equation 4 we can state that the real power bandwidth between the grid and the back-to-back inverter rectification stage is 0-20kW dependant on the phase difference between the two.

5. 3. 1. 3. DC-Link Capacitor

Using Equation 5 with the values T is the fundamental period equal to 20ms, V_{peak} is the highest voltage point equal to 600V, R_{load} is the load resistance equal to 53Ω and desired V_{ripple} equals 10% DC link capacitance required was calculated to be 1.88mF.

5. 3. 2. Results

Figure 5-4 illustrates the input and output voltage from the back-to-back inverter. By inspection of Figure 5-4 it can be seen that the output voltage is shifted by 171° leading.

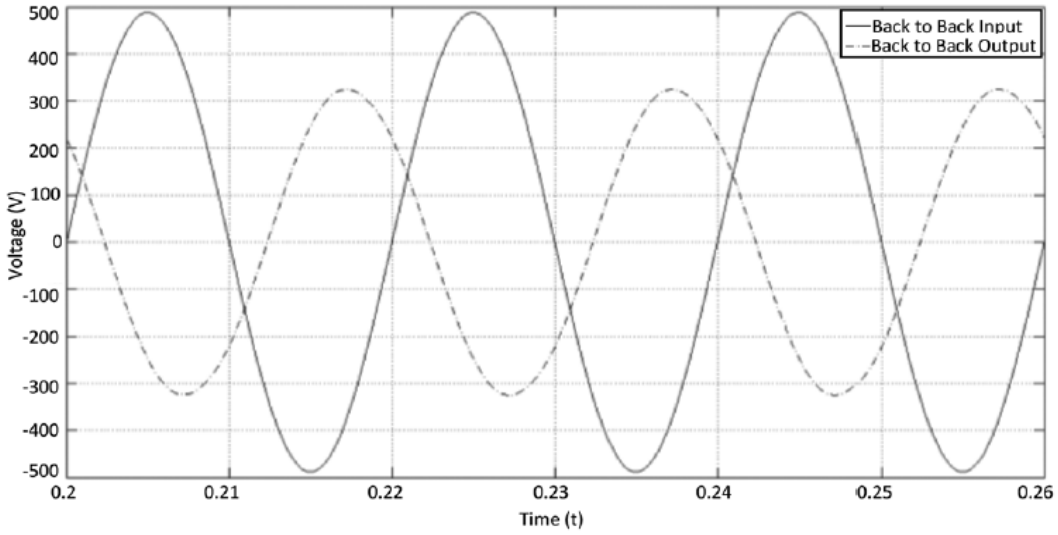

Figure 5-4: Input and Output Voltage of the Back-to-back Converter with 171° Phase Shift

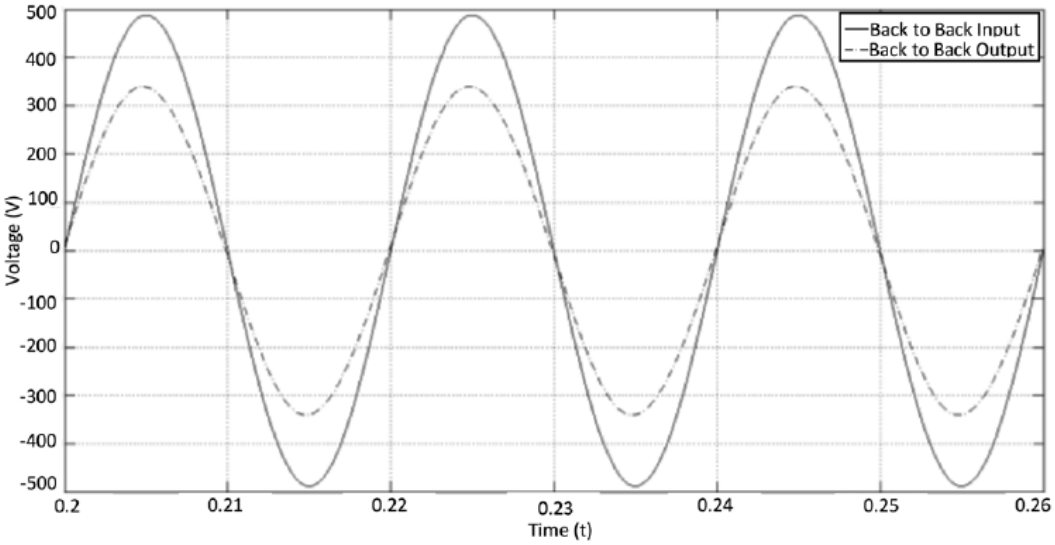

Figure 5-5: Input and Output Voltage of the Back-to-back Converter After Phase Difference Compensation

5. 3. 3. Discussion

The back-to-back inverter deconstructs the voltage into DC. The back-to-back inverter can then synthesise an AC voltage of any phase, magnitude and frequency. Therefore the control of the input and output stage are decoupled. The phase shift can be compensated for in the control, this is shown in Figure 5-5.

5. 3. 4. Summary

A back-to-back inverter has been designed which operates at a switching speed of 30kHz and has input inductance, $L_{1,}$ equal to 20mH, DC-link capacitance, $C_{1,}$ equal to 1.88mF and an output filter, L_2 and C_2, equal to equal to 2mH and 0.6μF respectively.

5. 4. Comparison of Converter Architectures for PUVR

The two topologies presented in the previous section have been tested in simulation and results for their performance in several areas compared. They were compared in the following areas:

- Losses
- Power Quality
- Complexity
- Control
- Transient Behaviour
- Protection

5. 4. 1. Losses

5. 4. 1. 1. Methodology

Calculations were undertaken using the data in the device datasheets [79, 80] and the loss calculation methods used in the relevant literature [53, 81, 82]. The method of calculating loss in semi-conductors was previously described in Section 2. 2.

The switching losses for both of the topologies were calculated, using a switching frequency of 33kHz. The energy loss for each time the devices switched was taken from the device datasheet.

5. 4. 1. 2. Results

Table 5-1: Summary Table of Device Losses; Switching and Conduction

	$P_{conduction}$ (W per arm)		$P_{switching}$ (W per arm)		Total (W)		Total (%)	
	Calc.	PLECS	Calc.	PLECS	Calc.	PLECS	Calc.	PLECS
Back-to-back Inverter	2.01	2.7	10.3	9.3	98.5	96	9.8	9.6
AC Chopper	2.2	3.2	4.5	5.9	27	36.4	2.7	3.6

The results of these calculations are shown in Table 5-1. In order to validate the calculations the back-to-back inverter and AC Chopper were both modelled in PLECs.

The models calculated the conduction and switching losses, with a current profile for each device created from information in the device datasheets [79, 80]. These results indicate that the back-to-back inverter generates approximately 6%-7% more total loss than the AC Chopper.

It is worth noting that the switching losses are quite high due to the fast switching frequency. A reduction in switching frequency from 30kHz will reduce the switching losses at the cost of increased harmonics. The harmonics generated are discussed further in Section 5. 4. 2. 1.

5. 4. 2. Power Quality

5. 4. 2. 1. Total Harmonic Distortion

Two Matlab models using idealised lossless devices were implemented to study the effect of non-linear loads on power quality delivered to the end user. The THD of both topologies was found with a standard linear load of 53Ω. Subsequently both topologies were tested with non-linear loads added in parallel with the linear load. The 5 non-linear loads were a TV, laptop, games console, desktop PC and desktop PC moniter. These were modelled as a diode bridge rectifier attached to a resistance with a parallel capacitance; the value of resistance was calculated using the power draw of these loads. The power draw data was gained from examining the power electronic transformers of these loads (See Appendix B).

Table 5-2: Summary table of THD on both topologies

Device and Configuration	V_{in} THD (%)	I_{in} THD (%)	V_{out} THD (%)	I_{out} THD (%)
AC Chopper (Linear)	0	0.81	0.44	0.44
AC Chopper (Non-Linear)	0	58.9	16.1	58.8
Back-to-back Inverter (Linear)	0	0.29	0.17	0.17
Back-to-back Inverter (Non-Linear)	0	3.05	3.45	69.9

Table 5-2 is a summary of the effects of total harmonic distortion (THD) on both topologies. It was found that adding a switching device would introduce a small amount of THD at each end-user; if PUVR were implemented this would have to consist with industry standards.

It can be observed that the back-to-back inverter has a much lower level of THD at the input when subjected to large non-linear loads. In reality the THD of these non-linear loads is much less, as conducted harmonic emissions are restricted by standards. However for the purposes of this study a worst case scenario has been assumed. The back-to-back inverter topology shows a decrease in harmonic content from the output to the input.

For the back-to-back inverter the initial rectifying stage can be controlled in order to gain the necessary power for the rest of the circuit, for a detailed description see Section 2. 3. 5.

With the DC link capacitor acting as a buffer the source and the load are decoupled, see Section 2. 3. 2. 2. for more detail. Therefore it is reasonable to expect that in terms of power quality the back-to-back inverter will perform better as the AC Chopper has no similar function. For a detail description of AC Chopper control see Section 2. 4. 4.

5. 4. 2. 2. Non-Unity Power Factor Loading

Each topology was examined with a resistive load (R) of 53Ω (see Section 3.1.1) and then subsequently tested with the same resistive load in series with an inductive load (L) of 17.2mH. The value of reactive load was chosen to give a power factor in the region of 0.9.

The effect of reactive loading on the idealised models of both topologies can be seen in Table 5-3. It was observed that under reactive loading the AC Chopper demands the extra 100VAr required for the load directly from the source. In contrast the back-to-back inverter topology requires no additional reactive power from the source. Based on these observations, the back-to-back inverter is the superior topology with regard to power quality as it has been shown to reject load harmonics and load reactive power draw.

Table 5-3: Summary table of power with and without reactive load

	P_{in} (W)	Q_{in} (VAr)	P_{out} (W)	Q_{out}(VAr)
AC Chopper (R)	1,000	15	1,000	0
AC Chopper (R+L)	990	86	990	101
Back-to-back Inverter (R)	997	0	997	0
Back-to-back Inverter (R+L)	988	0	988	101

5. 4. 2. 3. Loading Extremes

Although an average load of 1kW has been assumed, the maximum power that can be drawn in a UK household is 20kW, 90A through a combination of fuses. The result of changing the power drawn is shown in Table 5-4. It was found that the back-to-back inverter delivers better power quality at different extremes of loading. In experiencing greater loads the AC Chopper required more reactive power for its passive filters, which caused a non-unity power factor.

Table 5-4: Power Quality Results from Varying the Load

Power Draw (kW)	Device	P_{in} (kW)	Q_{in} (VAr)	P_{out} (kW)	Q_{out} (VAr)	V_{in} THD (%)	I_{in} THD (%)	V_{out} THD (%)	I_{out} THD (%)
0.1	AC Chopper	0.1	-32.2	0.1	0	0	3.98	0.48	0.48
	Back-to-back Inverter	0.1	-0.2	0.1	0	0	3.12	1.83	1.83
1	AC Chopper	1	15	1	0	0	0.81	0.44	0.44
	Back-to-back Inverter	0.99	0	0.99	0	0	0.29	0.17	0.17
10	AC Chopper	10	1,700	10	0	0	0.77	0.42	0.42
	Back-to-back Inverter	10	-1	9.9	0	0	2.03	0.11	0.11
20	AC Chopper	20	7,100	20	0	0	1.15	0.61	0.61
	Back-to-back Inverter	20	2,480	19.9	0	0	4.98	0.06	0.06

5. 4. 3. Complexity and Cost

5. 4. 3. 1. Methodology

Table 5-5 provides a cost estimate comparison of the two solutions based on the principal components in both converter topologies. The costs are based on the semi-conductors used in Section 5. 4. 1. and includes the costing of the associated power filters required for each topology [83-85].

Table 5-5: AC Chopper and Back-to-back Inverter Primary Components Cost Comparison

	1 Module (£)	Cost to Convert an Urban Area (£)
AC Chopper	520	111,800
Back-to-back Inverter	1,070	228,300

5. 4. 3. 2. Results

Comparing the description of the operation of both devices given in Section 2. 3. and Section 2. 4. , it is clear that the AC Chopper is less complex. From the results in Table 5-5 it is clear that the cost of using the back-to-back converter topology to outfit the physical system described in Chapter 3. is more expensive than outfitting the system with the AC Chopper topology.

5. 4. 4. Control

5. 4. 4. 1. Development and Testing of Controlled AC Chopper

The response of the closed-loop control was tested by applying a load step to the output of the chopper. In order to improve dynamic performance, a closed voltage feedback control loop was placed around the AC Chopper. The closed loop control was tested via demand changes from 0.5kW to 1kW to 2kW and the voltage fluctuations measured.

Figure 5-6 shows that when the load is doubled from 0.5kW to 1kW after 1.35s the chopper output voltage remains at 230V and the current doubles from 2.1A to 4.2A. After 1.55s the load is further doubled to 2kW. The output chopper voltage remains at 230V AC and the current rises to 9A.

In response to the load steps, the output voltage was observed to dip slightly by 1.3V and 1.7V over 0.03 seconds for the first and second load steps respectively, which as a percentage of load is a dip of -0.4% and -0.5%. These dips are caused by the change in load which increases current demand. This results in a voltage dip due to the relationship between voltage and current.

The PI controller then adjusts the PWM of the switches to match the demand. The dips are within the British standards for voltage sag, which is 230V+10%-6% [11].

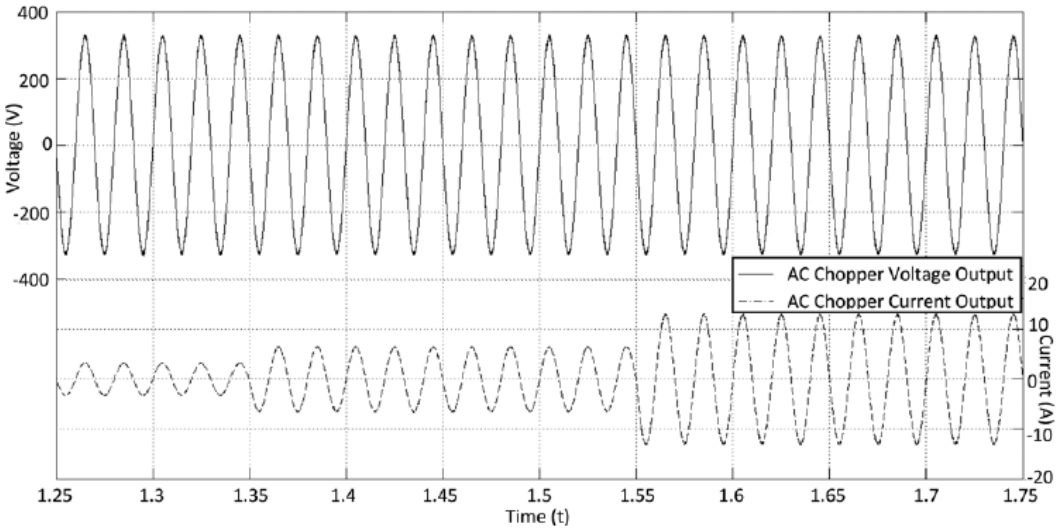

Figure 5-6: Dynamic Response to Step Changes

A block diagram with plant for the AC Chopper is shown in Figure 5-7, with values taken from the filter design section. The closed-loop transfer function was found to be cubic, shown in Equation 17.

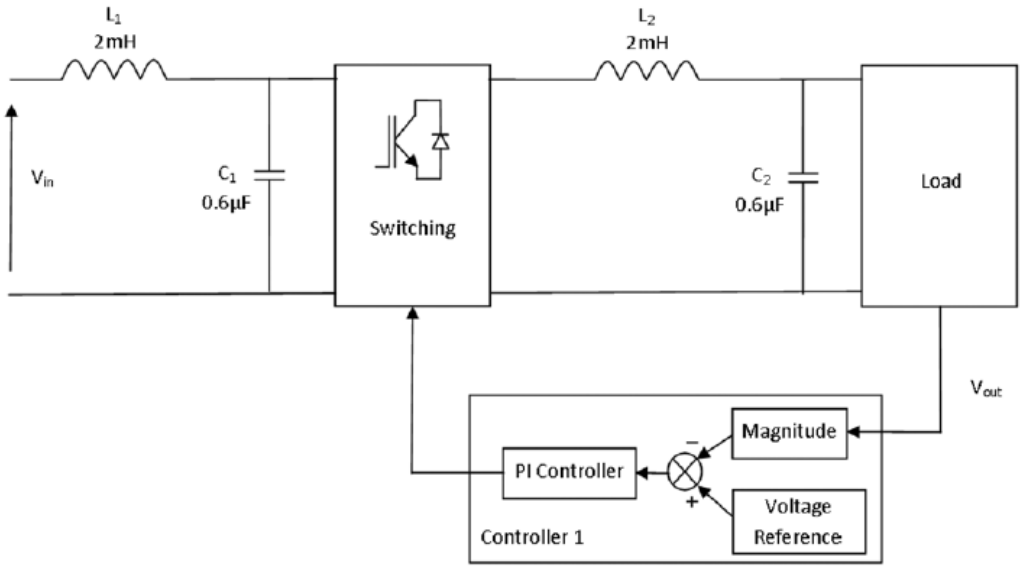

Figure 5-7: AC Chopper Control Block Diagram with Plant

The feedback based control for the AC Chopper has been described in Section 2. 4. 4. In order to tune the third order equation the good gain method was used [86]. Using this method to find approximate values then manual tuning, the ideal values for K_p and K_i were found. See Section 13. Appendix C for all calculated values of controller gain.

17

$$\frac{V_{out}}{V_{in}} = \frac{\frac{K_p}{L_2C_2}s + \frac{K_i}{L_2C_2}}{s^3 + \frac{1}{R_{load}C_2}s^2 + \frac{(K_p+1)}{L_2C_2}s + \frac{K_i}{L_2C_2}}$$

The response of the AC Chopper is shown in Figure 5-8. In order to demonstrate the stability of the controllers the poles of the control loops were plotted in Figure 5-13.

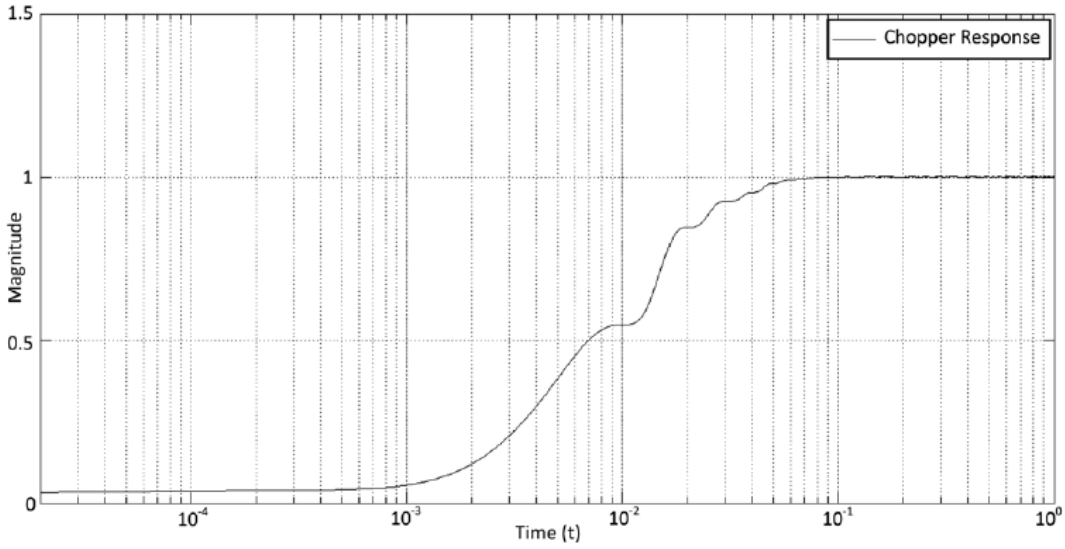

Figure 5-8: Step Response of AC Chopper Feedback Transfer Function

5. 4. 4. 2. Development and Testing of Controlled Back-to-back Inverter

The response of the closed-loop control was tested by applying a load step to the output of the back-to-back inverter. In order to improve dynamic performance, a closed voltage feedback control loop was placed around the load of the back-to-back inverter.

Controller 1 was tested using the same means as the AC Chopper, demand changes from 0.5kW to 1kW to 2kW and the voltage fluctuations measured.

The results are shown in Figure 5-9. It is observed that the back-to-back inverter can supply the load with a steady 230V AC at the different loads. In response to the load steps, the output voltage was observed to dip slightly by 1.9V and 2.1V over 0.03 seconds for the first and second load steps respectively, which as a percentage of load is a dip of -0.6% and -0.65%; this is within the British standards for voltage sag, which is 230V+10%-6% [11].

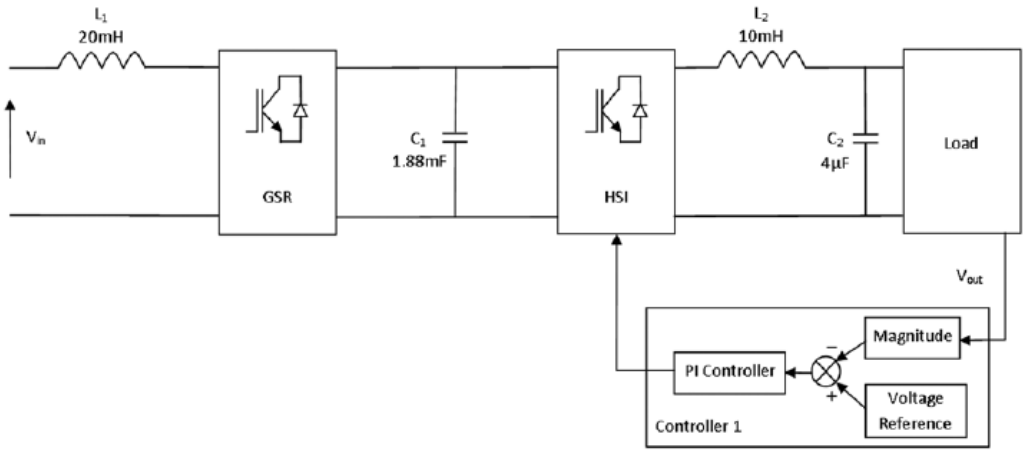

Figure 5-9: Back-to-back Inverter Controller 1 Block Diagram with Plant

It can be observed that the inversion stage of the back-to-back inverter in Figure 5-9 is identical to the output of the AC Chopper in Figure 5-7 but with different values of L_2 and C_2. Therefore Equation 17 can be used to describe the control of the inversion stage.

In order to control the power flow into the back-to-back inverter from the distribution grid, an additional control loop is required at the grid side rectifier (GSR) as shown as Controller 2 in Figure 5-10.

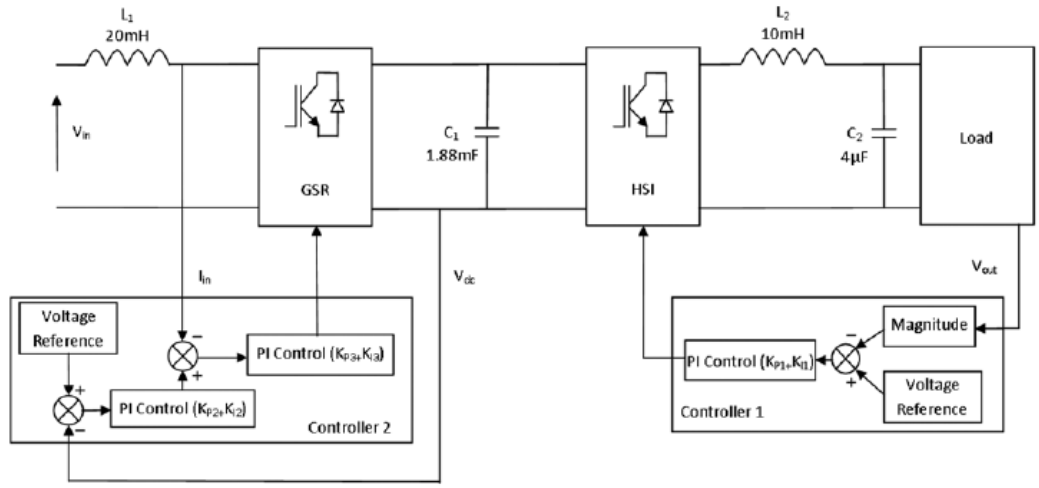

Figure 5-10: Back-to-back Inverter Controller 2 Block Diagram with Plant

The cascading feedback based control for the back-to-back inverter rectification stage has been described in Section 2. 3. 5. 2. From this section and the loop described in Figure 2-7 two equations can be derived which describe the outer loop and the inner loop.

These are Equation 18 for the outer loop and Equation 19 for the inner loop (where R is a small line resistance of 1mΩ). Using these two equations the controller gain vales were calculated. Appendix C catalogues the calculated values of controller gain.

The step response for Equations 17, 18 and 19 is shown in Figure 5-11. This demonstrates the speed of the controllers to be sufficiently different, to allow them to be considered decoupled from each other.

It was found that these calculated values had an overshoot response despite being tuned for over-damping (ξ=1), this is due to the ignored differential term in the numerator of Equation 18 and Equation 19. Controller 2 was manually tuned by increasing K_{p2} and $K_{p3,}$ the result of this is shown in Figure 5-12. The final control values are catalogued in 14. Appendix D.

In order to demonstrate the stability of the controllers the poles of the control loops were plotted in Figure 5-13.

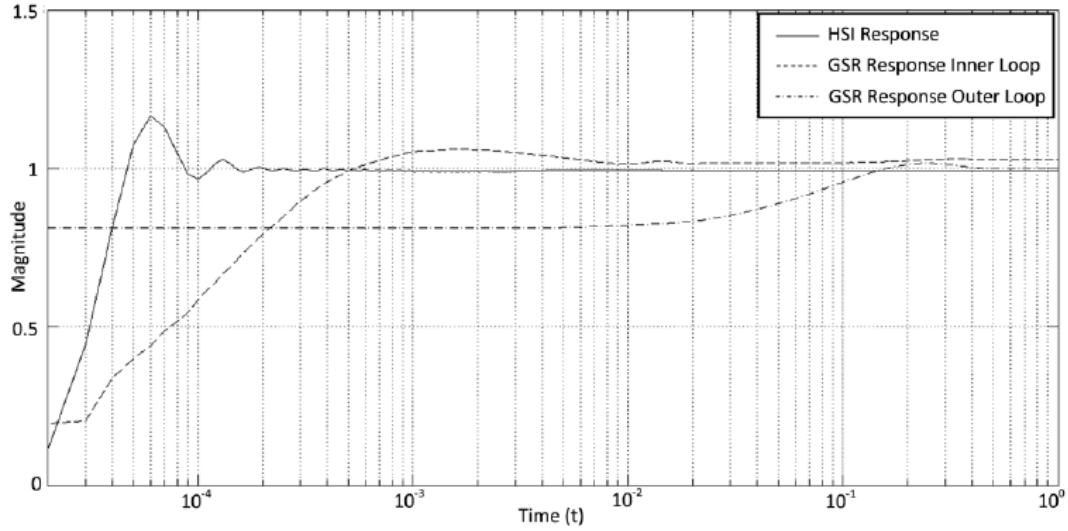

Figure 5-11: Step Response of Back-to-back Inverter Feedback Transfer Function with Calculated Gain Values

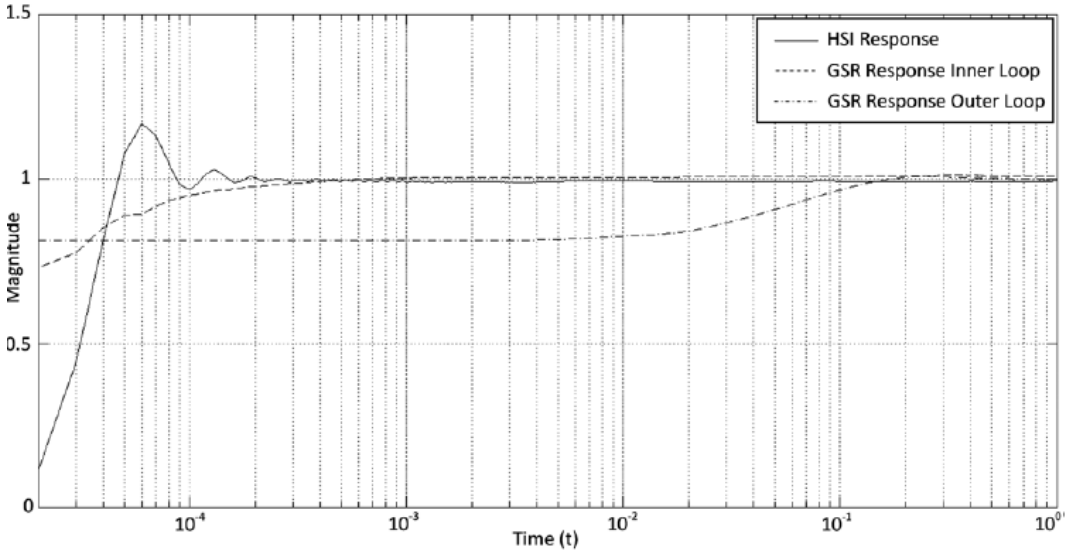

Figure 5-12: Step Response of Back-to-back Inverter Feedback Transfer Function with Manually Tuned Gain Values

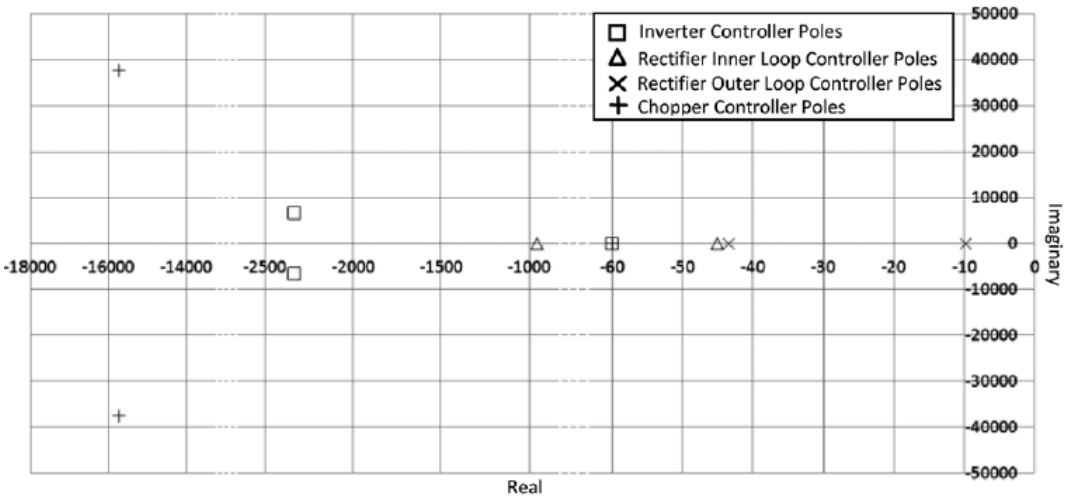

Figure 5-13: Poles and Zero of the AC Chopper and Back-to-back Inverter

18

$$\frac{V_{out}}{V_{in}} = \frac{\frac{K_{i2}}{C_1}}{s^2 + \frac{K_{p2}}{C_1}s + \frac{K_{i2}}{C_1}}$$

19

$$\frac{V_{out}}{V_{in}} = \frac{\frac{K_{i3}}{L_1}}{s^2 + \frac{(R + K_{p3})}{L_1}s + \frac{K_{i3}}{L_1}}$$

5. 4. 5. Transient Behaviour

The time taken to reach steady-state was found to be 0.1s for the back-to-back inverter compared to 0.05s for the AC Chopper shown in Figure 5-8 and Figure 5-12. Both topologies are sufficiently fast.

5. 4. 6. Protection

The proposed converter location is shown in Figure 5-14. To ensure that the breaker on the main feeder does not activate in case of a fault on the converter hardware, the converter must be placed after the fuses on the distribution network. This will prevent a fault in any single converter causing a trip that affects other customers.

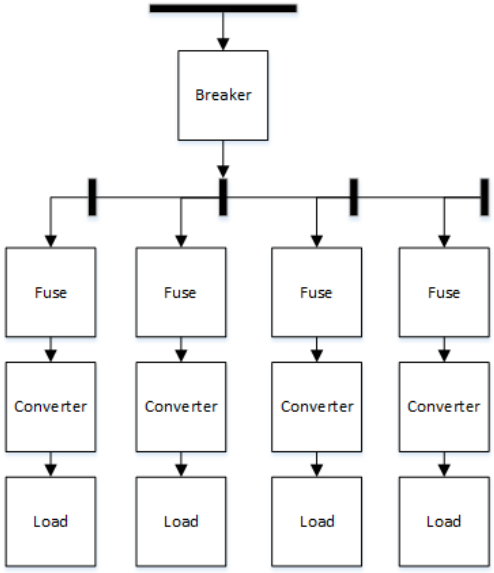

Figure 5-14: Proposed Converter Location

However this means that any present protection system must be rated higher than 346V phase, otherwise it must be replaced. This will not be problematic as British Standards fuses have a voltage rating of up to 1kV line AC [87].

A standard 3 bedroom home will have a series of fuses with upstream reclose devices on the main feeder or breakers on the local transformer [88].

Increasing the power density in the network increases the fault level substantially, consider a short circuit across the load of 0.1Ω and Equation 20 [89].

20 $$P_f = \frac{V_{rms}^2}{R_f}$$

With the present system where V_{rms}=230V the resulting fault level, P_f, is equal to 0.53MW. With V_{rms}=346V the resulting fault level is 1.2MW, an increase of 0.7MW. Therefore both converter types share this common disadvantage. However if the installation follows IET wiring standards, which considers low voltage to be under $1kV_{3ph}$ or $600V_{ph}$, there will be no comprise to safety by increasing the voltage [90].

5. 5. Discussion

It was found that the AC Chopper produces 6%-7% less total power loss through modelling validated through calculation. Converter losses have been previously discussed in Section 4. 1. 3. and must be as low as possible for PUVR to be considered viable. The minimum efficiency value required was found to be 93.3%, comparing the efficiency values gained of 90.2%-90.4% for the back-to-back inverter and 96.4%-97.3% for the AC Chopper; it is clear that the AC Chopper is the better choice of architecture in terms of losses.

It is worth noting that the initial rectification stage can only 'boost' the V_{DC}, therefore the voltage is not able to go below the peak V_{IN} of 490V. This means the modulation index of the inverter stage will be low and this will lead to more loss in the switching of the inverter stage [91].

The power quality of the two architectures was assessed through three tests on the Matlab simulations. The first test evaluated the THD generation of the converters and how they interact with non-linear loads. The tests found that each device generates an acceptably low level of THD.

However the back-to-back converter architecture was demonstrated to have a superior interaction with non-linear loads as much of the high magnitude, low order harmonic currents were not passed through the converter. This is due to the decoupling of the back-to-back inverters conversion stages as described in Section 2. 3.

The second test evaluated a non-unity power factored load; the results showed that the back-to-back inverter had a superior interaction as again the conversion stages are decoupled allowing the inverter to supply a load that has a non-unity power factor without affecting the power factor of the rectifier.

The final test evaluated the converters under the maximum possible load of a UK household 20kW. The results found that both converters perform within standards for the full operating range of the converter. However at maximum operating point the power factor of the converters drop to 0.94 lagging for the AC Chopper and 0.99 lagging for the back-to-back inverter.

This is still within UK standards of power factor and any household is rarely going to reach maximum power draw. However it is worth noting that the back-to-back inverter generates less reactive power and that smaller filters may be required for the AC Chopper.

It is also worth noting that radiated electromagnetic interference (EMI) is a problem associated with the use of power electronics. However at these power levels well established rules for enclosures, connection layout and semi-conductor gate drive devices can be used to ensure EMI is minimised [77].

From the results shown Table 5-5 in the cost reduction in using the AC Chopper over the back-to-back inverter will make PUVR more viable in terms of cost benefit.

The control of both topologies was found to perform well within industry standards for voltage fluctuation and the topologies were both found to be sufficienctly fast. However the control of the back-to-back converter was found to be more complex with a second controlled required that incorporates a cascaded PI control.

Neither converter has any significant advantage in protection nor were any protection issues found as the IET wiring regulations define LV equipment as 1kV or lower and the end-user shall still receive $230V_{AC}$ phase.

It is also worth noting from a reliability perspective that the large storage device required for the back-to-back inverter will dramatically increase required maintenance and device failure rates [54]. The AC Chopper does not require this large capacitance.

In addition, if PUVR is implemented, household protection would need to be modified. Miniature Circuit Breakers (MCBs) and fuses presently operate for a specified amount of current; if the amount of current the end-user can access is increased it follows that household protection systems will need to account for this increase.

5. 6. Chapter Summary

Of the two possible system architectures considered, it is clear that an AC Chopper architecture has several advantages over a back-to-back inverter system. The AC Chopper was found to generate less loss, cost less to build, require smaller filters and have simple control. Cost and efficiency was found in Section 4. 1. 3. to be the most important factors in implementing PUVR.

However, the back-to-back inverter was found to be better in maintaining power quality seen by both the grid and consumer. The AC Chopper is not decoupled from the grid, there is no intermediary buffer, and power quality suffers as a result.

If the AC Chopper could improve the power quality seen by the end-user it would make it comparable to the back-to-back inverter but without the problems found with the back-to-back inverter architecture.

CHAPTER 6

6. Practical Implementation

On order to be able to fully justify the simulated results, a physical demonstration of the AC Chopper circuit must be produced. This will validate the simulated results recorded in Chapter 5.

In this Chapter a full description of all equipment will then be provided followed by a methodology describing how this equipment was used in order to implement an AC Chopper circuit. The results recorded from the circuit will then be shown numerically and graphically. The results will then be considered and compare to simulated results.

Subsequent to this a second architecture will be introduced, the AC Chopper and Auto-Transformer Hybrid. Any additional equipment used and how this circuit is implemented will be described. Results from this circuit architecture will then be presented followed by a discussion of the gained results and their relevance compared to results from Chapter 5. Finally a section will summarise the main points of interest that can be taken from this work.

It is worth stating that size of converter is considered beyond the scope of this thesis. It is desirable to keep converter size to a minimum, if the converter is to be installed in the household. If the converter is placed outside the household in an IP rated box there are less size restrictions, however this may require trench work adjacent to the consumer household. Clearly this is not a trivial matter and therefore should be researched thoroughly before an implementation strategy is decided upon.

6. 1. AC Chopper Circuit

This section will describe the equipment used in the AC Chopper circuit and how the equipment was implemented in order to produce the circuit. A circuit diagram of the practical AC Chopper circuit is shown in Figure 6-1. The difference between this circuit and the AC Chopper modelled in Chapter 5. is the inclusion of filter resistances, non-ideal switching and a 1:2 ratio transformer which doubles the input voltage of the circuit from $230V_{AC}$ to $460V_{AC}$.

In practice it was also required to redesign the IGBTs and more efficiency higher rated IGBTs have been used for the practical implementation than in Chapter 5.

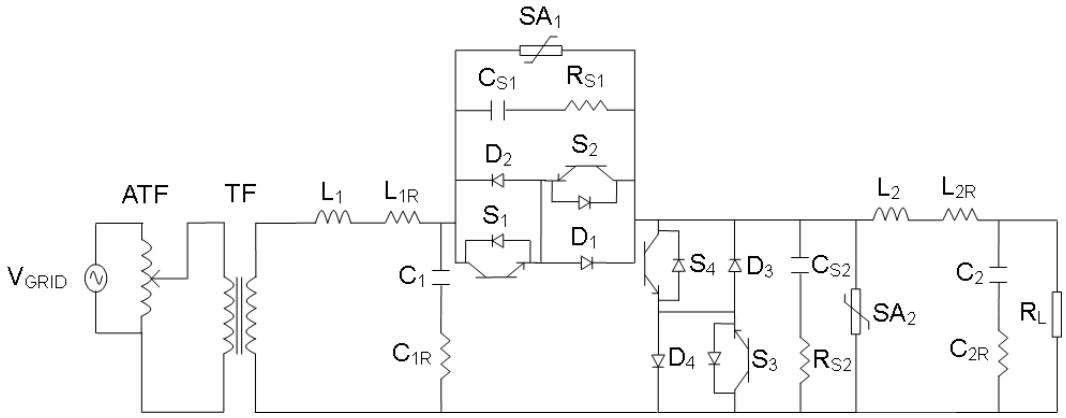

Figure 6-1: Practical AC Chopper Circuit Diagram

6. 1. 1. Equipment

A description of each element in the practical circuit including the function of the equipment, how it operates and why this equipment is necessary.

6. 1. 1. 1. Isolating Transformers

Isolating transformers are simply standard 1:1 ratio transformers used for galvanic isolation of circuits. With galvanic isolation circuits become electrically separate; this in-turn has two beneficial effects. Separation of circuits allows for testing of the prototype and any accidents which occur will trip the fuse of the isolating transformer rather than a breaker further upstream.

Electrical isolation also limits the effect of noise generated by switching operations on the very sensitive measurement units, microcontroller and control circuits. Therefore the main electricity supply to the circuit was isolated via a grey 2kVA. Control elements of the circuit were also electrically isolated via smaller isolating transformers with smaller ratings; a blue 750VA isolating transformer A second yellow 750VA isolating transformer was used to isolate the supply to the microcontroller.

The supply isolation transformer would not be necessary if this circuit were to be used in a real system. Controller power would likely be provided using an isolated AC-DC converter stage which is standard for many power electronic systems.

6. 1. 1. 2. Variac (Auto-transformer)

A single auto-transformer was connected to the isolating transformer in order to supply electricity to the AC Chopper, shown diagrammatically in Figure 6-1 as component ATF. This allowed gradual testing and aided in the debugging of the chopper circuit. This also allowed the switching arrangement to be operated at different power levels allowing an efficiency curve to recorded, see Section 6. 3. The auto-transformer rated steady state values are 230V and 6A.

If implemented in a product for use outside laboratory confirnes this step would not be necessary as a varied voltage input for experimental testing is not necessary.

6. 1. 1. 3. Transformer

As the voltage rating of the auto-transformer is only $230V_{AC}$ (phase to ground), a 1:2 ratio transformer was required in order to double the voltage to an appropriate level shown diagrammatically in Figure 6-1 as component TF. This allowed a maximum voltage of 460V to be reached at the input appropriate for testing the AC Chopper which shall reduce any input voltage to $230V_{ac}$. The transformer used in the experiments has a power rating of 4kVA.

This transformation stage would not be necessary in the real system as input (phase to ground) voltage of the real system would already be above $230V_{AC}$.

6. 1. 1. 4. Measurement Units

In order to record results measurement units must be utilised. In this case voltage, current, power factor, voltage output total harmonic distortion, input current total harmonic distortion was measured by Voltec PM100 single phase power analysers at the input to the circuit, after the filters, after the switching arrangement and at the output stage. Therefore power loss at all stages can be measured.

A long averaging function built into the analysers was used to record the measurements in order to increase the accuracy of results which may be distorted.

Waveforms of voltage and current were recorded using voltage/current transducers and oscilloscopes.

Although care was taken to remove noise from the measurements by using isolating transformers to supply the mains to these devices, there is background noise in the system from switching operations which was not possible to completely eliminate.

In a real system these measurements would not be necessary as there is no requirement in the distribution system to measure properties of the electricity at the loading point of the distribution network.

6. 1. 1. 5. Input Filter

As discussed in Sections 2. 3. 2. low pass filtering is required in order for the switching arrangement to operate within the harmonic limits presented in Section 2. 1. The size of filter used within the modelling is also described in these sections.

The input filter is shown diagrammatically in Figure 6-1 as components L1, C1 with resistances $L1_R$, $C1_R$. The values of these components are 3mH and 4x470nF (1.88µF in parallel), however the measured value of these components are 2.79mH and 1.8µF respectively. The ratings of these components are a steady state current of 10A though the inductance and 1kV across the capacitors.

6. 1. 1. 6. Switching Arrangement

The AC Chopper circuit is described in detail in Section 2. 4. The circuit produced to gain experimental results is presented in Figure 6-2. In Figure 6-2 the individual IGBTs, diodes, driver circuits, snubbers and varistors are shown.

It is also worth noting that the heat sink used is overrated to provide a safety margin during testing and could be redesigned to reduce the converter volume and mass.

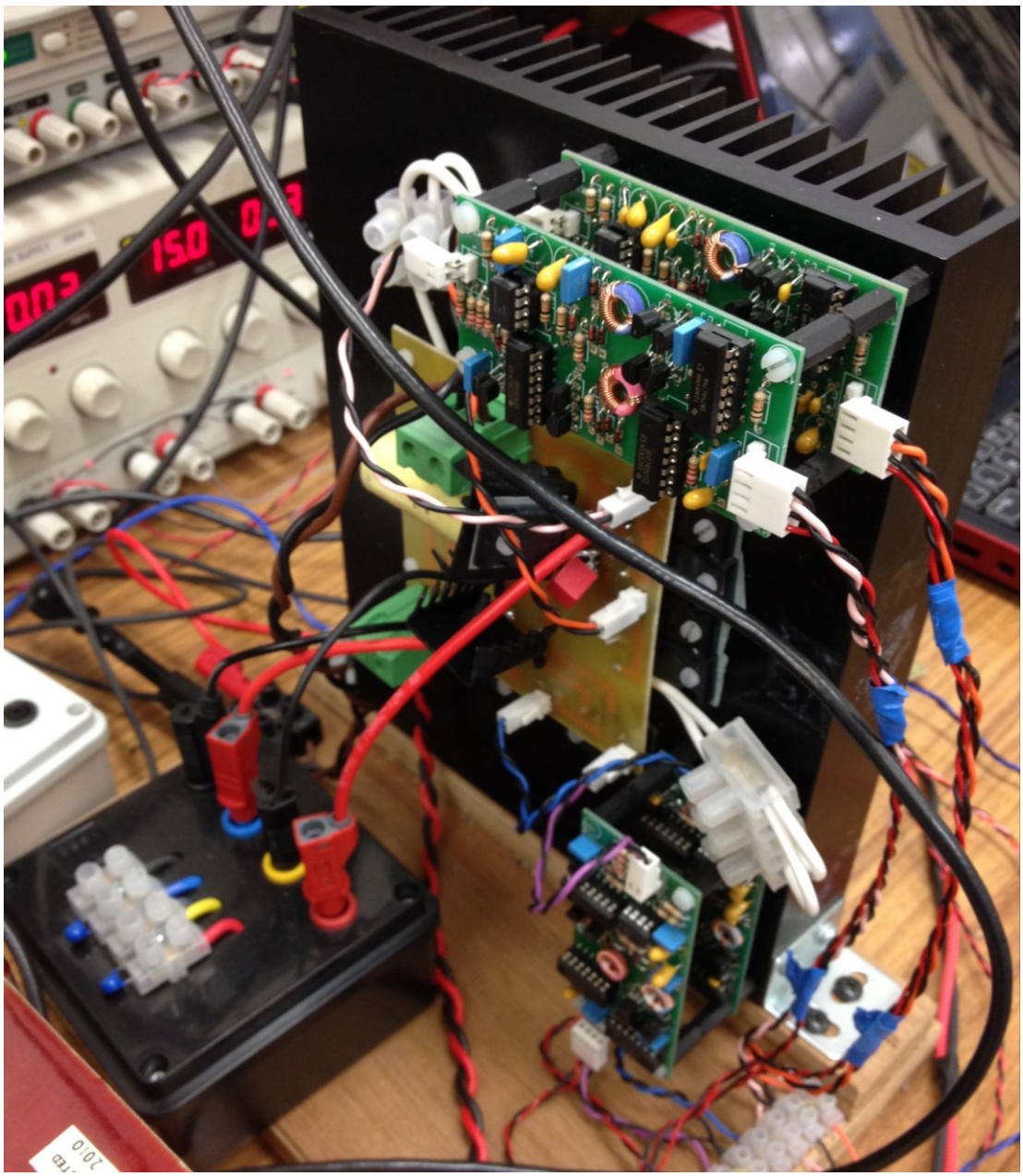

Figure 6-2: Practical AC Chopper circuit

6. 1. 1. 7. IGBTs

The discrete Insulated Gate Bipolar Transistors (IGBTs) that were used to demonstrate the AC Chopper circuit are International Rectifier IRG7PH50UPbF and they are shown in Figure 6-2 and shown diagrammatically in Figure 6-1 as components S1-S4. These IGBTs in particular were chosen due to their high collector-to-emitter voltage of 1.2kV, low losses and high quality load current vs frequency characteristic.

At first glance a collector emitter voltage of 1.2kV may seem inappropriate for an input voltage of $345V_{AC}$, however when considering that the peak of this voltage would be $488V_{peak}$ and that the voltage may overshoot during switching a 600V device does not offer enough headroom to be considered robust.

The voltage across the collector emitter when switched on is 1.7V-2.1V dependant on junction temperature (lower temperature equates to smaller voltage). The device also turns on and off very quickly with a maximum turn on time of 115ns (turn on time plus rise time), and a maximum turn off time of 710ns (turn off time plus fall time).

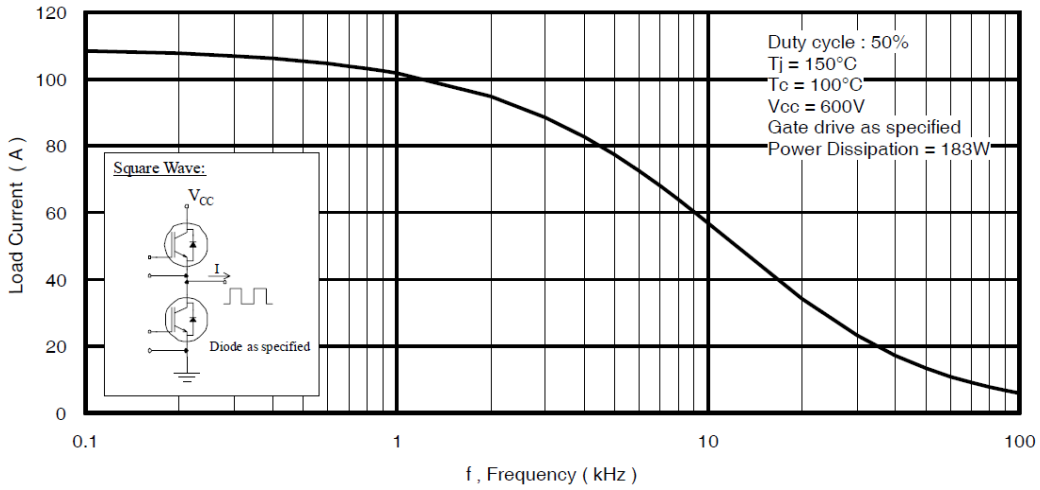

Figure 6-3: Typical Load Current vs Frequency [92]

The load current vs frequency characteristics of this IGBT are shown in Figure 6-3. From this graph the maximum load current can be observed for a given switching frequency. Some results are shown in Table 6-1. Note that 90A is the maximum household power draw and that 10kHz and 30kHz are switching frequencies used in simulations or experiments throughout this thesis. For a 1kW demonstration prototype these IGBTs are more than sufficient.

Table 6-1: Combinations of switching frequency and load current

Switching Frequency	Load Current (Approximate)
1kHz	90A
10kHz	55A
30kHz	22A

6. 1. 1. 8. Diodes

The discrete diodes are Fairchild Semiconductor RHRG75120, also shown in Figure 6-2 and shown diagrammatically in Figure 6-1 as components D1-D4. They have blocking voltage of 1.2kV; this is in line with the IGBT collector-emitter voltage when turned off. The reasoning behind this relatively high blocking voltage is also described in Chapter 6. 1. 1. 7. These diodes also support a high forward current of 75A and can recover very quickly under this current, in 100ns [79]. The voltage over the device when on is also low at from 2.6-3.2V dependant on junction temperature.

6. 1. 1. 9. Snubber Circuit

Snubbers allow high frequency transient currents to bypass the IGBT and diode bridge these are shown diagrammatically in Figure 6-1 as components C_{S1}, C_{S2}, R_{S1}, R_{S2}. This in turn causes switching to be smoother and reduced stressed on power electronic devices increasing reliability [53], however this comes at the cost of power losses.

The prototype circuit is made out of discrete components with a relatively large electrical distance between them compared to a surface mount or packaged circuit. Therefore parasitic (or stray) inductance will be greater in this prototype circuit than in any finished product as conductors will always have intrinsic inductive and capacitive components and greater conductor length will directly increase the intrinsic inductive component associated with it [10]. Therefore a snubber circuit was used in this prototype to limit the effects of parasitic inductance however it may not be necessary in a refined circuit.

Section 2. 3. 6. describes the sizing of the capacitor and resistor used in the snubber; the snubbers used can be observed in Figure 6-2 as small red squares. They have a size of 2.2 μF and 4.7 ohms.

Theoretical values for the snubber size were calculated in Section 2. 3. 6. However as the prototyping process is circular, these values were later re-determined as other constraints became apparent; this is further discussed in Section 6. 1. 2. 6.

6. 1. 1. 10. Surge Protection

In the AC Chopper architecture there is the possibility of incorrect commutation which may result in interruption of the current path with no alternative current path for the output inductive element. This could result in failure without surge protection.

The varistors are shown diagrammatically in Figure 6-1 as components SA_1, SA_2. The need for varistors is due to inductance in the circuit, any sudden changes in current may damage the IGBTs and diodes in the circuit. This is due to the well-known relationship between inductance and rate of change of current defined in Equation 21.

21
$$V_{drop} = L \times \frac{di}{dt}$$

It is possible to circumvent these extremely large transient voltages via use of surge arrestors i.e. varistors. The varistors used in the circuit can be seen in Figure 6-2 and they have a breakdown voltage of 1kV. This limit is below the maximum operating voltage of the IGBTs but is well above the expected operating voltage.

Varistors have a low resistance at a high voltage; therefore in this case if a voltage of 1kV is applied over the varistors, the varistors will become very conductive and shunt the current away from the relevant component(s) protecting them from damage. The high current due to the high conductivity will also clamp the voltage over the IGBT to 1kV [93].

6. 1. 1. 11. Output Filter

In order for the output of the switching arrangement to be useable, any high frequency components must be filtered out of the waveform. This is part of the regulations of the UK grid described in Section 2. 1. 4. Therefore a low pass filter is required at the output of the switching arrangement; how a low pass filter is designed is described in Section 2. 3. 2. 4.

For the practical implementation the AC Chopper, the output filter is shown diagrammatically in Figure 6-1 as components L2, C2 with resistances $L2_R$, $C2_R$. The inductance has a value of 10mH and a measured value of 7mH.It also has a current rating of 30A steady-state, and therefore it is over-rated for the purposes of this experiment, however it is not expected that this will affect the experimental results in any way.

The capacitor used in the output filter has a value of 0.47μF and a measured value of 0.45μF. It has a voltage rating of 1kV.

6. 1. 1. 12. Test Loads

Three household loads were simulated in the experiments, these are:
Firstly, a unity power factored load i.e. a load that is purely resistive and linear such as heating elements. They are represented diagrammatically in Figure 6-1 as component R_L. For the unity power factor tests a resistance of 44Ω was used, as this was the closest value available to a 230V, 1kW load.
Secondly, a non-unity power factored load i.e. a load that is resistive and inductive but still behaves linearly such as a washing machine. These loads have a value of 20mH, 20mH and 10mH; these are place in series with a resistive load of 17.7Ω to create a non-unity power factored load of 0.75.
Finally, a non-linear load was tested. These types of load are named as such as they do not vary voltage with current in a linear fashion and are, most commonly, loads based on semi-conductor technology. A standard 800W microwave found commonly in the modern UK household was used.
More information on the types of loads used in UK households is available in Section 2. 5. 2.

6. 1. 2. Methodology

This Methodology describes in detail how the equipment described in Section 6. 1. 1. was used in order to produce the practical circuit.

6. 1. 2. 1. Semi-Soft Switching

There are various methods in switching the four semi-conductors in the matrix converter circuit [61]. The method used in this practical implementation is the four-steps commutated semi soft-switching method. This will give 50% less switching loss than hard switching the device [61]; a two-steps commutated method is also possible, but requires a more elaborate zero-crossing detection method involving intelligent gate drives [61]. The zero crossing detection method used is discussed in Section 6. 1. 2. 2. and the methods available discussed in Section 2. 4. 4. 4.

In order to correctly use this method information is required on the input current waveform. The microcontroller which controls the switch must be aware of the current direction of electric current drawn from the grid.

6. 1. 2. 2. Zero-Crossing Detection

The direction of the input current to the AC Chopper is measured by a current transducer at the input to the device; this isolated the control circuit from the main circuit and outputted a representative voltage measurement which was then passed to a comparator circuit.

The comparator essentially generates a square voltage waveform from the voltage outputted from the current transducer that is based on whether the current direction is positive or negative.

This square voltage waveform is then passed to a buffer circuit which makes the square wave compatible with the microcontroller input/output (IO) pins. This information then informs the microcontroller about whether the current is positive or negative and therefore the correct commutation mode is chosen. This process is shown in Figure 6-4 and how the microcontroller detects the current direction change and implements the soft-switching algorithms is described in Section 6. 1. 2. 1.

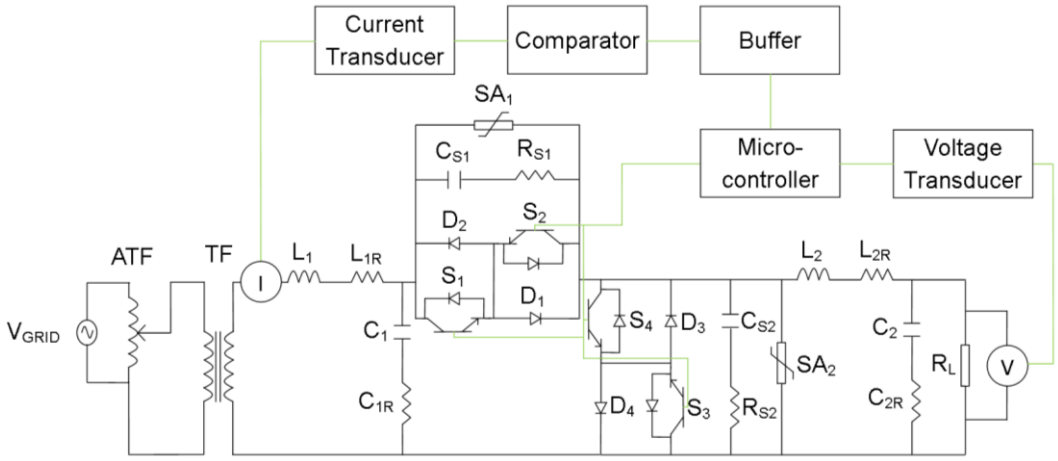

Figure 6-4: AC Chopper with Control Stages Circuit Diagram

6. 1. 2. 3. Closed Loop Control

It can be observed from Figure 6-4 that a voltage transducer measures the output voltage across the load. The transducer isolates the control circuit from the main circuit and outputs a representative voltage waveform that is compatible with the analogue-to-digital (ADC) of the microcontroller.

This information was then used to modify the duty cycle of the switches to keep the voltage over the load at a constant 230V. The theory of how to design a closed loop control of an AC Chopper circuit is fully described in Section 2. 4. 4. and Section 5. 4. 4. 1. How the microcontroller processes the information and modifies the duty cycle is described in Section 6. 1. 2. 4.

6. 1. 2. 4. Microcontroller

The microcontroller used for the practical experiment was the Texas Instruments TMS320 F2833, and the program was coded in C++. A flowchart for the program is shown in Figure 6-5 and from this it can be observed that it is necessary to understand the following parts of the microcontroller.

- Pulse-Width Modulation (PWM)
- General Purpose Input and Output (GPIO)
- Interrupts
- Analogue-to-Digital Converter (ADC)

The full code used in the program is available in a separate compact disc, supplied with this thesis. The following sections will provide some commentary on particular sections of code.

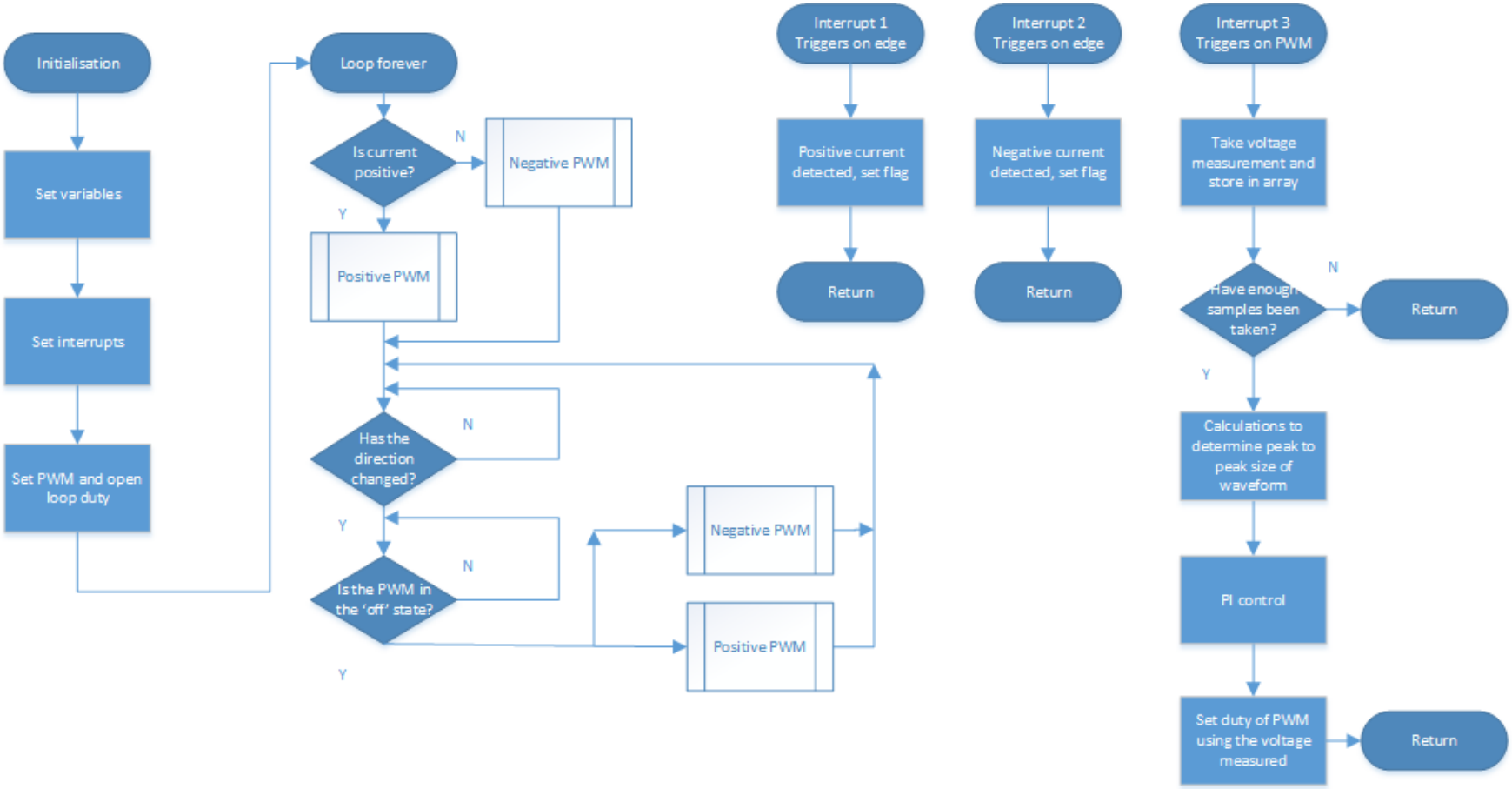

Figure 6-5: Program Flowchart

The sections referred to as *InitEPWMx();* set up the pulse width modulation pins to produce input pulses to the external driver circuits. Note that despite only four semi-conductors needing to be switched, all six PWM pins are necessary. There are three reasons for this.

Firstly complementary pins are not unusable with the matrix converter switching arrangement. Complementary pins are designed to be used with an H-bridge configuration. This is due to the way that deadbands are applied to the master and complementary pins. The master pin will receive either the Rising Edge Delay (RED) or the Falling Edge Delay (FED) shown in Figure 6-6, the complementary pin will receive the opposite delay. This is exactly what is required for the operation of an H-bridge circuit, however for a soft-switched matrix converter circuit a PWM pin must have both FED and RED in order to operate correctly. A solution was devised in which a phase delay was added to each pin and then appropriate FED added to each PWM pin. Therefore, in this case, four master pins must be used and no complementary pins.

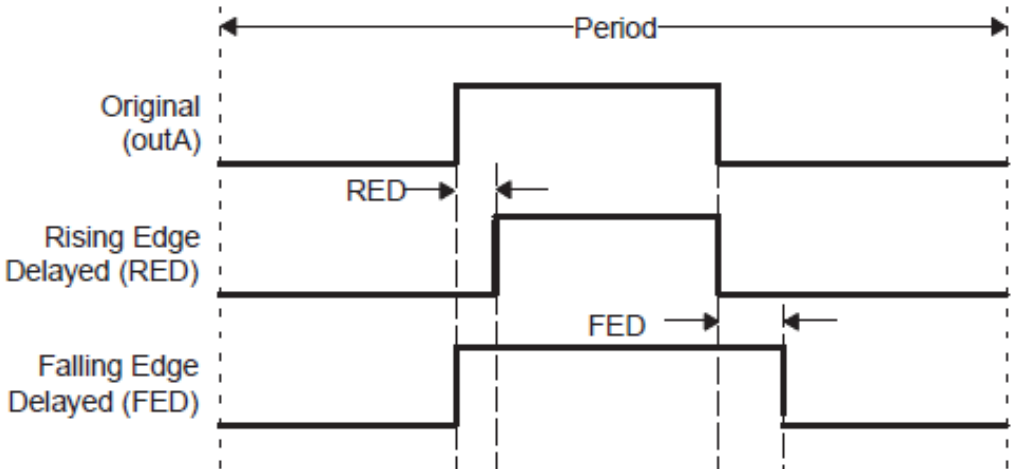

Figure 6-6: Deadbands in PWM [94]

Secondly, in order for the phasing of the PWM pins to operate as intended PWM1A must be used as a master (or reference) pin in order to correctly apply phase differences to 4 pins simultaneously[94].

The required inputs for the switching arrangement have been previously described in Section 2. 4. 4. 3.

Finally the last PWM pin is used for a timed interrupt in order to measure and store the value held in the ADC; this can be observed in the section of code “interrupt void epwm6_timer_isr(void)”. This code will be elaborated upon further later in this section.

The GPIO pins serve as simple input and output digital signals; the most significant GPIO pins in the code are the pins used for interrupting. Through the control circuits which were described in Section 6. 1. 2. 2. Two GPIO pins receive square waveforms that are in anti-phase with each other. These square waveforms describe whether the current is positive or negative and when a rising (or falling) edge is detected it is known that the current is transitioning from one state to another.

Two interrupts are set to trigger from these GPIO pins; these interrupts set flags that inform the rest of the program that a current transition has occurred and to take steps to instantaneously change the commutation method. This ensures that the commutation method switches over quickly and therefore no mal-operation occurs.

These GPIO pins are highly qualified i.e. the sensitivity to change is very low. To elaborate, the same result must be measured several times before the result is considered valid enough to change. This stops any nuisance changes due to any interference from the switching of the main circuit.

There are three interrupts in this program; these have been described somewhat already. The order of importance of these interrupts is as follows

1. GPIO interrupt 1
2. GPIO interrupt 2
3. PWM timer interrupt

Therefore it is possible that during the code that forms part of interrupt 3, a second interrupt occurs from interrupt 1 or 2. This is an important distinction to have in the program as the PI control of the switching outputs which is controlled by interrupt 3 is far less important than ensuring proper commutation which is controlled by interrupts 1 or 2. Also note that it is impossible for interrupts 1 and 2 to activate at the same time.

Another important note to make with interrupts is that the timer interrupt operates at the very fast rate in order to have a high sampling frequency. With this in mind it is important to "protect" certain important sections of code, such any code that re-configures the PWM pins, by temporarily switching off the interrupts at the beginning of these sections of code and subsequently re-enabling interrupts post the code.

The Analogue-to-Digital Converter or ADC is used to take the measured output voltage from the voltage transducer and process this information so the microcontroller can make informed decisions based on the measurement. The ADC is set to continuously sample the voltage waveform from the transducer, however the actual sampling rate is determined by the PWM interrupt which takes a measurement and stores in a matrix it at a rate of 2kHz (40 samples per sine wave).

In order to limit to influence of interference from the main circuit a coaxial cable was used to transmit the transducer voltage waveform to the microcontroller. This was found to be a very effective way of limiting the effects of noise. Other routes taken to increase the accuracy of the information are, akin to the GPIO pins, a high qualification rate. This ensures that any “spikes” or “dip” in the waveform are not counted as valid results, this lowers the sample rate of the ADC but the ADC samples extremely quickly and the rate at which the ADC samples is far greater than the rate that the PWM samples therefore this is not an issue.

Using the waveform data stored in a matrix from the PWM sampling of the ADC, the data is processed and a voltage output voltage is determined. This value is then utilized to change the duty of the switching. This can be observed in the section of the code entitled “interrupt void epwm6_timer_isr(void)”.

The information taken from the ADC is a 16-bit unsigned integer; this means that the sampled signal is assigned a value in the range of 0-65535 (2^{16}).

The first step is to find the maximum and minimum values of the waveform; this informs us of the peak-to-peak value of the sine wave in digital steps. The peak-to-peak value is then converted to “voltage” by multiplying by a constant.

It is important at this point that all numbers used in calculation are floating point numbers. This is due to the overflow problems with other number formats.

The measured signal is compared with the target output voltage; this produces an error signal. This error is then passed through PI control and the controlled error signal is added to the present value of duty cycle.

The proportional control is achieved simply multiplying the error signal by a constant. The integral control is achieved via the following algorithm shown in Equations 22, 23, 24 and 25 which can be used to provide integral control for discrete systems (Z-Domain) [95].

22 $$v = v\_1 + (f_s \times e)$$

23 $$v\_1 = v$$

24 $$PI_e = ((K_p \times e) + (K_i \times v))$$

25 $$d = d + PI_e$$

Where:

v is the integral error

v_1 is the previous integral error

f_s is the switching frequency

e is the error

K_p is the proportional gain

K_i is the integral gain

PI_e is the combined error feedback

d is the duty cycle

One of the issues with this type of control is that in debugging, the v and v_1 values can become extremely large and the algorithm will no longer function correctly. This is why it is important to be able to reset the integral error value. In lieu of this function, the integral values have a positive and negative limit of 10,000 and -10,000 respectively. This was found to stop any problems caused by erroneous integrator values.

6. 1. 2. 5. Electromagnetic Interference

Due to the switching of the IGBTs electromagnetic interference (EMI) will radiate from the circuit. This causes errors in measurement such as the additional distortion added to the output current measurement shown in Figure 6-7. This was confirmed as, upon a change in equipment, the EMI visibly reduced.

While this is a nuisance, it will not affect the circuit operation, however it will cause measured THD results to be higher than expected.

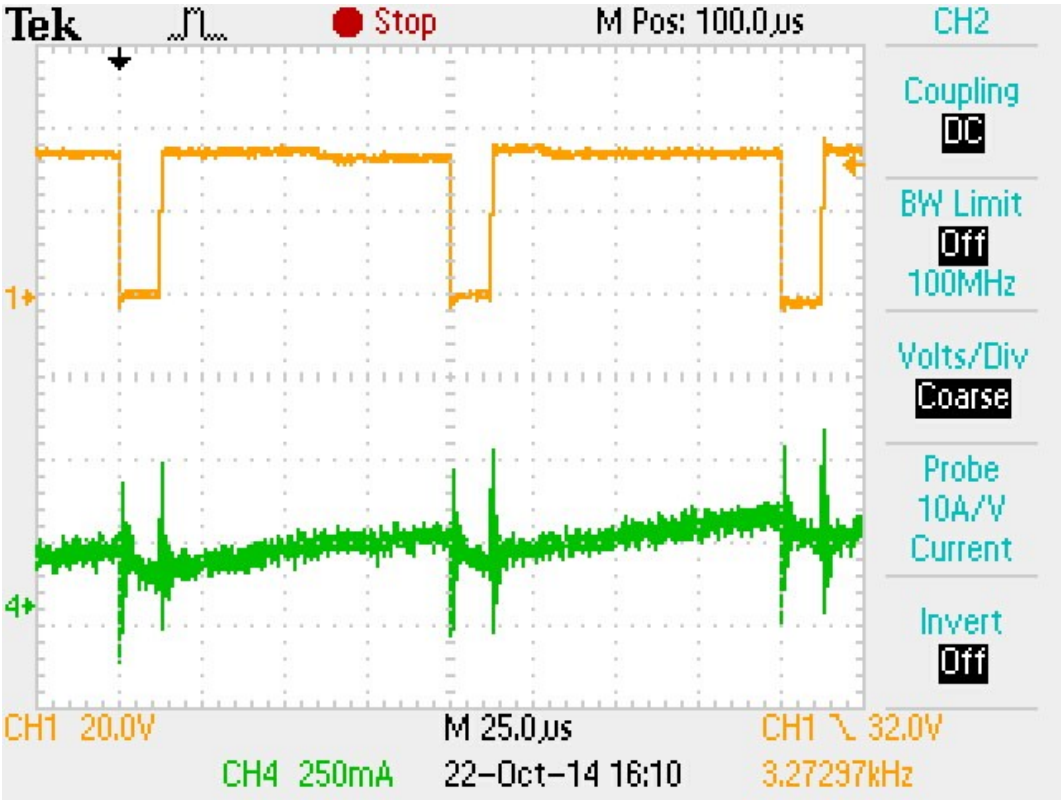

Figure 6-7: Interference on the measurement of the current waveform

6. 1. 2. 6. Optimization of switching frequency, filter size and IGBT

A study was performed in Matlab Simulink with the aim of optimising the filter size for the AC Chopper, while paying particular attention to the various loads used in the average UK household.

Figure 6-8 to Figure 6-15 show the variety of simulations run to determine the appropriate size of inductance and capacitance. All inductance values are in mH and capacitance values in μF. THD_I and THD_V are the input current total harmonic distortion and the output voltage total harmonic distortion; these values are measured in %.

Figure 6-8 to Figure 6-11 show the results from a value sweep of the input and output filters of the AC Chopper at a switching frequency of 30kHz. These tests were run against for various types of load typical in the UK household, so the resulting filter design will be extremely robust.

Figure 6-12 to Figure 6-15 show the same tests run with a AC Chopper operating at a switching frequency of 10kHz.

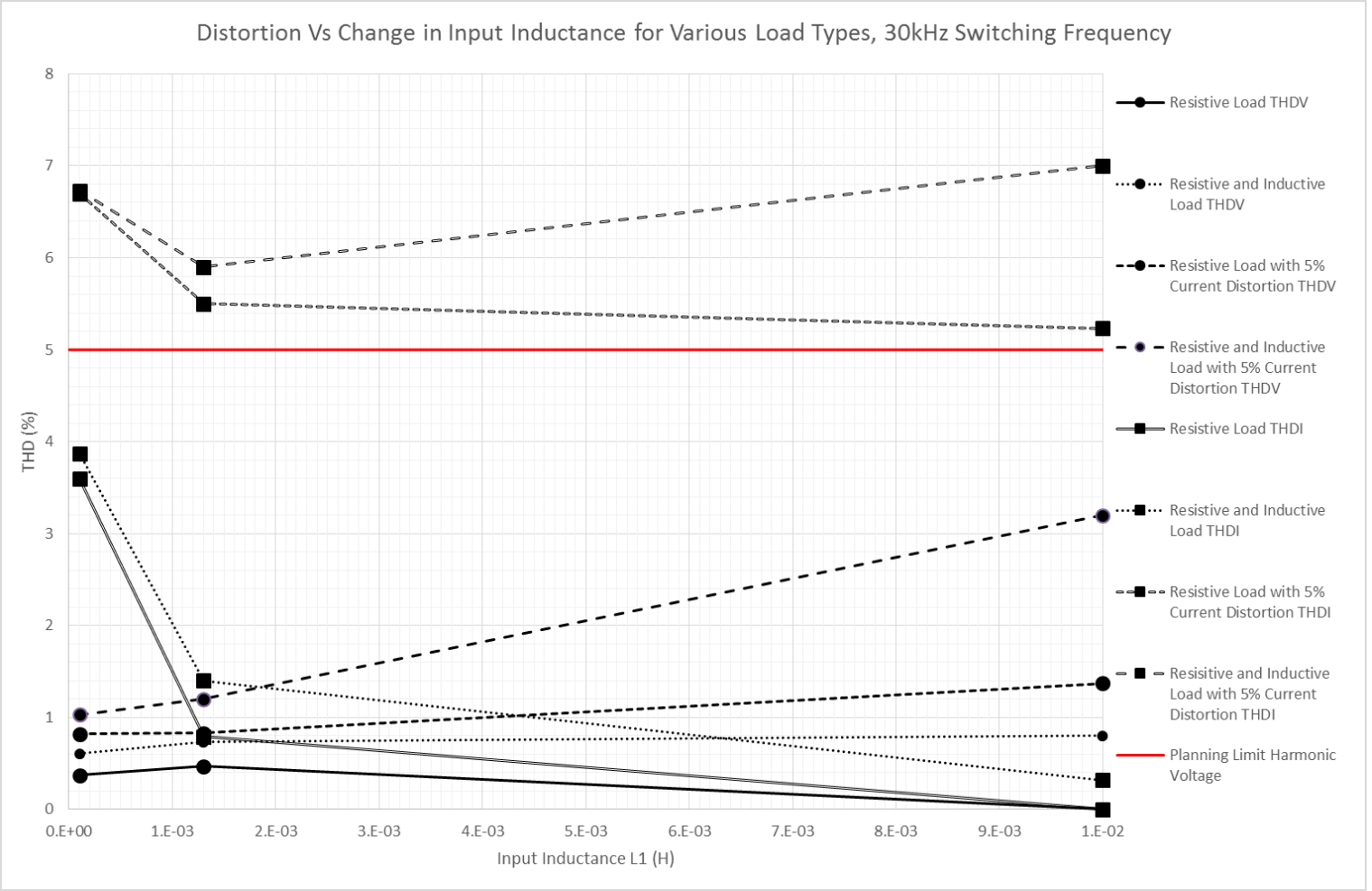

Figure 6-8: Voltage and Current THD for Various Load Types, Changing L1, Switching Frequency 30kHz

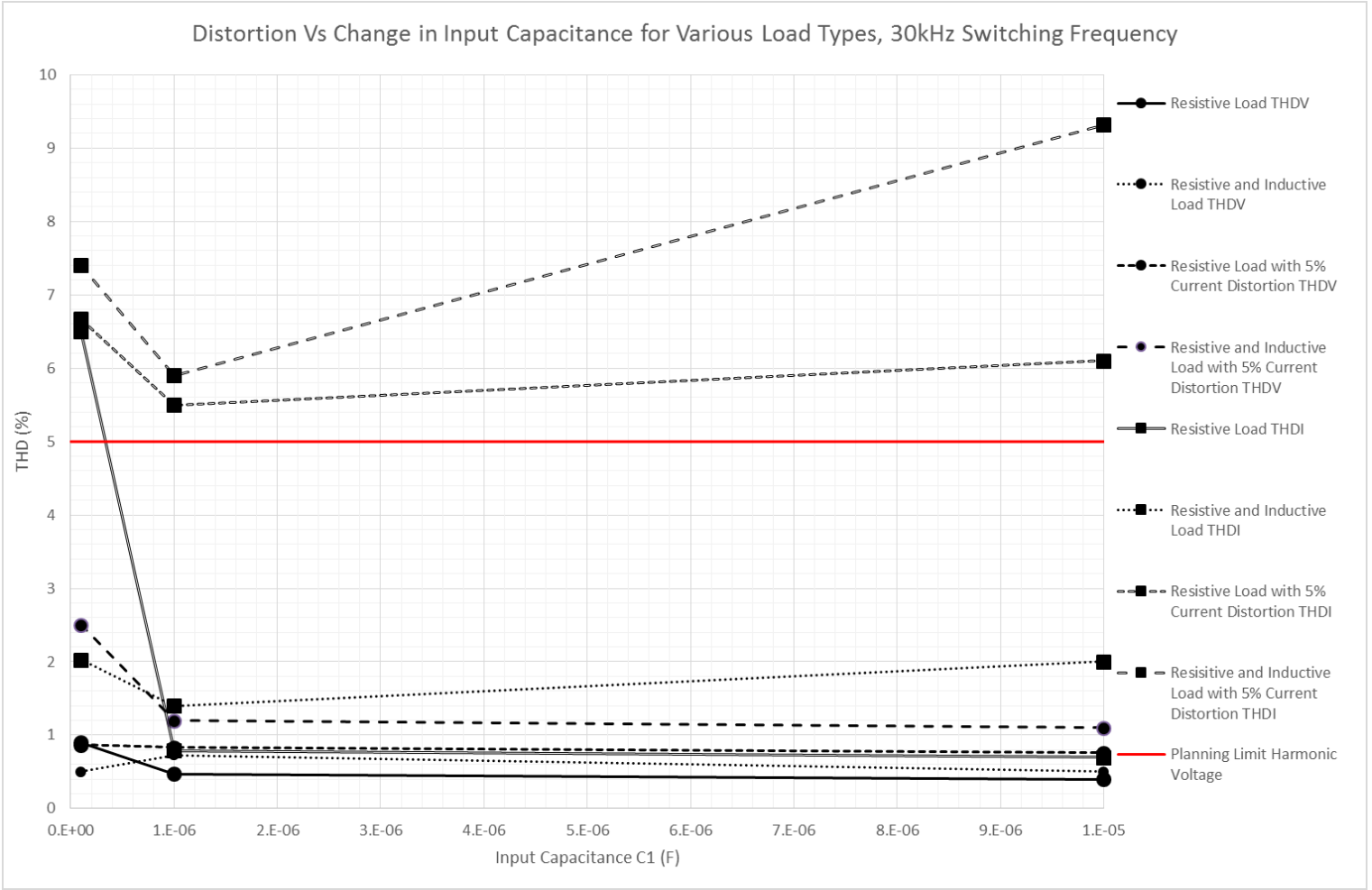

Figure 6-9: Voltage and Current THD for Various Load Types, Changing C1, Switching Frequency 30kHz

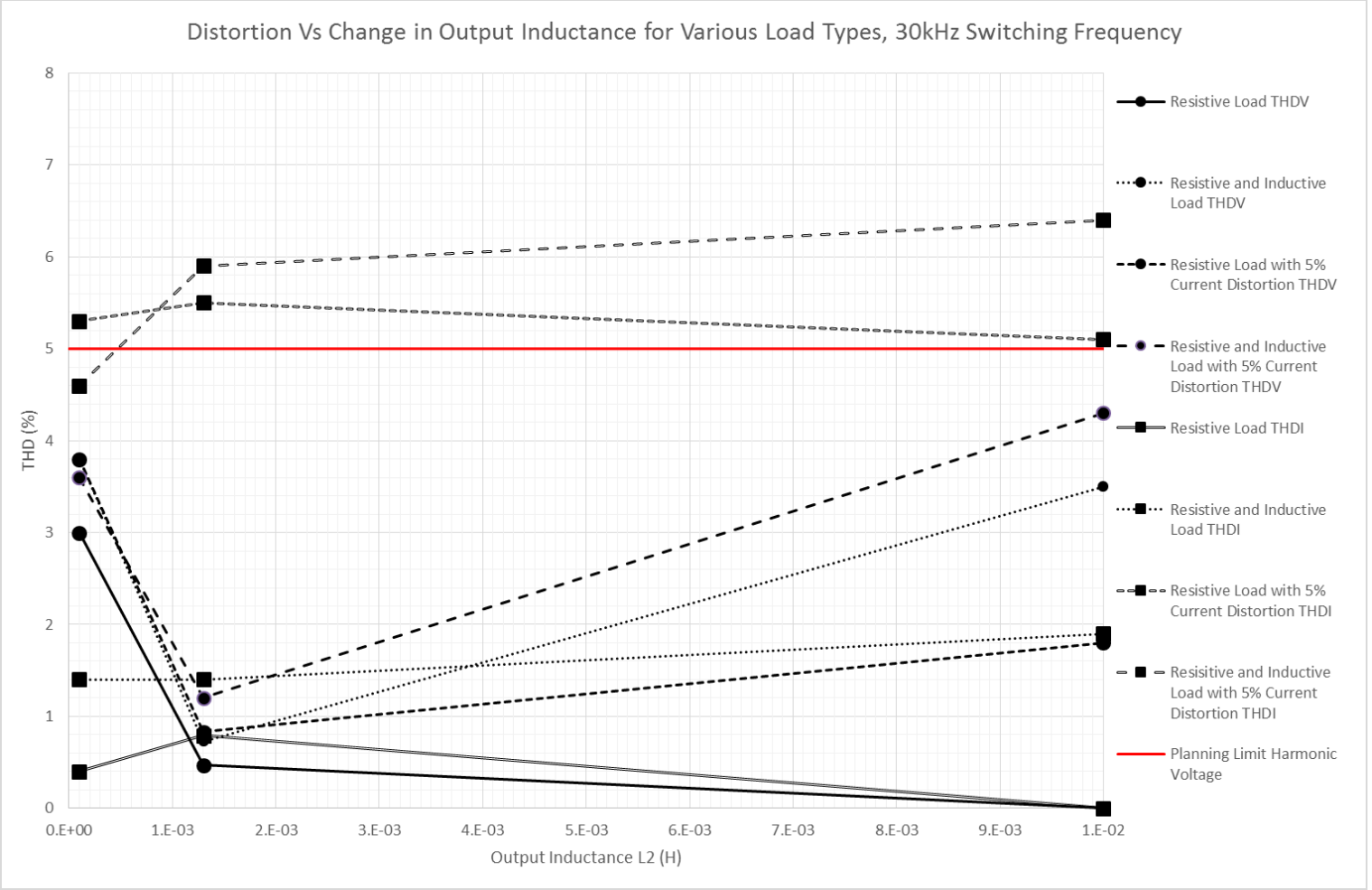

Figure 6-10: Voltage and Current THD for Various Load Types, Changing L2, Switching Frequency 30kHz

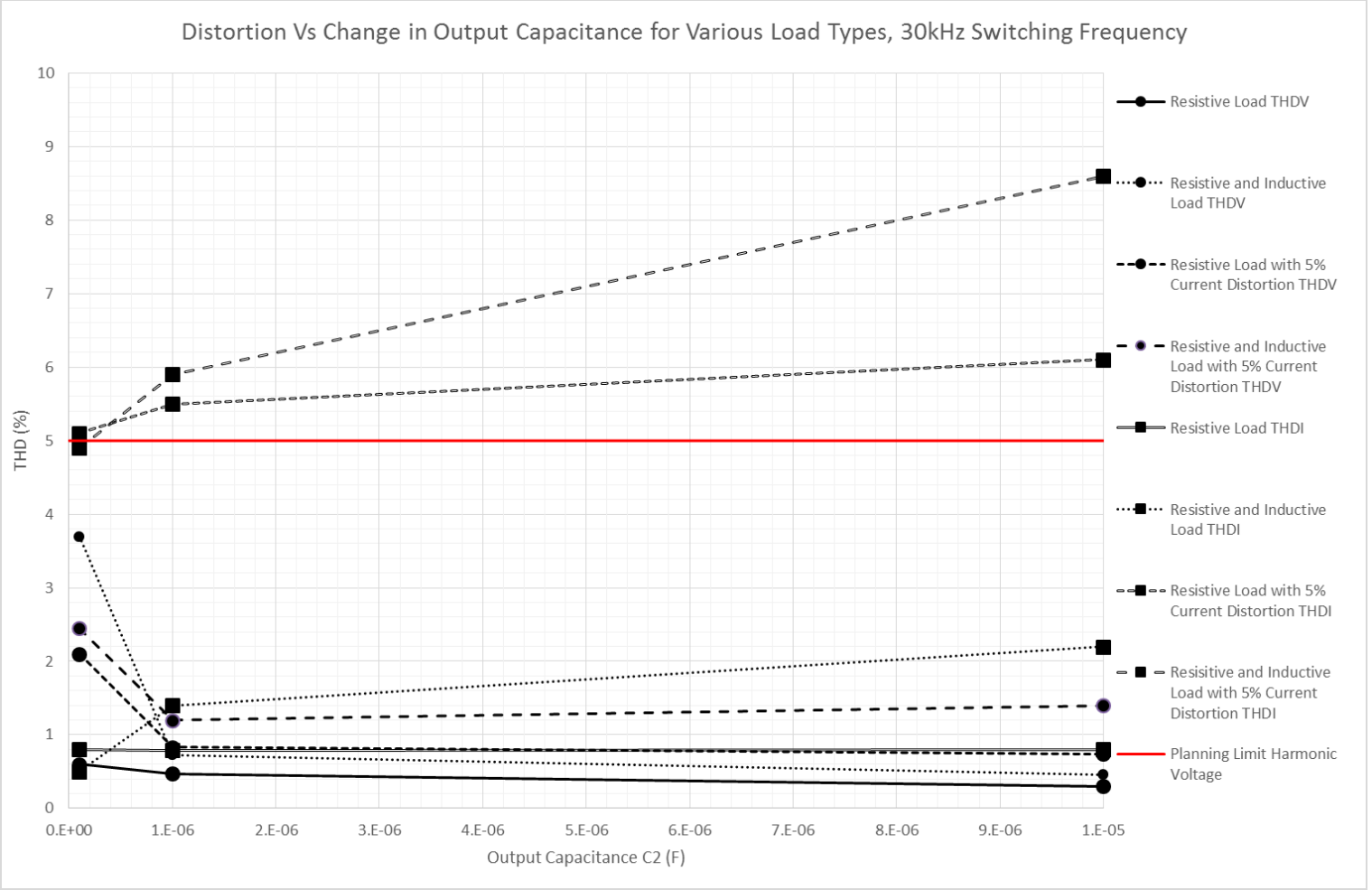

Figure 6-11: Voltage and Current THD for Various Load Types, Changing C2, Switching Frequency 30kHz

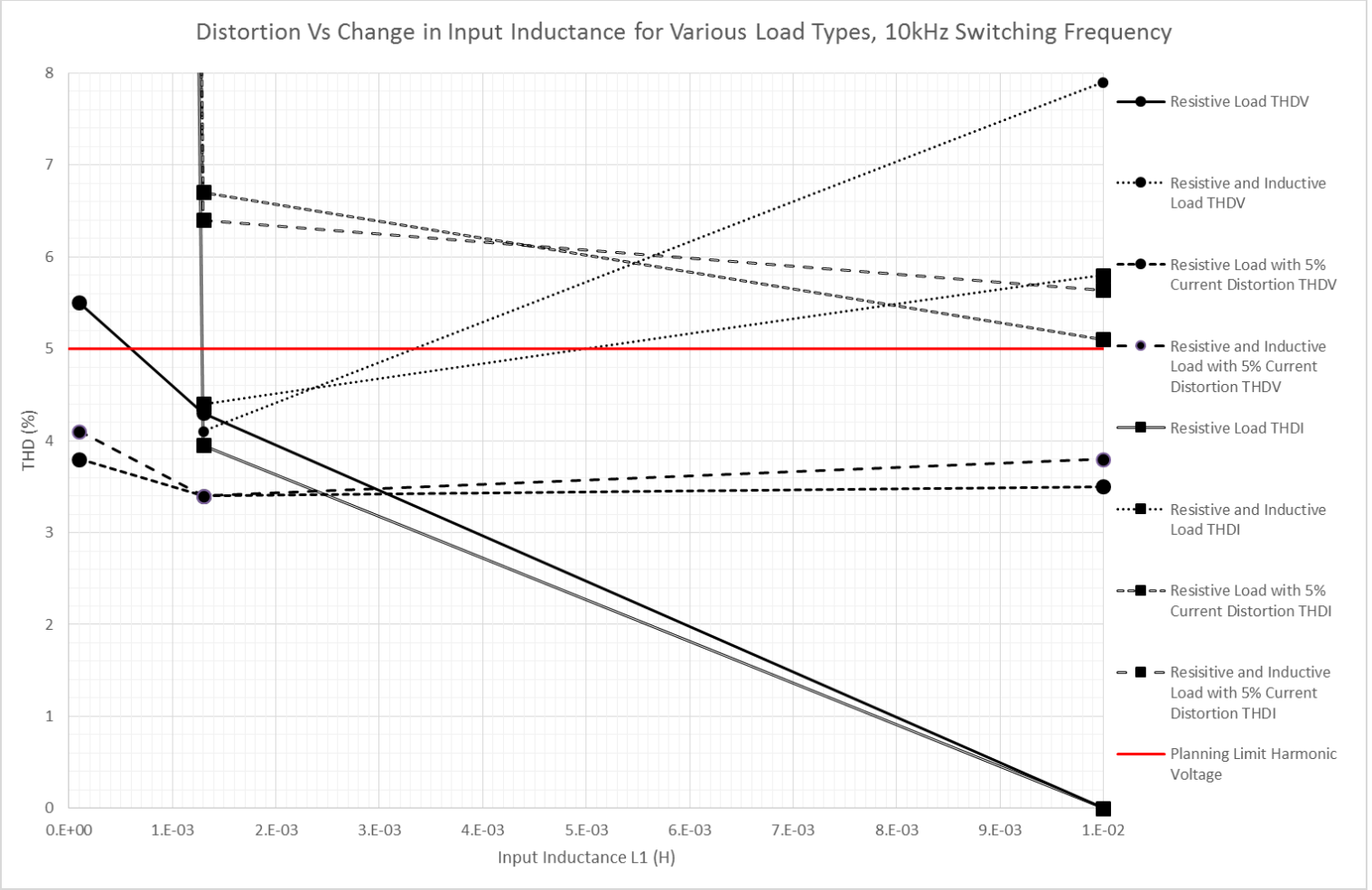

Figure 6-12: Voltage and Current THD for Various Load Types, Changing L1, Switching Frequency 10kHz

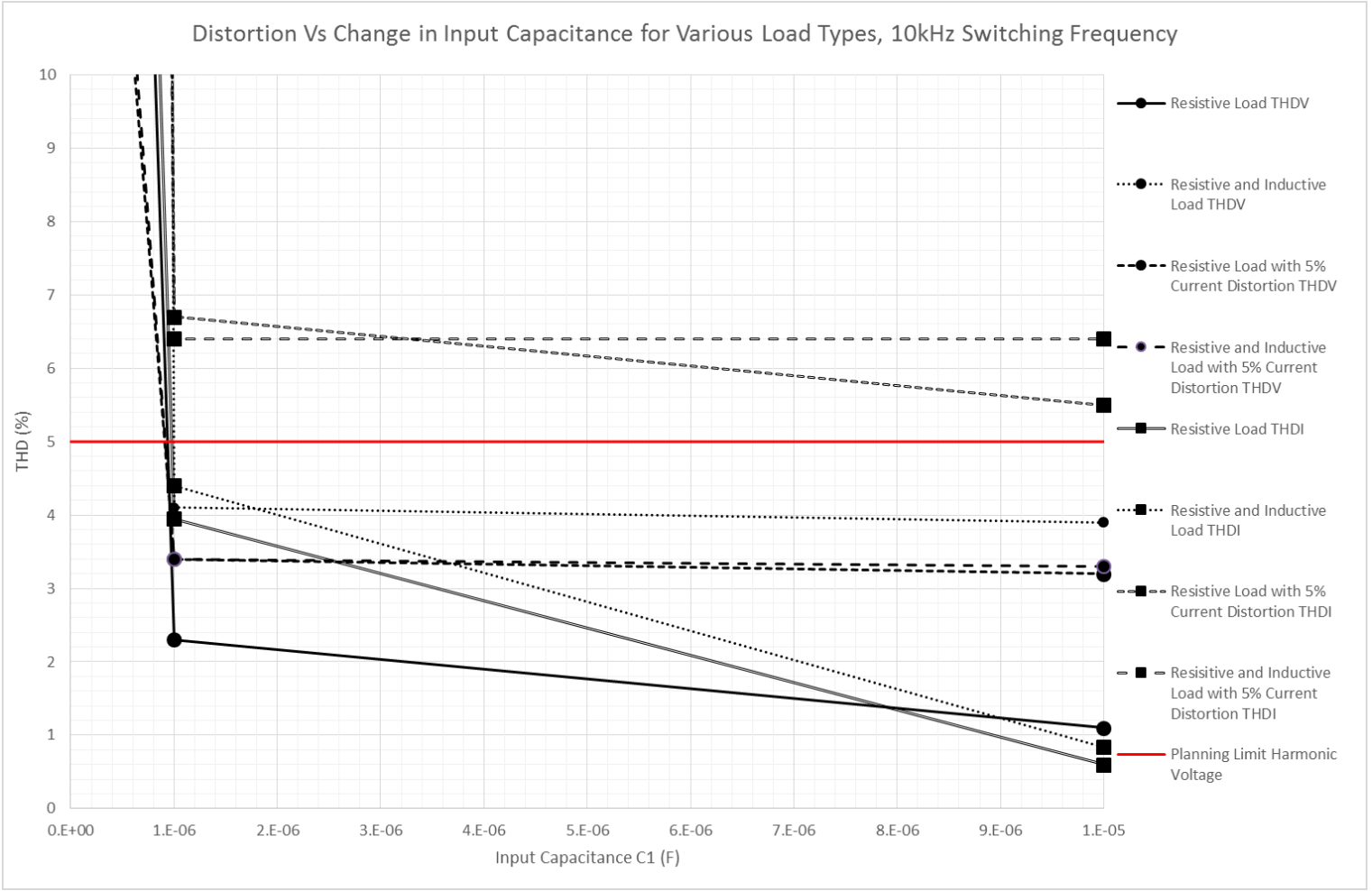

Figure 6-13: Voltage and Current THD for Various Load Types, Changing C1, Switching Frequency 10kHz

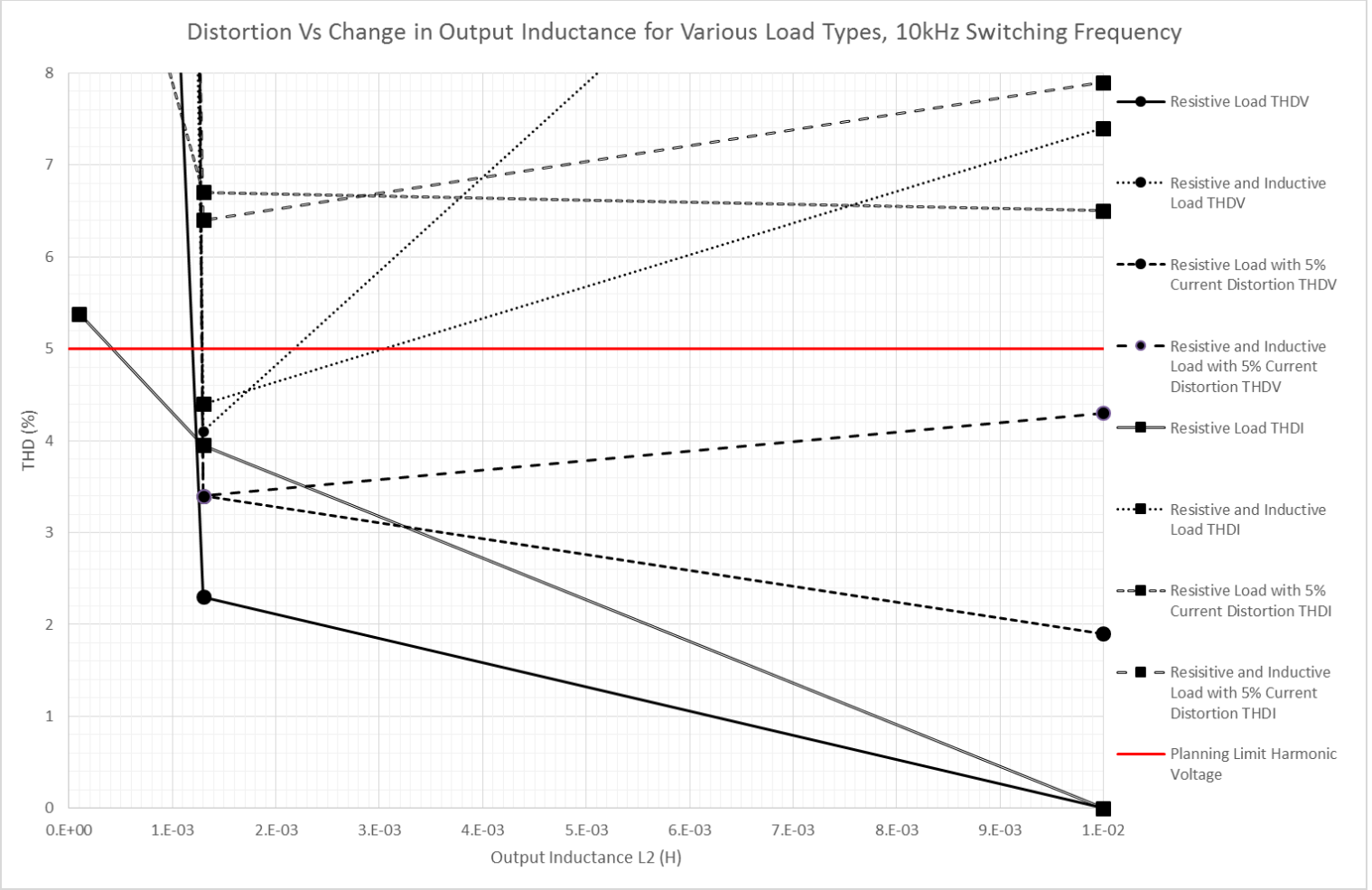

Figure 6-14: Voltage and Current THD for Various Load Types, Changing L2, Switching Frequency 10kHz

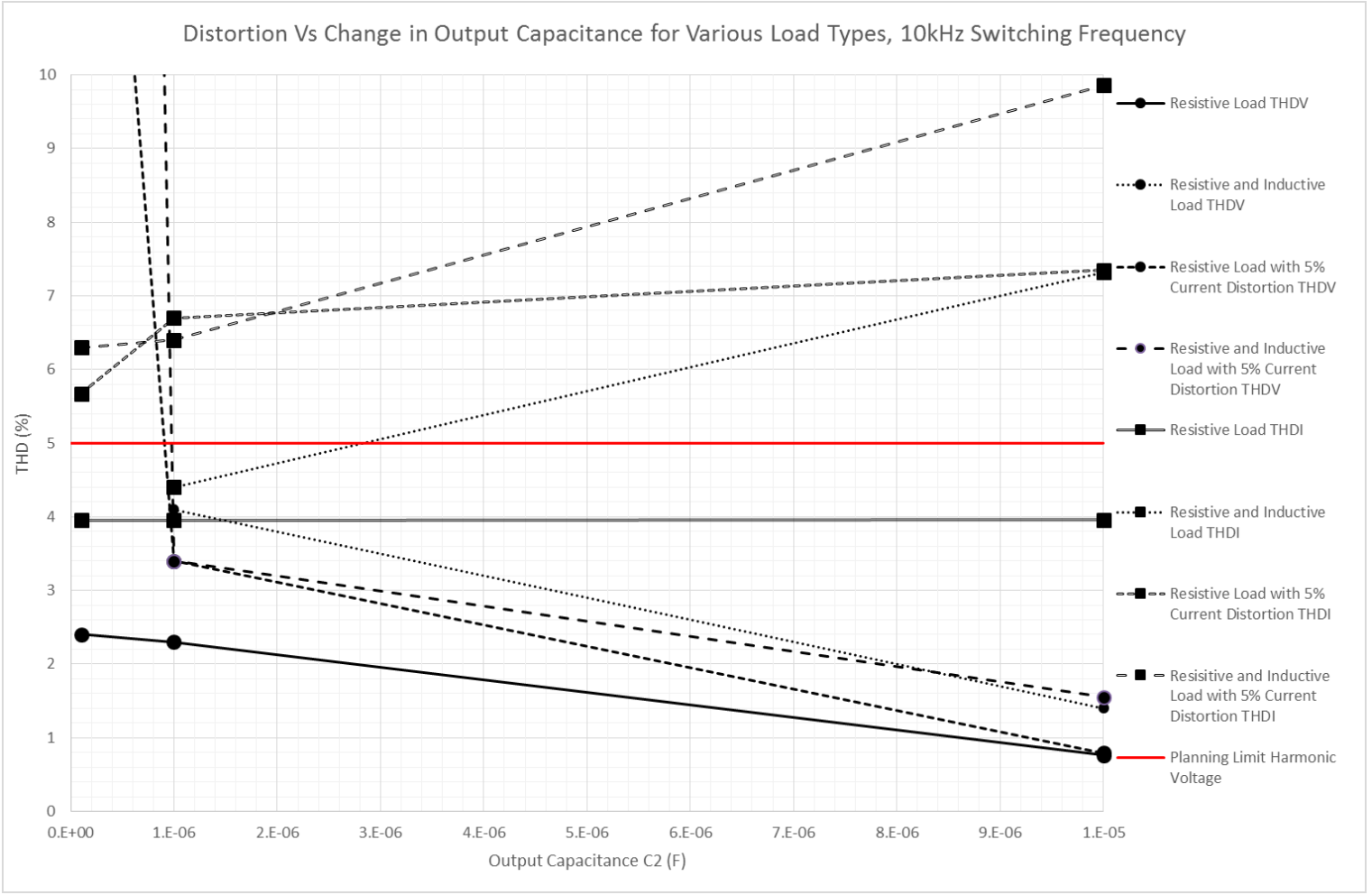

Figure 6-15: Voltage and Current THD for Various Load Types, Changing C2, Switching Frequency 10kHz

From the using the previous studies as a starting point, filter values were found, these values were tested using the same method as the simulations in Figure 6-8 to Figure 6-15. The results are shown in Table 6-2 and Table 6-3 for 30kHz and 10kHz respectively.

Table 6-2: Filter Value Tests - Switching Frequency 30kHz - Row 1: 20kW, Row 2: 0.75pf, Row 3: 5% THD, Row 4: 0.78pf and 5% THD

L1	C1	L2	C2	$F_{co}1$	$F_{co}2$	P_{in}	Q_{in}	THD_I	THD_V	Pf
1	1	0.3	0.3	5	16.7	20.9	1.89	0.45	1.37	1.00
1	1	0.3	0.3	5	16.7	0.94	0.73	0.6	4.24	0.79
1	1	0.3	0.3	5	16.7	1.07	-0.07	4.7	3.3	1.00
1	1	0.3	0.3	5	16.7	1	0.695	4.4	3.4	0.82

Table 6-3: Filter Value Tests - Switching Frequency 10kHz - Row 1: 20kW, Row 2: 0.75pf, Row 3: 5% THD, Row 4: 0.78pf and 5% THD

L1	C1	L2	C2	$F_{co}1$	$F_{co}2$	P_{in}	Q_{in}	THD_I	THD_V	Pf
2.5	1.5	2	0.45	2.6	5.3	21	8.5	0.86	0.82	1.00
2.5	1.5	2	0.45	2.6	5.3	0.92	0.66	1.1	4.4	0.79
2.5	1.5	2	0.45	2.6	5.3	1.02	-0.07	5	3	1.00
2.5	1.5	2	0.45	2.6	5.3	0.96	0.7	5	3.2	0.82

From Figure 6-8 to Figure 6-15 it is clear that a higher switching frequency gives a better power quality. However as discussed in Sections 2. 2. 4. and 2. 3. 6. higher switching speeds results in higher losses in the IGBTs and snubbers. A higher switching frequency will also reduce the load current though the IGBT, see Section 6. 1. 1. 7. for more detail. Therefore a decision must be made regarding the best possible switching frequency to use.

During experimental work it was found that a switching frequency of 30kHz generated too much switching loss in the IGBT. This can be observed in Figure 6-16 which was operating at 500W (half-load). The IGBT temperature was very high at 77.7°C therefore to increase the circuit reliability a new lower switching frequency of 10kHz was used in subsequent experiments.

As a higher operating temperature is indicative of device stress and will reduce device lifetime. This is described in Section 2. 2. 3.

The effect of adding the snubbers of value 2.2nF and 4.7Ω to the circuit is shown in Figure 6-17. It can be observed that a much cleaner transient was achieved that has no overshoot at device turn on.

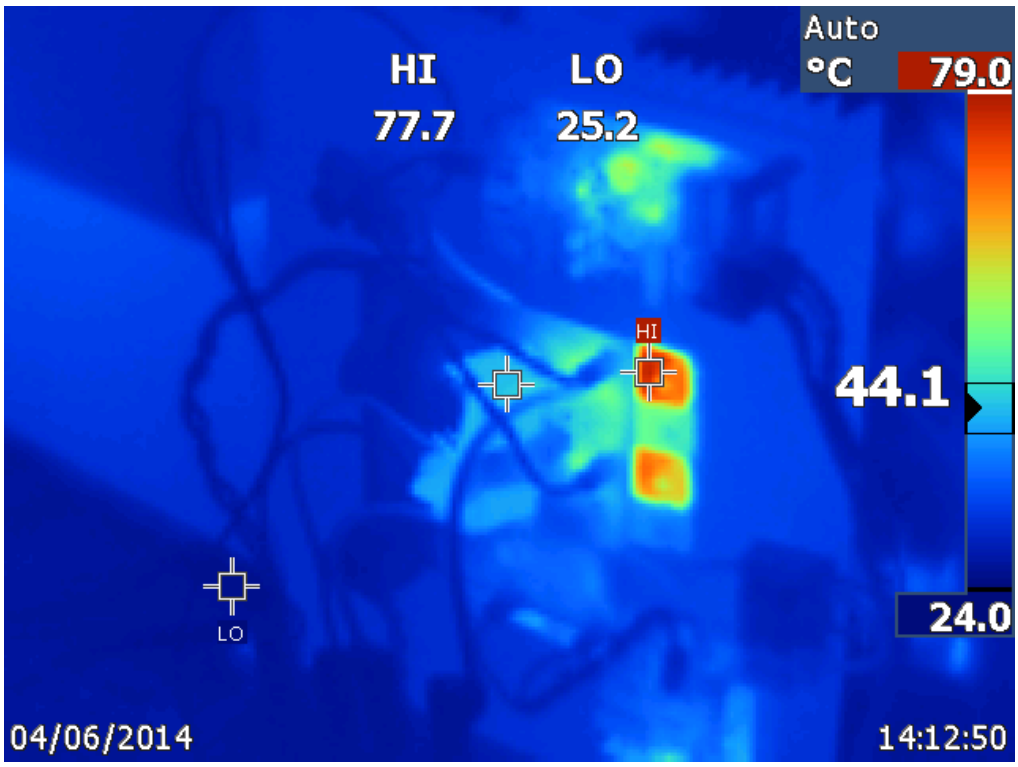

Figure 6-16: Operation of AC Chopper at half load, 30kHz

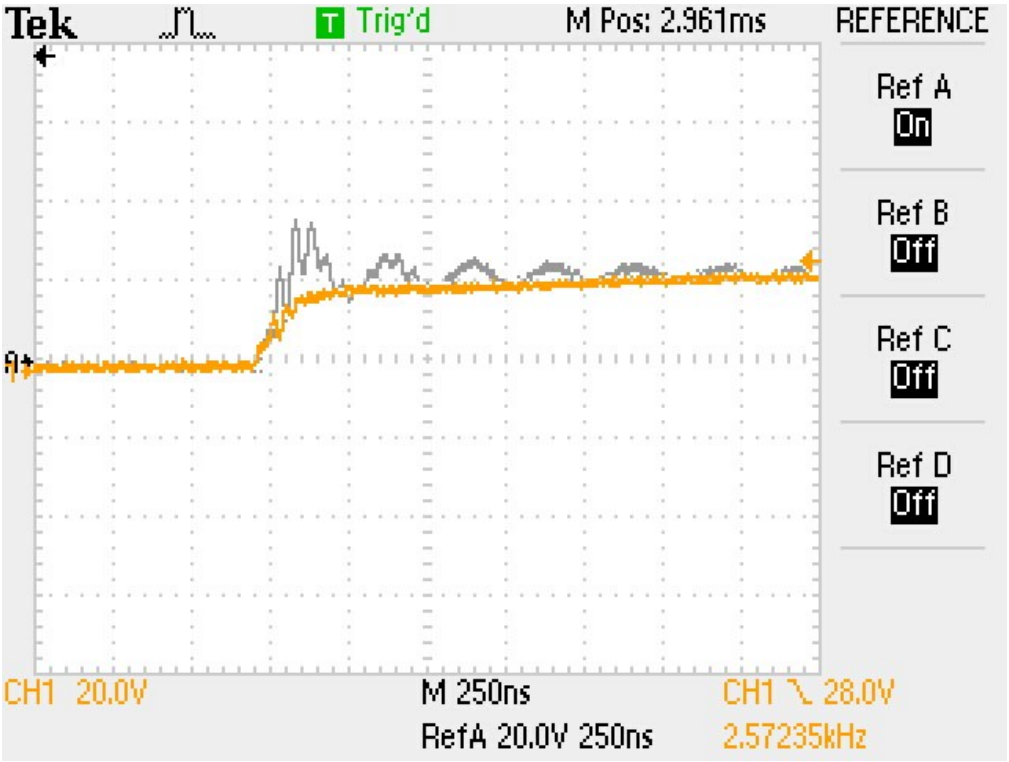

Figure 6-17: Practical effect of snubbers on switching waveform, gray waveform without snubber, yellow with snubber

From the results presented in Section 6. 1. 2. 5. we have determined that the most suitable switching frequency for the IGBTs presented in Section 6. 1. 1. 7. is 10kHz From Table 6-1 we can therefore obtain the maximum load current value of 55A, this is acceptable for the AC Chopper demonstration prototype. In order to use this circuit in a real household a load current value of 90A is required, see Section 2. 1. 3. for more detail. From Table 6-1 this means that if the circuit were to be practically implemented in the household the switching frequency must be 1kHz in value. From Figure 6-8 to Figure 6-15 it can be observed that the drop in switching frequency in-turn means a drop in power quality. As the filters must be larger in order to eliminate the lower frequency harmonics, this in-turn causes the circuit to absorb more reactive power.
This may breach the power quality aspects of G59/3, described in Section 2. 1. 4. In such a case, an IGBT with a better switching frequency vs load current must be selected or a newer technology used with a faster switching frequency such as SiC MOSFETs [96].
The filter sizes for a switching frequency of 10kHz were found to be an input inductance of 2.5mH, a input capacitance of 1.5μF, an output inductance of 2mH and a output capacitance of 0.45μF. These values provided good performance under all loading conditions and do not absorb too much reactive power.

6. 1. 2. 7. Testing

The objective of the practical studies is to discover the efficiency of the converter at various power levels up to a maximum of 1kVA. This was achieved via power measurement devices described in Section 6. 1. 1. 4. These were placed at the input to the converter and the output of the converter. Therefore the power lost over the converter could be measured via the difference of these values. The power lost can be used to determine the efficiency of the converter.

The THD of the circuit was also measured; this was achieved via two more power measurement devices placed at the input to the circuit and the load of the circuit. These measured the input current THD and the output voltage THD. Therefore the results gained will be a series of efficiency and THD values for various power levels.

6. 2. Grid Conditions

It is worth noting that due to the extremely high amount of electronics at the University of Strathclyde, the voltage waveform is slightly flat topped, this was measured as 1.77% voltage THD.

6. 3. AC Chopper Results

For the equipment described in Section 6. 1. 1. and using the method described in Section 6. 1. 2. the AC Chopper demonstration prototype produced the following results.

For the equipment described in Section 6. 1. 1. an identical circuit was also simulated in Matlab Simulink; this is the same model used in Chapter 5. However the model was updated with new component values to validate experimental results. Two simulation curves were generated from the models which indicate a best and worst case as the voltage drop and resistance of the IGBT is highly dependent on the temperature and operating point respectively.

From Figure 6-18 it can be observed that in this case the best and worst possible voltage drop across the IGBT is 1.7V and 2.1V.

Figure 6-19 shows the resistance of the IGBT and the voltage across it and the current through it changes (V_{GE}=10V).

From this graph a value of 0.008Ω was calculated as the best case value of R_{on} with a current of 30A or greater flowing through the device while a worst case value of 0.5Ω was calculated with a current of 3A or less flowing through the device.

Similarly for the diodes in the circuit the best case V_{drop} and R_{on} are 3.2V and 0.033Ω, and the worst case is 3.2V and 0.9Ω. These values can be gained from the diode datasheet [80].

Electrical Characteristics @ T_J = 25°C (unless otherwise specified)

	Parameter	Min.	Typ.	Max.	Units	Conditions
$V_{(BR)CES}$	Collector-to-Emitter Breakdown Voltage	1200	—	—	V	V_{GE} = 0V, I_C = 100μA ③
$\Delta V_{(BR)CES}/\Delta T_J$	Temperature Coeff. of Breakdown Voltage	—	1.0	—	V/°C	V_{GE} = 0V, I_C = 1mA (25°C-150°C) ③
$V_{CE(on)}$	Collector-to-Emitter Saturation Voltage	—	1.7	2.0	V	I_C = 50A, V_{GE} = 15V, T_J = 25°C ②
		—	2.0	—		I_C = 50A, V_{GE} = 15V, T_J = 150°C ②
		—	2.1	—		I_C = 50A, V_{GE} = 15V, T_J = 175°C ②
$V_{GE(th)}$	Gate Threshold Voltage	3.0	—	6.0	V	V_{CE} = V_{GE}, I_C = 2.0mA
$\Delta V_{GE(th)}/\Delta TJ$	Threshold Voltage temp. coefficient	—	-17	—	mV/°C	V_{CE} = V_{GE}, I_C = 1mA (25°C - 175°C)
gfe	Forward Transconductance	—	55	—	S	V_{CE} = 50V, I_C = 50A, PW = 80μs
I_{CES}	Collector-to-Emitter Leakage Current	—	2.0	100	μA	V_{GE} = 0V, V_{CE} = 1200V
		—	1700	—		V_{GE} = 0V, V_{CE} = 1200V, T_J = 175°C
I_{GES}	Gate-to-Emitter Leakage Current	—	—	±200	nA	V_{GE} = ±30V

Figure 6-18: IGBT Electrical characteristics [92]

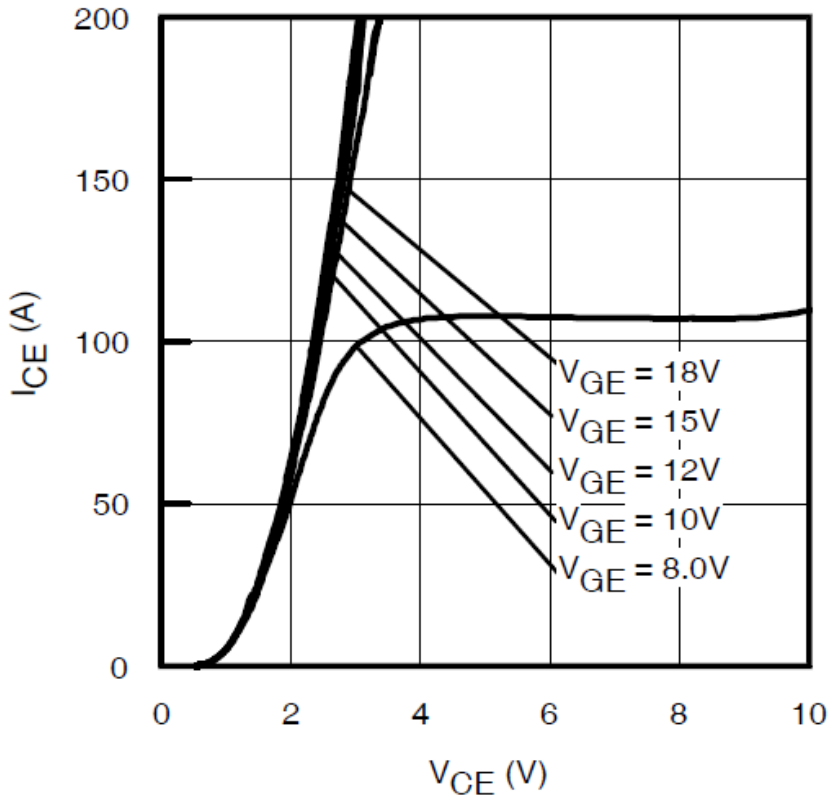

Figure 6-19: IGBT Resistance Curve [92]

6. 3. 1. Unity Power Factor Load

For a power level of up to 1kVA the results recorded are shown graphically in each individual section. An excel spreadsheet entitled "All Practical Results", is supplied on the accompanying CD which details each data point recorded. The first study records the efficiency and THD of the AC Chopper with a load of unity power factor. A sample result is shown in Figure 6-20 which demonstrates the waveforms found with the operation of the AC Chopper driving a unity power factor linear load.

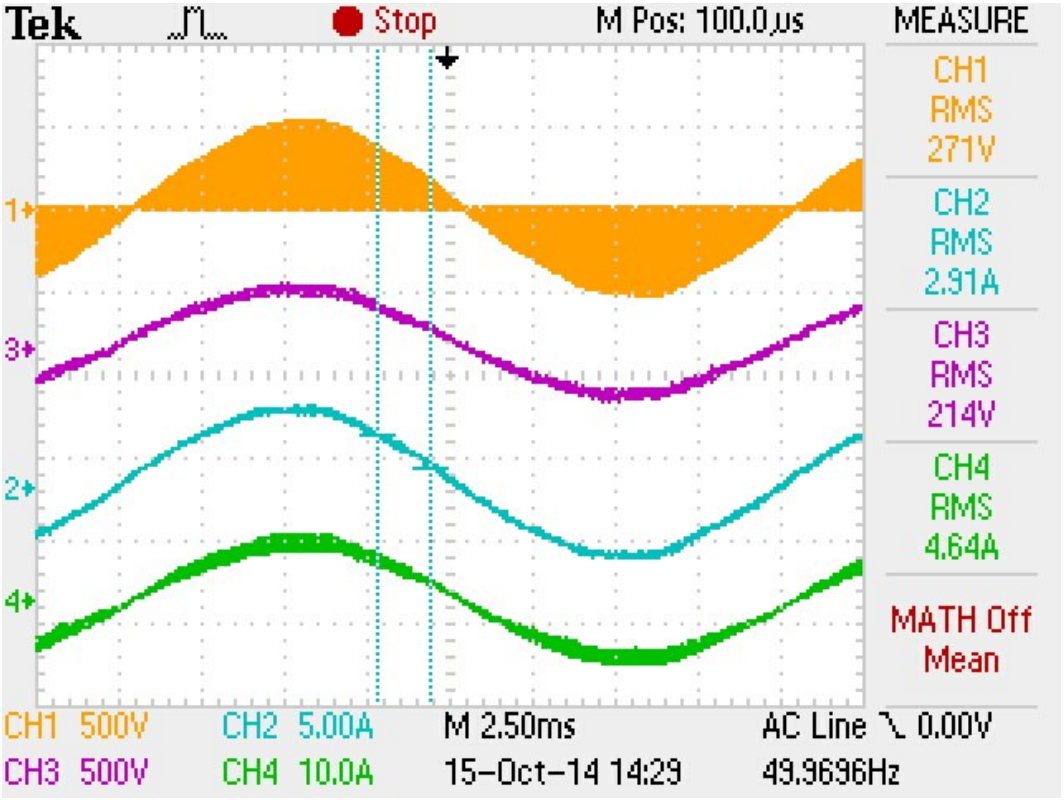

Figure 6-20: Sample Result of AC Chopper Operating with a Unity Power Factor Load. The Yellow Waveform is the "chopped" Voltage Input, the Purple Waveform is the Filtered Voltage Output, the Blue Waveform shows the Input Current, the Green Waveform shows the Output Current.

6. 3. 1. 1. Efficiency Results

Figure 6-21 shows the results from the study plotted graphically. It was observed that the results fall within the expected region. The curve of simulation results that was observed in the simulated results can also be observed in the practical results. This curve exists at the IGBT devices become more efficient as the circuit operating point comes closer to the rated values of the IGBTs.

It is also worth noting that the Matlab Simulink does not take into account all switching losses as only the current fall time is modelled in simulation therefore there will be a loss generated at device turn-off but not at device turn-on. The switching loss at turn-off will be greater than the switching loss at turn-on, due to the greater time required to switch off the device [92].

In summary it was expected that the simulated model would have greater efficiency than the practical model and this was verified.

The results show that the maximum efficiency of the AC Chopper is approximately 97% and the maximum efficiency from the simulation is slightly higher than 97%. The minimum efficiency is approximately 87.5% at near zero active power drawn. All results conform in terms of form and magnitude, therefore the practical results are validated.

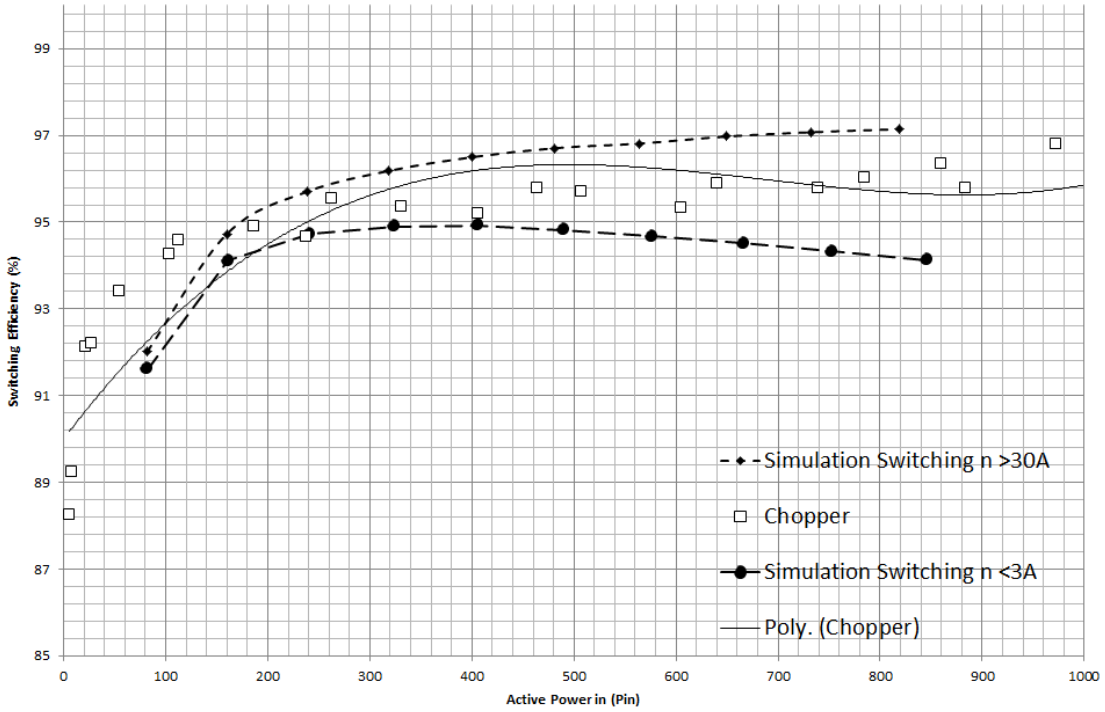

Figure 6-21: AC Chopper - Resistive Load - Switching Efficiency at Various Power Levels. The Simulation Results Use Semiconductor On-State Resistance Characteristics at <3A and >30A in order to provide a Window for the Results

6. 3. 1. 2. THD Results

From Section 6. 1. 2. 5. it was expected that the value of distortion would be greater in a practical circuit than in a simulated circuit. This was confirmed and is shown graphically in Figure 6-22. It can be observed that the initial harmonic distortion of the circuit is approximately 2.8% which decreases to a steady value of approximately 1.9% THD under full load.

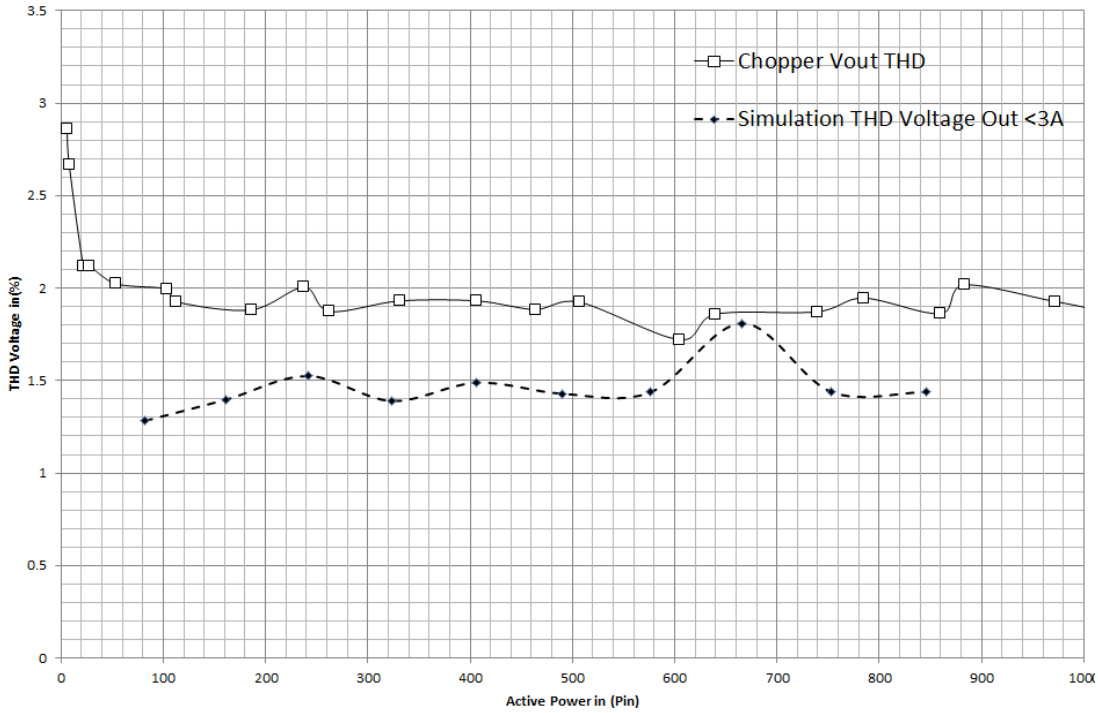

Figure 6-22: AC Chopper - Resistive Load - Total Harmonic Distortion of Output Voltage

The levels of distortion shown in Figure 6-22 are far below the limits described in Section 2. 1. 4. and considering the initial grid voltage THD of 1.9% described in Section 6. 2. very little harmonic content has been introduced to the voltage waveform as a result of switching. The simulation did not account for distorted grid voltage of the effects of EMI on distortion measurement. The simulation consistently measured 1.5% THD other than a small anomalous spike to 1.75% THD. Despite the external factors the values conform in terms of form and magnitude, therefore the practical results are validated.

Figure 6-23 shows the THD of input current, as before these measurements were subject to external factors of the EMI and initial grid distortion. The practical results indicate a consistent input current THD of 1.9% while the simulated results indicate a consistent input current THD of 1%. As before despite the external factors the values conform in terms of form and magnitude, therefore the practical results are validated.

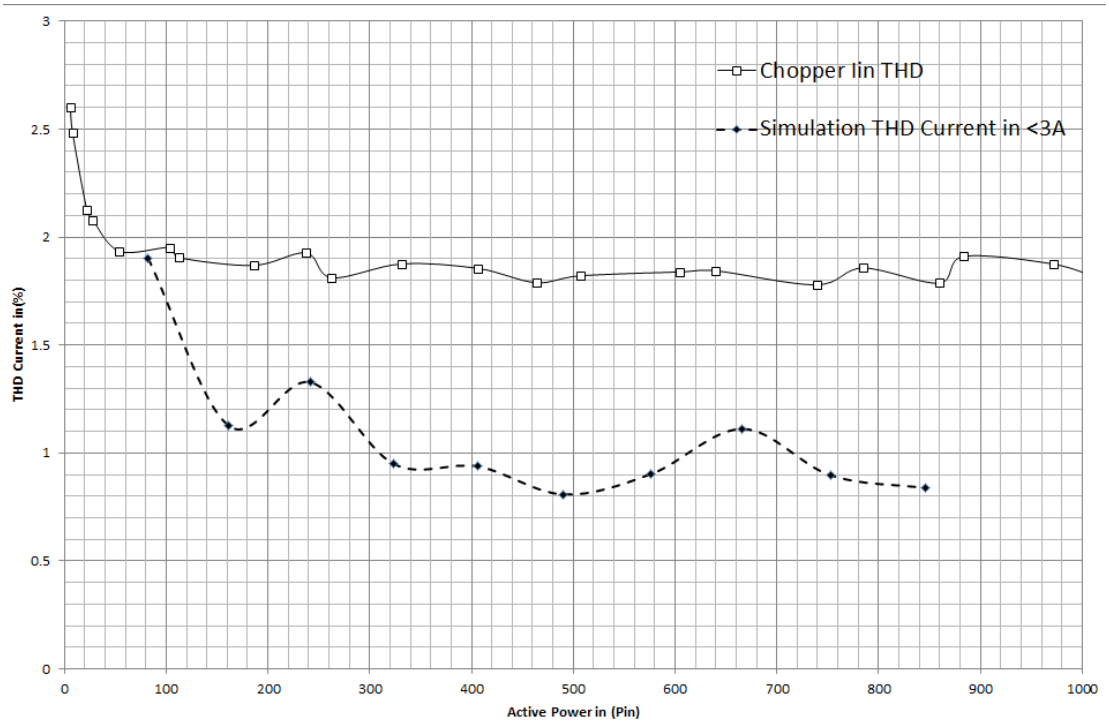

Figure 6-23: AC Chopper - Resistive Load - Total Harmonic Distortion of Input Current

6. 3. 2. Non-Unity Power Factor Load

The second study records the efficiency and THD of the AC Chopper with a load of non-unity power factor. A sample result is shown in Figure 6-24 which demonstrates the waveforms found with the operation of the AC Chopper driving a non-unity power factor load.

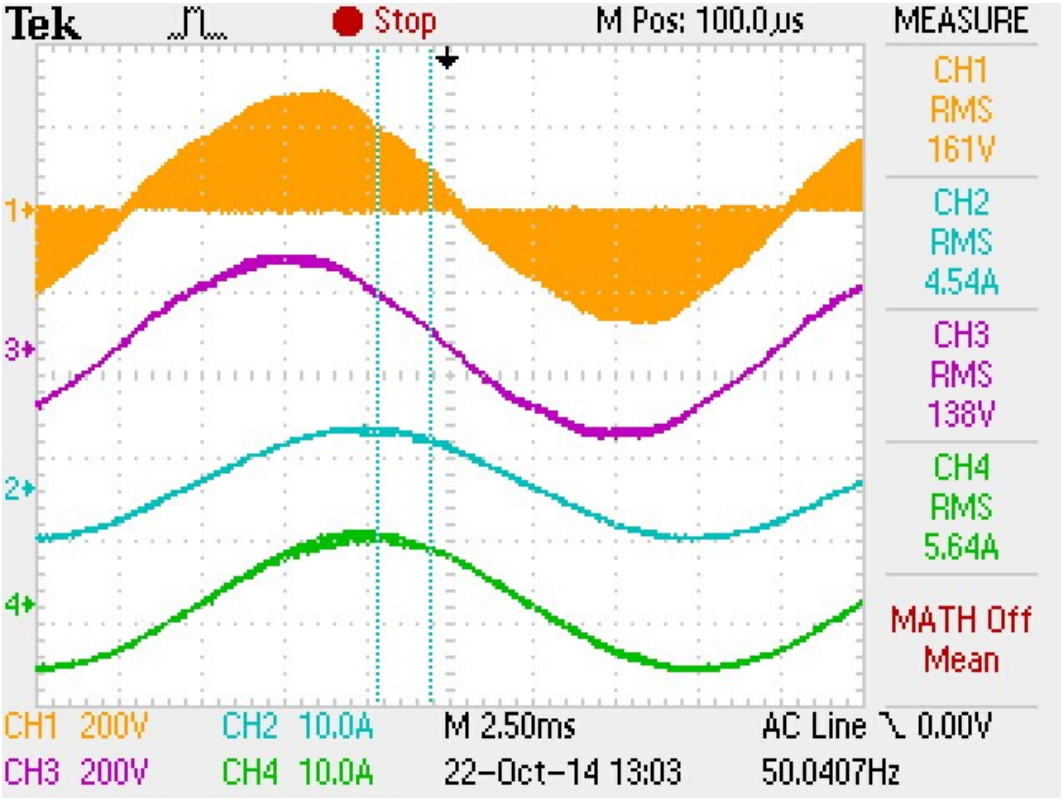

Figure 6-24: Sample Result of AC Chopper Operating with a Non-Unity Power Factor Load. The Yellow Waveform is the "chopped" Voltage Input, the Purple Waveform is the Filtered Voltage Output, the Blue Waveform shows the Input Current, the Green Waveform shows the Output Current.

6. 3. 2. 1. Efficiency Results

The presented results shown in Figure 6-25 provide evidence that the maximum efficiency of the AC Chopper is approximately 96.8% and the maximum efficiency from the simulation is slightly higher than 97.1%.

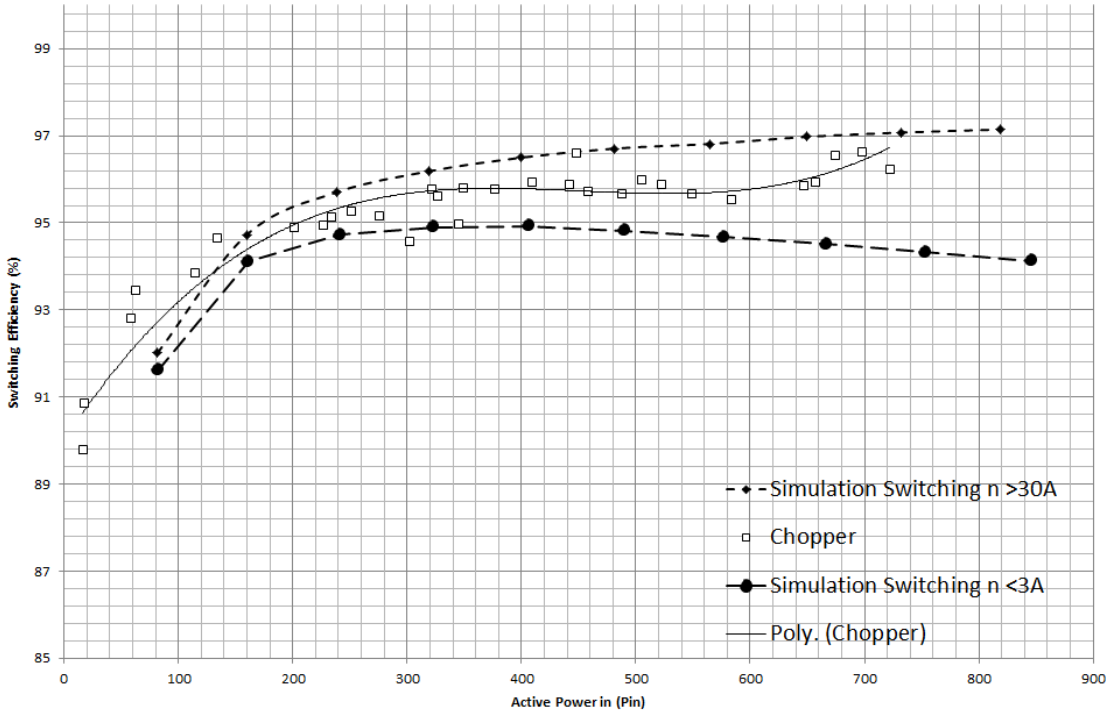

Figure 6-25: AC Chopper - Resistive and Inductive Load - Efficiency. The Simulation Results Use Semiconductor On-State Resistance Characteristics at <3A and >30A in order to provide a Window for the Results

The minimum efficiency is approximately 90% at near zero active power drawn. All results conform in terms of form and magnitude, therefore the practical results are validated.

6. 3. 2. 2. THD Results

Figure 6-26 shows the THD of output voltage, as before these measurements were subject to external factors of the EMI and initial grid distortion.

The practical results indicate a consistent output voltage THD of 2.4% while the simulated results indicate a consistent output voltage THD of 1.5%. As before despite the external factors the values conform in terms of form and magnitude, therefore the practical results are validated.

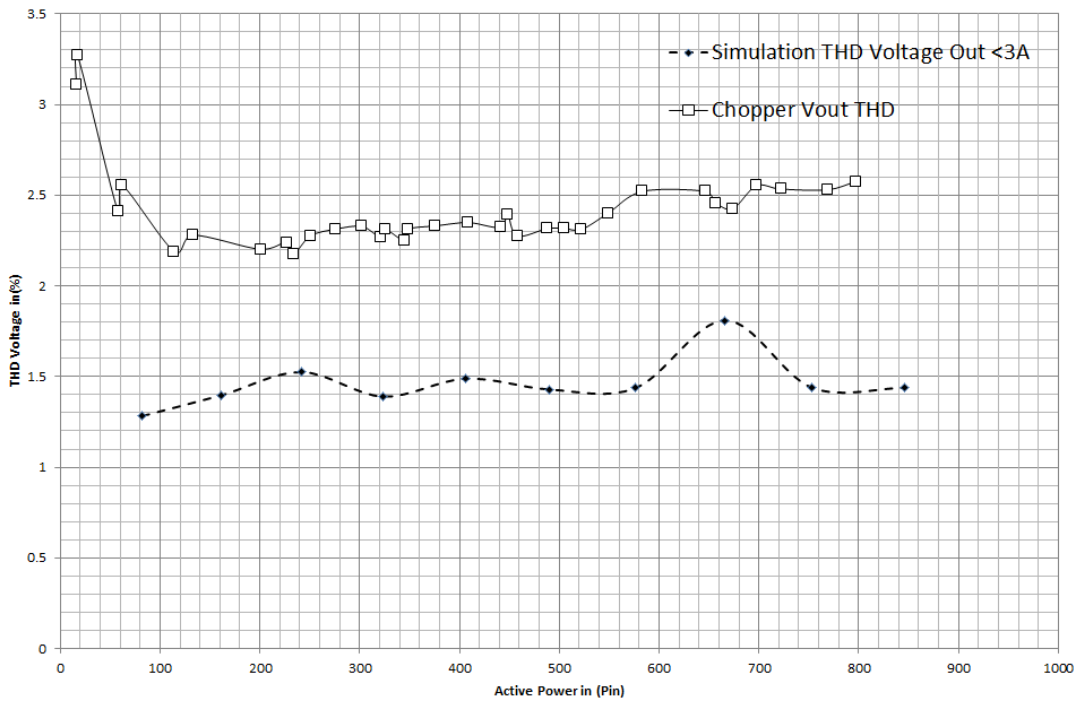

Figure 6-26: AC Chopper - Resistive and Inductive Load - Voltage THD

Figure 6-27 shows the THD of input current, as before these measurements were subject to external factors of the EMI and initial grid distortion.

The practical results indicate a consistent input current THD of 1.2% while the simulated results indicate a consistent input current THD of 0.9%. As before despite the external factors the values conform in terms of form and magnitude, therefore the practical results are validated.

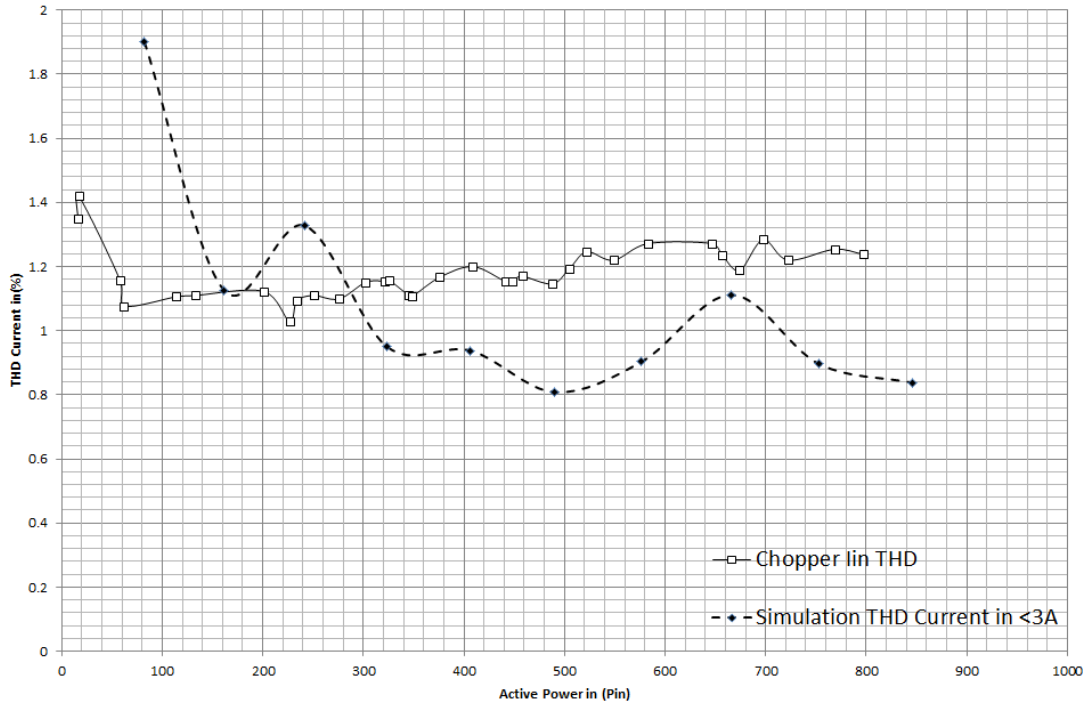

Figure 6-27: AC Chopper - Resistive and Inductive Load - Current THD

6. 3. 3. Non- Linear Load

The non-linear load is practically modelled via a microwave. Unlike the other load types this non-linear load only has one operating point and therefore only one set of results can be taken. A demonstration of this circuit is available in the supplied CD. The results taken are shown in Table 6-4, note that the long averaging technique used for measurements in Section 6. 3. 1. and Section 6. 3. 2. could not be used in this instance due to the transient nature of the microwaves operation therefore results are subject to greater measurement error.

The results show that standard operation of the microwave without using the chopper circuit generates a very high amount of harmonic current. The waveforms of the microwave operation are shown in Figure 6-28 and Figure 6-29.

From the table it can be observed that in line with results from previous sections at low power levels the efficiency of the AC Chopper is low at approximately 20.7%. However at high power levels the efficiency is very high at 98.1%. It can also be observed that the voltage distortion is 4.9% and current distortion 22.3%. From the waveforms it is clear that the current is extremely distorted and that despite this the AC Chopper behaves as normal.

Table 6-4: AC Chopper - Microwave Load - Efficiency, Voltage THD and Current THD

Microwave	η (%)	V_{THD} (%)	I_{THD} (%)
Standard	-	1.75	24.35
Standby	20.7	2.08	19.72
Full Load	98.1	4.9	22.3

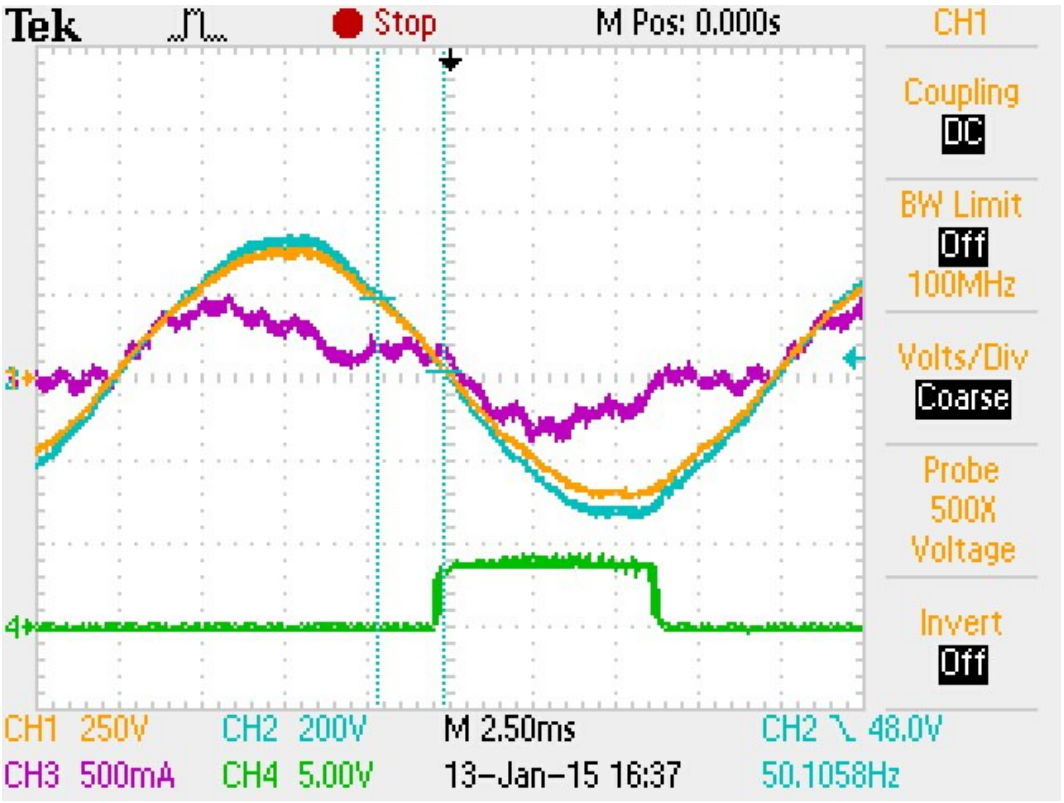

Figure 6-28: AC Chopper - Microwave Operation - Standby Mode. The Yellow Waveform is the Voltage Input, the Purple Waveform is the Current Output, the Blue Waveform shows the Voltage Output, the Green Waveform shows the Control Circuitry Operation Which Changes the Current Commutation Mode

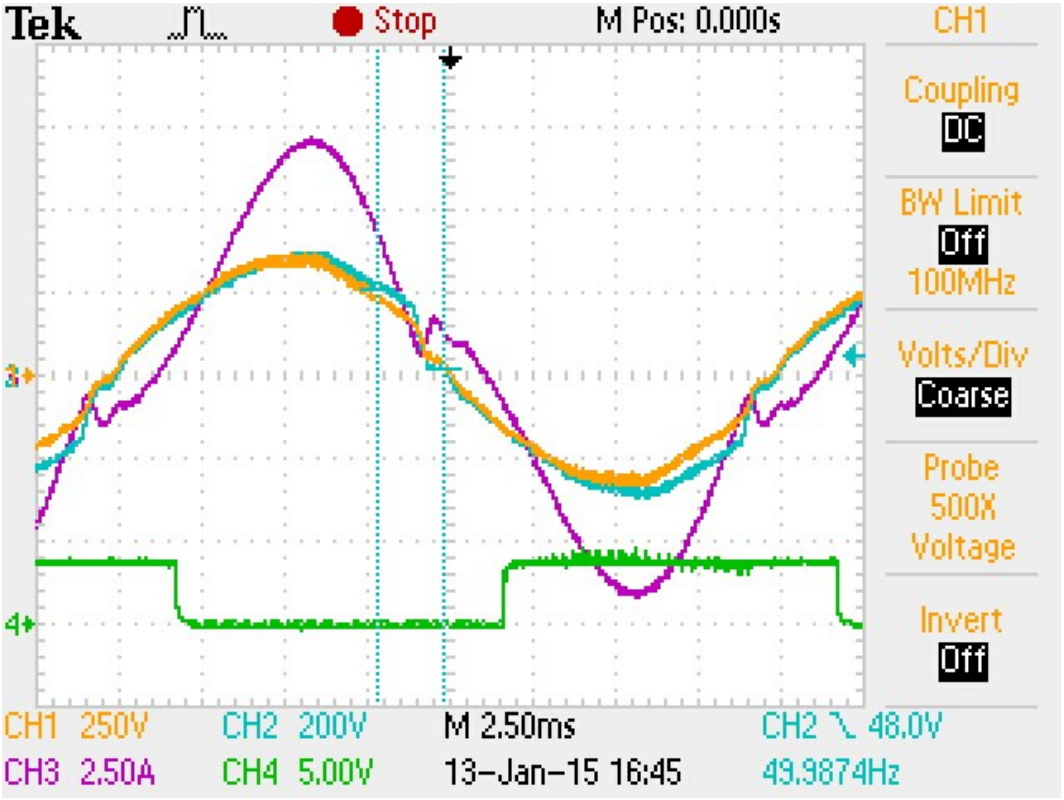

Figure 6-29: AC Chopper - Microwave Operation - Full Load. The Yellow Waveform is the Voltage Input, the Purple Waveform is the Current Output, the Blue Waveform shows the Voltage Output, the Green Waveform shows the Control Circuitry Operation Which Changes the Current Commutation Mode

6. 4. AC Chopper Discussion

This section will discuss the results from the practical circuit. Sections 4. 1. 2. 3. and 5. 2. simulated the AC Chopper circuit and found it to be a viable method of enhancing the LV distribution infrastructure but only if three important conditions were met.

1. The circuit must have an extremely high efficiency
2. The circuit must be able to provide a high quality waveform to the end-user
3. The circuit must be affordable

These are not the only aspects to consider, problems such as size and maintainability are also important. However these three issues were considered vital.

From the results in this section we address the first two points. It was found that no matter what type of load was used the AC Chopper has a high efficiency of 95% or higher. The only exception to this is when a low amount of power is drawn and arguably in these circumstances the amount of power drawn is so small that the efficiency of the circuit is not as important.

It was also found that the power quality of the circuit is always below 5% voltage distortion seen by the consumer. In fact considering the initial grid voltage distortion of 1.77% the voltage distortion "seen" by the consumer was found to be 2-2.5%, therefore very little harmonic distortion has been added to the waveform.

The most intriguing results are those provided via the use of a microwave oven. Overall the amount of current distortion "seen" by the network has lessened, but a greater voltage distortion is "seen" by the user.

Whilst still not outside any regulatory limits as described in Section 2. 1. 4. , the inclusion of the AC Chopper circuit has increased the level of voltage distortion. The increased voltage distortion may be due to the harmonic voltage drop across the filter.

The issue of cost will be further explored in Chapter 7.

Therefore from the results collected so far, PUVR via the use of an AC Chopper is a viable prospect. However an exploration of ways to further increase the power quality in particular that of the output voltage waveform would be recommended as a next step.

6. 5. AC Chopper and Auto-Transformer Hybrid Circuit

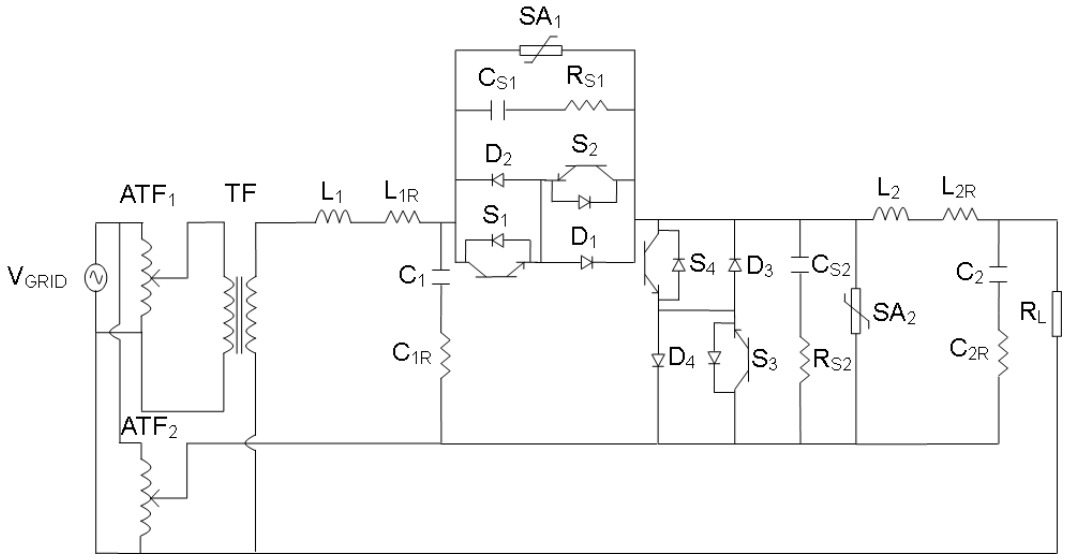

Figure 6-30: Practical AC Chopper with Auto-Transformer Circuit Diagram

In order to increase the power quality of the AC Chopper circuit a variant of the circuit was tested which included an additional auto-transformer with the premise that, if the voltage is partly transformed and partly converted by the chopper circuit the distortion generated should be diminished. However the output voltage will still maintain the level of control offered by the use of power electronics over traditional transformers.

The architecture shown in Figure 6-30 was known to not be the most optimal experimental set up.

To elaborate, best practice would be to have the transformer, TF, before the auto-transformers, ATF1 and ATF2. It can be observed in Figure 6-30 that the galvanic isolation provided by transformer, TF, is not utilised. The reason behind this is purely due to equipment constraints in that the rated voltage of the auto-transformers is 230V and therefore cannot be placed after the transformation up to 460V.

It is recommended that if any future attempt is made at demonstrating this architecture, the boosting transformer will first transform the voltage to 460V and subsequently two 460V rated auto-transformers are supplied from this in parallel operation.

6. 5. 1. Additional Equipment

Only one additional piece of equipment was required to implement this architecture, an additional autotransformer.

6. 5. 1. 1. Additional Variac (Auto-transformer)

The additional auto-transformer required is shown diagrammatically in Figure 6-30 as component ATF_2. As with the first auto-transformer it has a rating of 230V at a steady state current of 6A.

6. 6. AC Chopper and Auto-Transformer Hybrid Results

With the initial equipment described in Section 6. 1. 1. , the additional equipment described in Section 6. 5. 1. and using the original methodology described in Section 6. 1. 2. the following results were gained.

As before, these results compare the efficiency of the AC Chopper circuit and the voltage and current total harmonic distortion against increasing input power. The input power is increased via the auto-transformers. In general ATF_1 and ATF_2 are increased equally. However during operation a fault in the circuit was perceived and therefore, for the sake of diligence, the maximum supplied voltage of ATF_2 is 80V. After collecting results the perceived fault was identified to be an incorrect setting on a measurement transducer. Therefore there is no reason to believe that there is any inherent fault due to the circuit architecture. Results were not re-recorded as the recorded results are still valid. Section 6. 6. 3. is the only exception to this as these results were recorded after finding the fault. In this section only 75V of the waveform was chopped and the remaining voltage transformed by ATF_2.

The results have been overlaid with the results from Section 6. 3. to provide a clear comparison.

6. 6. 1. Unity Power Factor Load

For a power level of up to 1kVA the results recorded are shown graphically in each individual section.

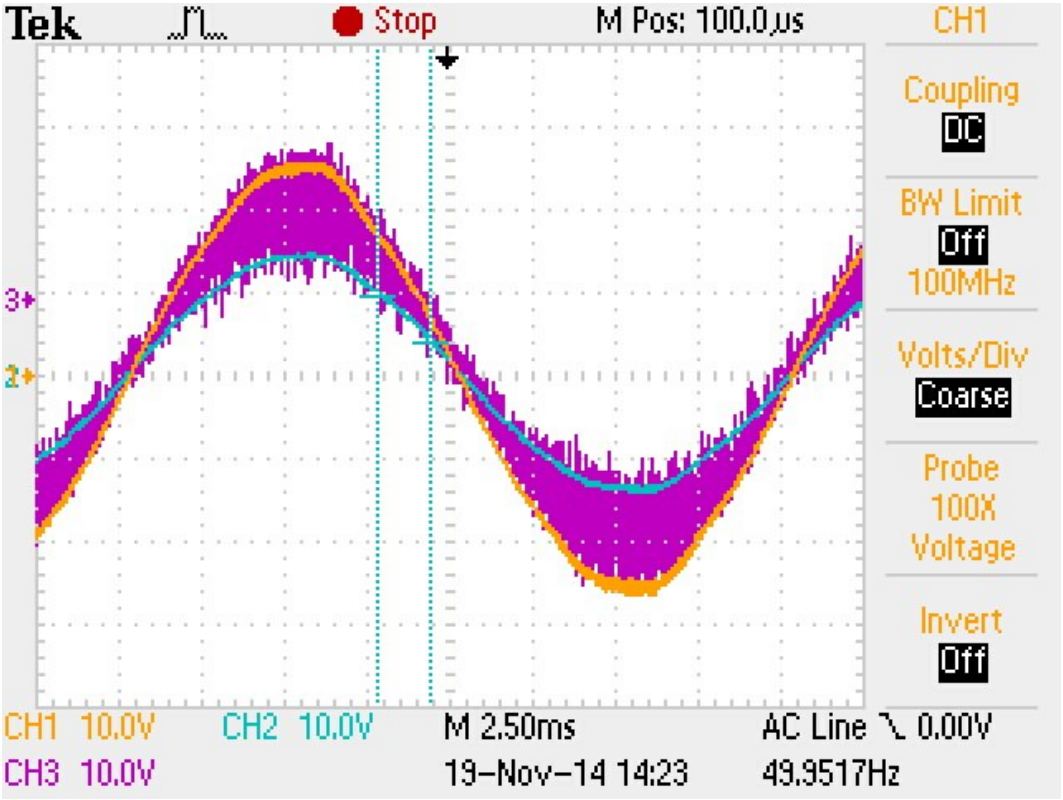

Figure 6-31: Sample Result of AC Chopper and Auto-Transformer Hybrid Operating with a Unity Power Factor Load. The Yellow Waveform is the Input Voltage, the Blue Waveform is the Magnitude of Transformed Voltage, the Purple Waveform is the Magnitude of Converted Voltage.

An excel spreadsheet entitled “All Practical Results”, is supplied on the accompanying CD which details each data point recorded. The first study records the efficiency and THD of the AC Chopper and auto-transformer hybrid circuit with a load of unity power factor.
A sample result is shown in Figure 6-31 which demonstrates the waveforms found with the operation of the AC Chopper with auto-transformer hybrid driving a unity power factor linear load.

6. 6. 1. 1. Efficiency Results

The results are shown graphically in Figure 6-32. It can be observed that results fall within the expected region of efficiency providing validation. Interestingly the curve of the efficiency is less steep and takes a greater amount of power to plateau. Upon consideration this is sensible as the nature of this curve was previously attributed to the conduction loss and the relative magnitude of the conduction loss in comparison to the operating power level, described in Section 6. 3. 1. 1.
Considering that a part of the voltage is now being transformed it is reasonable to assume that less power is being converted by the AC Chopper. This results in a shift backwards in operating point, therefore the shallower slope also serves to validate the results gained.
The maximum efficiency observed was approximately 97% with a rising trend; this is different to previously gained results for the standalone AC Chopper which suggested a plateau of approximately 97% efficiency.

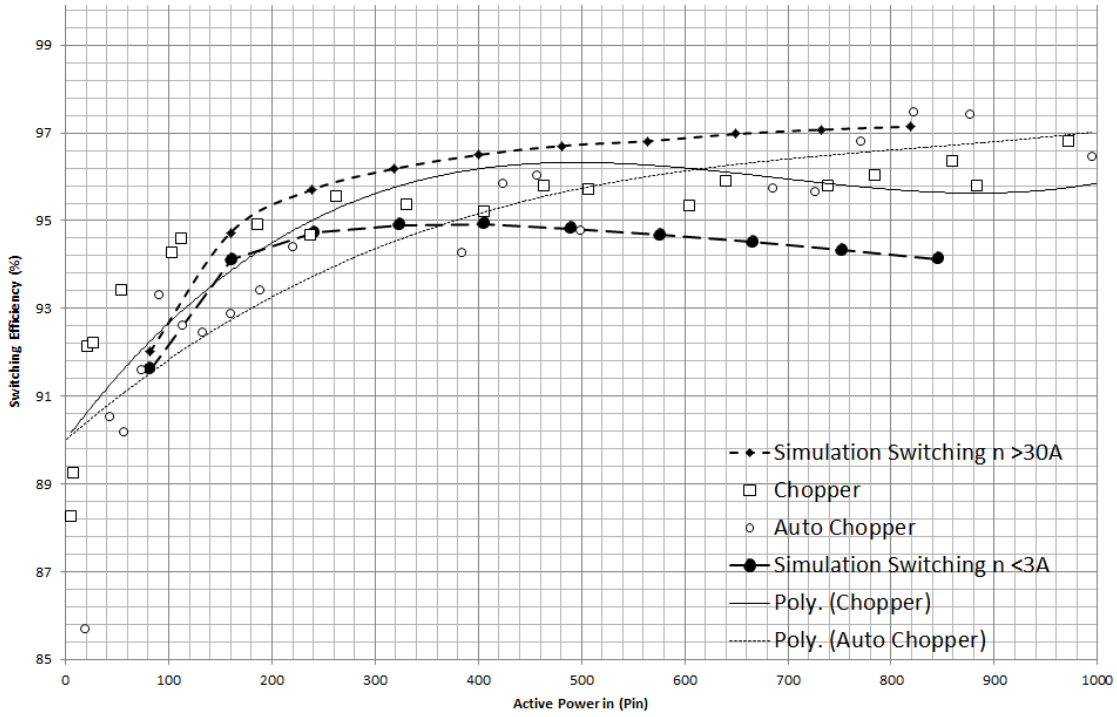

Figure 6-32: AC Chopper and Auto-Transformer Hybrid - Resistive Load - Switching Efficiency at Various Power Levels. The Simulation Results Use Semiconductor On-State Resistance Characteristics at <3A and >30A in order to provide a Window for the Results

This is in line with expectations as the hybrid converter switches at a lower voltage level but the level of current remains the same, therefore it is expected that the conduction loss is the same as the standalone AC Chopper architecture and that some efficiency gains would be made with regard to switching loss.

The marginal gain in efficiency is considered reasonable as the change in architecture was designed to facilitate a better power quality performance rather than an increase in operating efficiency.

6. 6. 1. 2. THD Results

The THD results gained from the practical implementation of the AC Chopper with auto-transformer is shown graphically in Figure 6-33 and Figure 6-34. From Figure 6-33 it can be observed that the AC Chopper and auto-transformer hybrid circuit delivers better power quality in terms of output voltage THD with an average operating voltage THD of 1.5% compared to the standard AC Chopper's average operating voltage THD of 2%. In fact, considering that the standard grid conditions were measured as 1.77% voltage THD the AC Chopper with auto-transformer hybrid was observed to improve power quality.

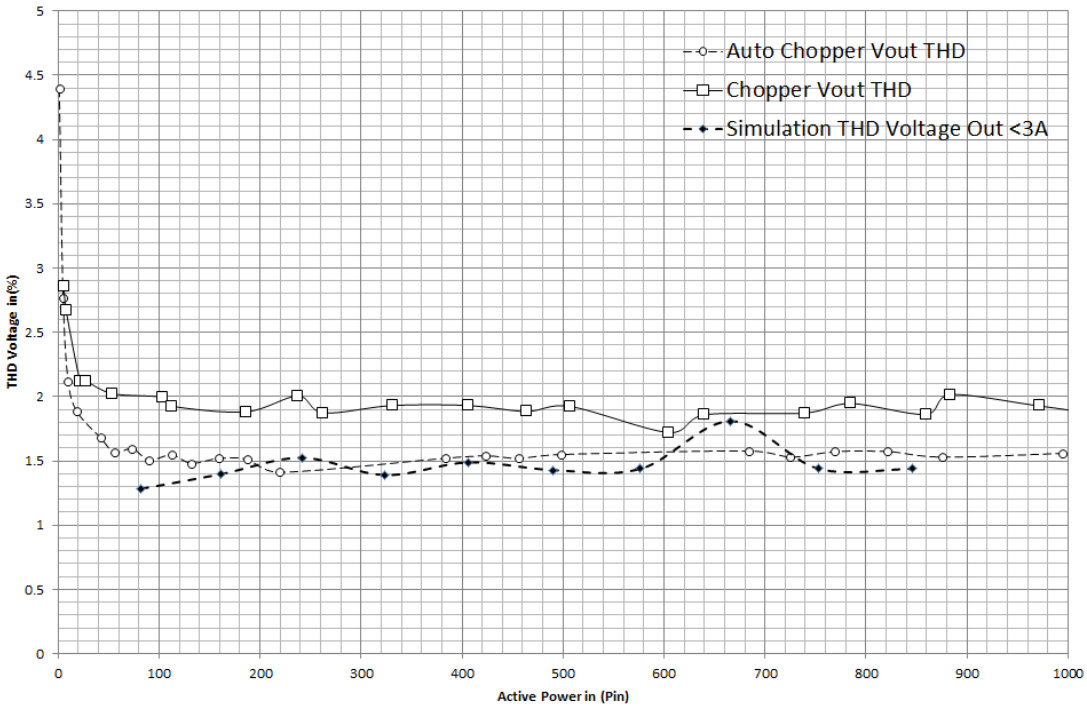

Figure 6-33: AC Chopper and Auto-Transformer Hybrid - Resistive Load - Output Voltage THD at Various Power Levels

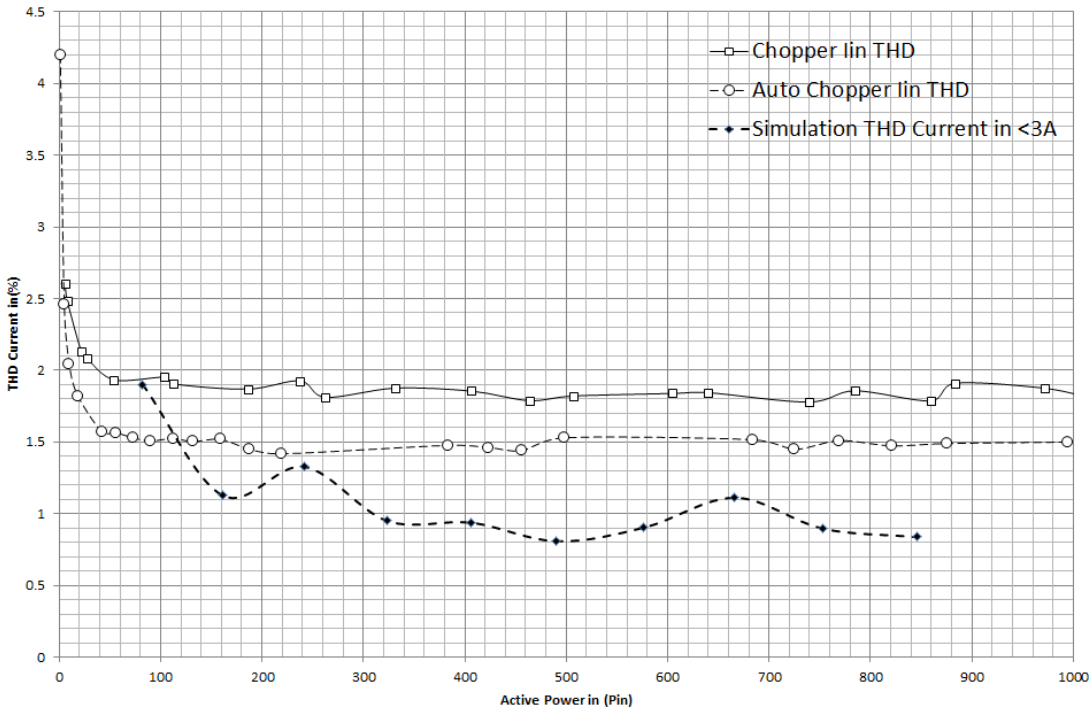

Figure 6-34: AC Chopper and Auto-Transformer Hybrid - Resistive Load - Input Current THD at Various Power Levels

Figure 6-34 shows the input current THD, as before it can be observed that harmonic content has dropped by 0.5% from 2% to 1.5% as a result of incorporating a second auto-transformer into the design.

6. 6. 2. Non-Unity Power Factor Load

The second study records the efficiency and THD of the AC Chopper incorporating an additional auto-transformer with a load of non-unity power factor. A sample result is shown in Figure 6-35 which demonstrates the waveforms found with the operation of the AC Chopper with auto-transformer hybrid driving a unity power factor linear load.

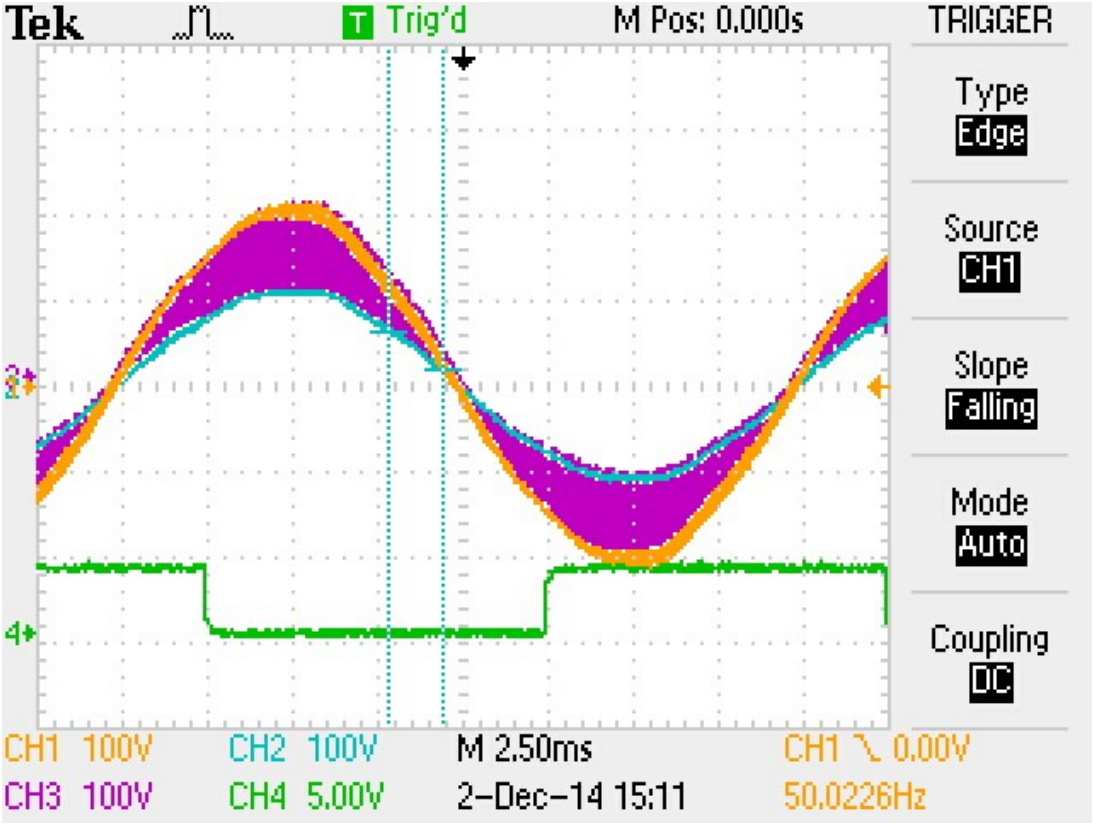

Figure 6-35: Sample Result of AC Chopper and Auto-Transformer Hybrid Operating with a Non-Unity Power Factor Load. The Yellow Waveform is the Input Voltage, the Blue Waveform is the Magnitude of Transformed Voltage, the Purple Waveform is the Magnitude of Converted Voltage, the Green Waveform shows the Control Circuitry Operation Which Changes the Current Commutation Mode

6. 6. 2. 1. Efficiency Results

The results shown in Figure 6-36 show the same trends as Figure 6-32, which further validates simulated and practical results.

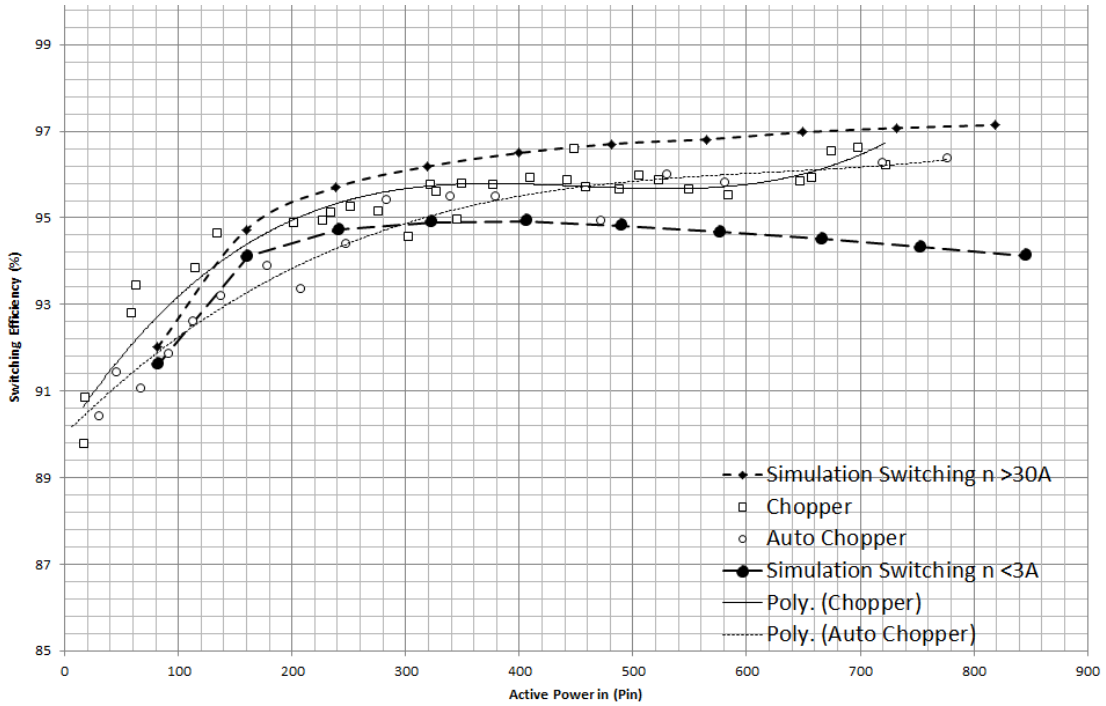

Figure 6-36: AC Chopper and Auto-Transformer Hybrid - Resistive and Inductive Load - Switching Efficiency at Various Power Levels. The Simulation Results Use Semiconductor On-State Resistance Characteristics at <3A and >30A in order to provide a Window for the Results

A maximum efficiency of approximately 96.7% is observed, maximum efficiency of the standard AC Chopper is shown to be approximately 96.8%. This comparison is considered to be reasonable as no increase in efficiency was anticipated.

6. 6. 2. 2. THD Results

The results from THD measurement are shown in Figure 6-37 and Figure 6-38. The output voltage THD is shown in Figure 6-37; the results clearly show a decrease in harmonic content when an auto-transformer is incorporated into the circuit.

The output voltage THD stays at approximately 0.9%, decreased from approximately 2.4%. Therefore a reduction of approximately 1.5% THD was observed in the voltage output.

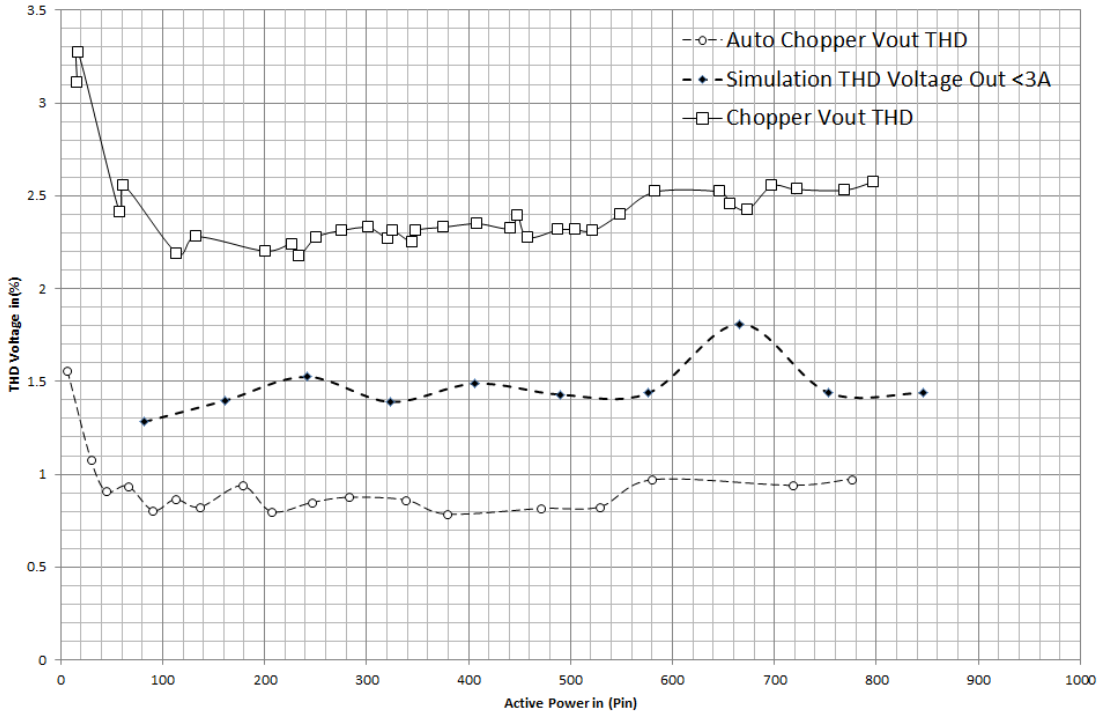

Figure 6-37: AC Chopper and Auto-Transformer Hybrid - Resistive and Inductive Load - Output Voltage THD at Various Power Levels

The current THD is shown in Figure 6-38, the harmonic content varies consistently so in this case it is difficult to approximate the THD as one value. However, it can be observed that the maximum input current THD from the AC Chopper with auto-transformer is equal to 1.2% compared to a maximum of 1.28% without the auto-transformer. It can also be observed that the THD of the auto-transformer variant is consistently lower.

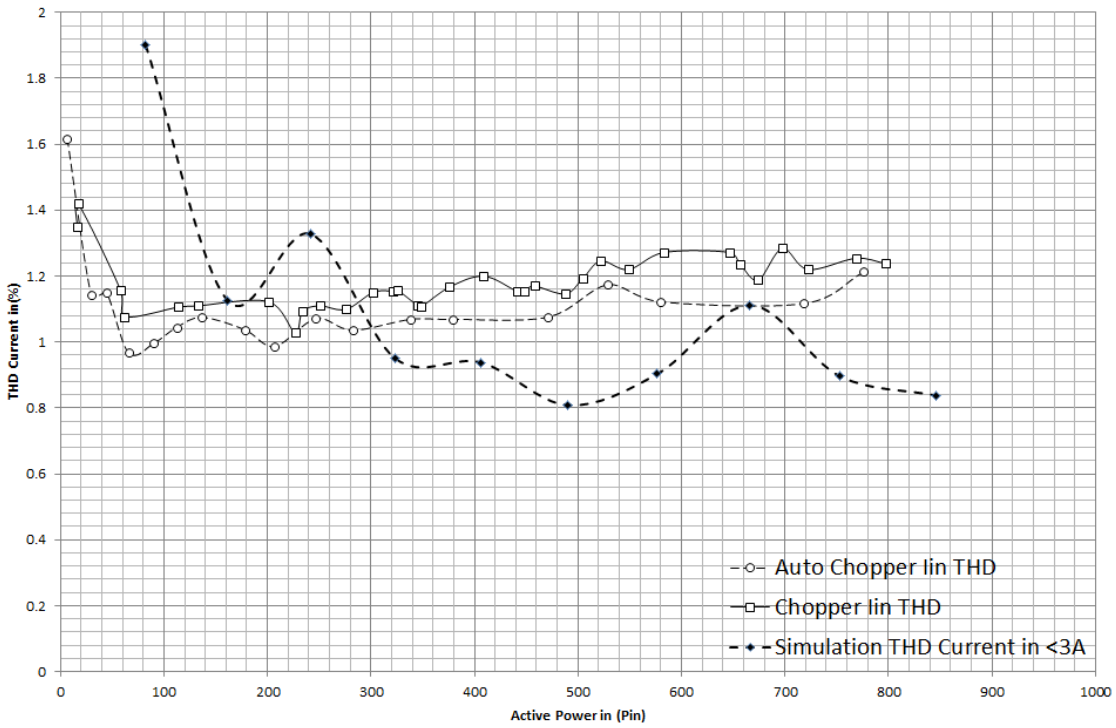

Figure 6-38: AC Chopper and Auto-Transformer Hybrid - Resistive and Inductive Load - Input Current THD at Various Power Levels

6. 6. 3. Non- Linear Load

The non-linear load is practically modelled via a microwave. Unlike the other load types this non-linear load only has one operating point and therefore only one set of results can be taken. A demonstration of this circuit is available in the supplied CD.

The results taken are shown in Table 6-4. Note that the long averaging technique used for measurements in Section 6. 3. 1. and Section 6. 3. 2. could not be used in this instance due to the transient nature of the microwaves operation therefore results are subject to greater measurement error.

The results show that standard operation of the microwave without using the chopper circuit generates a very high amount of harmonic current. The waveforms of the microwave operation are shown in Figure 6-28 and Figure 6-29.

Table 6-5: AC Chopper and Auto-Transformer Hybrid - Microwave Load - Efficiency, Voltage THD and Current THD

Microwave	η (%)	V_{THD} (%)	I_{THD} (%)
Standard	-	1.75	24.35
Standby	88.3	2.02	11.6
Full Load	97.2	9.49	20.9

From the table it can be observed that in line with results from previous sections at low power levels the efficiency of the AC Chopper is low at approximately 88.3%. However at high power levels the efficiency is very high at 97.2%. It can also be observed that the voltage distortion is 9.49% and current distortion 20.9%.

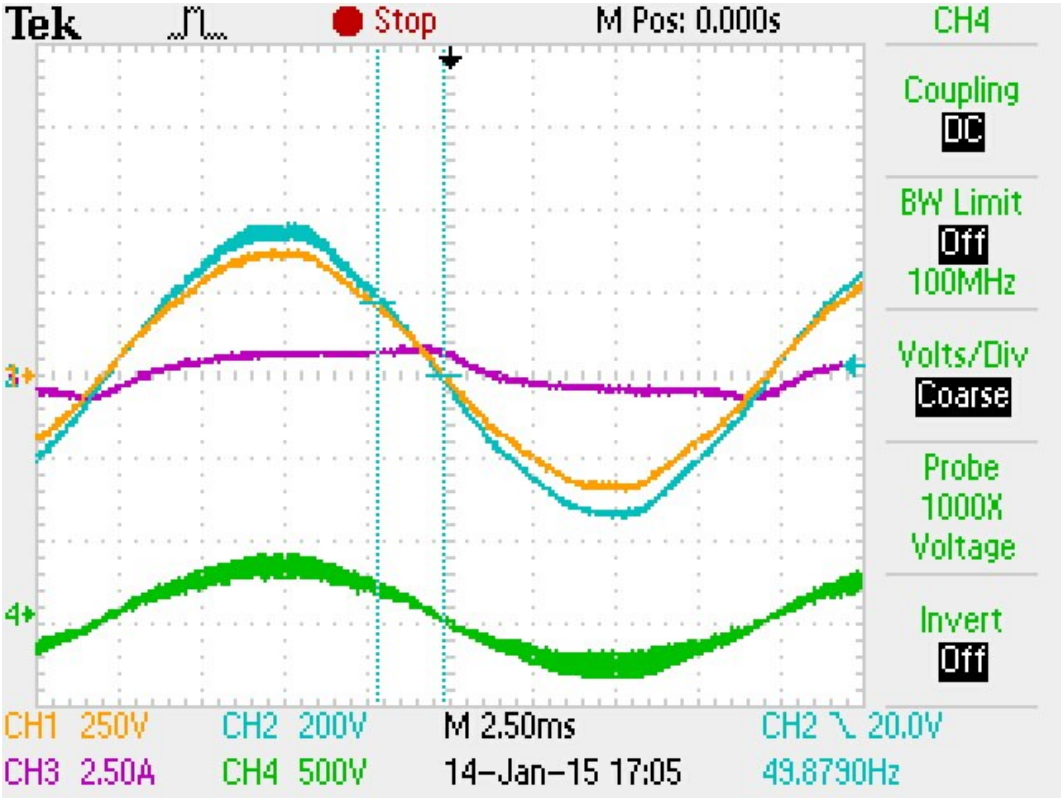

Figure 6-39 - AC Chopper and Auto-Transformer Hybrid - Microwave load - Standby Mode. The Yellow Waveform is the Voltage Input, the Purple Waveform is the Current Output, the Blue Waveform shows the Voltage Output, the Green Waveform shows the Magnitude of "chopped" Input Voltage.

From the waveforms it is clear that the current is extremely distorted and that despite this the AC Chopper behaves as normal.

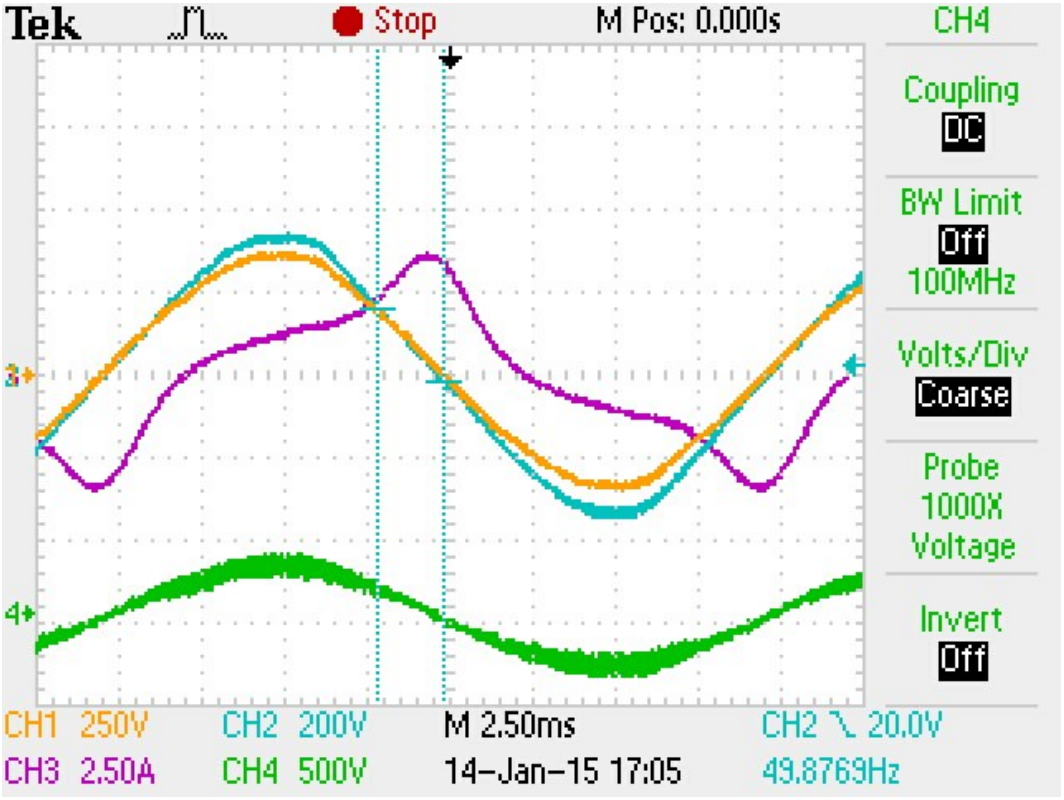

Figure 6-40- AC Chopper and Auto-Transformer Hybrid - Microwave load - Charging Mode. The Yellow Waveform is the Voltage Input, the Purple Waveform is the Current Output, the Blue Waveform shows the Voltage Output, the Green Waveform shows the Magnitude of "chopped" Input Voltage.

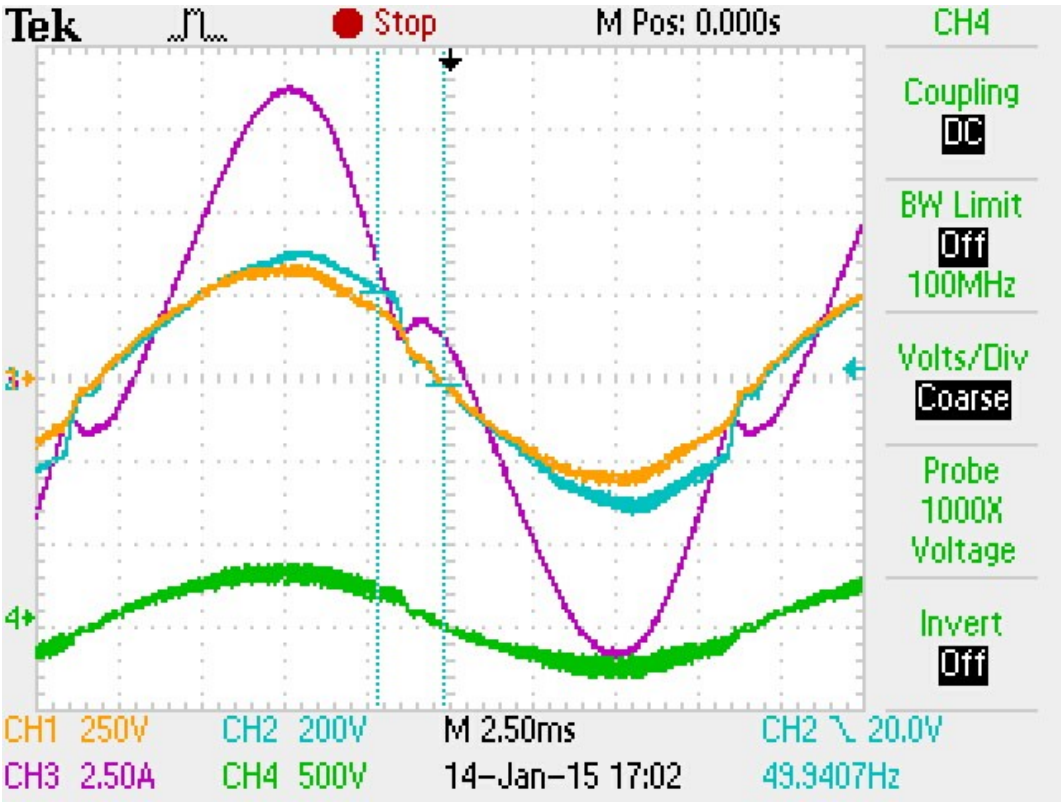

Figure 6-41- AC Chopper and Auto-Transformer Hybrid - Microwave load - Full Load. The Yellow Waveform is the Voltage Input, the Purple Waveform is the Current Output, the Blue Waveform shows the Voltage Output, the Green Waveform shows the Magnitude of "chopped" Input Voltage.

6. 7. AC Chopper and Auto-Transformer Hybrid Discussion

This section will discuss the results gained from Section 6. 1. and 6. 3. and ascertain if the AC Chopper and Auto-Transformer Hybrid is a more suitable architecture for PUVR.

6. 7. 1. Loss Comparison

A summary of efficiency results is tabulated in Table 6-6. From these results it is clear that the efficiency of the new architecture is similar to the efficiency of the old architecture. Therefore no efficiency gains were made by adding the auto-transformer to the circuit.

Table 6-6: Summary of Efficiency Results

Maximum Efficiency	Unity Power Factor (%)	Non- Unity Power Factor (%)	Non- Linear Load (%)
AC Chopper	97	96.8	98.1
AC Chopper and ATF Hybrid	97	96.7	97.2

However, as the amount of voltage that is converted can be varied it becomes possible to consider further changes in circuit design. In Figure 6-39, Figure 6-40 and Figure 6-41 it can be observed that the amount of voltage converted is very small (green waveform). The magnitude of the chopped waveform was a maximum of $75V_{RMS}$, with this level of voltage a 200V MOSFET could be used to replace the circuit IGBTs resulting in a circuit architecture shown in Figure 6-42.

This would further reduce the conduction loss due MOSFETs very low on-state resistance and reduce harmonic content due to the higher switching frequencies possible with MOSFETS [53].

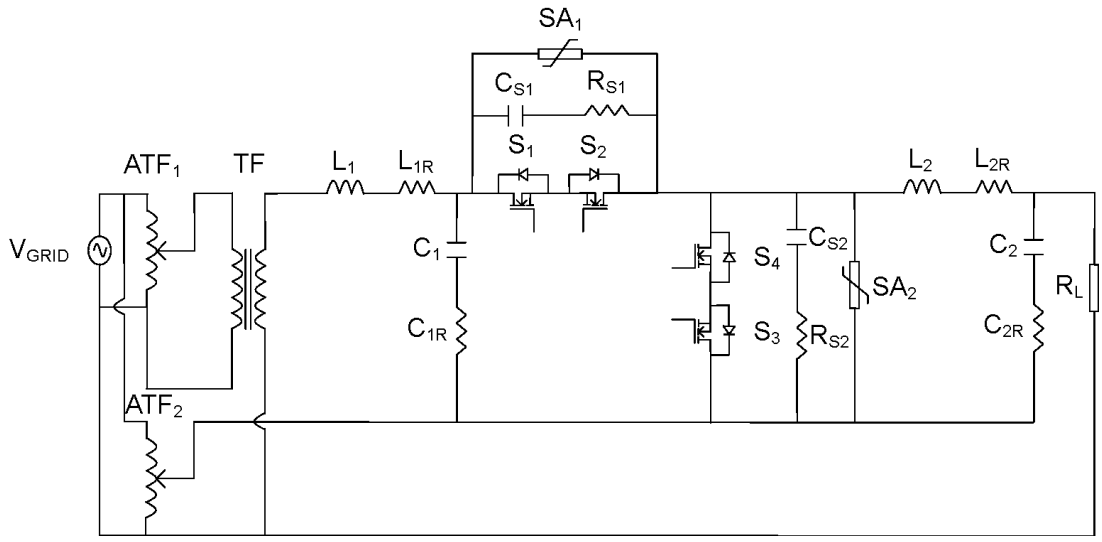

Figure 6-42: Practical AC Chopper with Auto-Transformer Hybrid MOSFET version

6. 7. 2. THD Comparison

A summary of results from the practical measurements is shown in Table 6-7. It was found that the AC Chopper and auto-transformer hybrid improved both the voltage and current THD for loads of power factor 0.75 or greater. This was in line with expectation as less of the waveform is subject to high frequency switching.

What was not expected was the large increase in voltage THD when a non-linear load was energised. This large increase is due to the line impedance added by the additional auto-transformer. Current distortion caused by non-linear loads can essentially be thought of as current sources in shunt with the load injected into the power system. When this injected current passes through a linear resistance a varied voltage is dropped over the element effectively causing voltage distortion [65].

Table 6-7: Summary of Power Quality Results

Average THD_V / Average THD_I	Unity Power Factor (%)	Non- Unity Power Factor (%)	Non- Linear Load (%)
AC Chopper	1.9	2.4	4.9
	1.9	1.2	22.3
AC Chopper and ATF Hybrid	1.5	0.9	9.49
	1.5	1.1	20.9

The current harmonics generated by the microwave load is substantial in terms of magnitude and level of distortion. While this is not against any regulations described in Section 2. 1. , it is cause for concern and any device which introduces a line impedance should be tested with this load so that the level of voltage distortion can be deduced.

6. 7. 3. Suggested Architecture

In terms of efficiency, there was no observed appreciable difference between the AC Chopper and the AC Chopper and auto-transformer hybrid. However it is expected that using the MOSFET version of the AC Chopper with auto-transformer, suggested in Section 6. 7. 1. , Figure 6-42, will be of greater efficiency due to higher switching frequency i.e. less switching loss and small $R_{DS(ON)}$ of MOSFETs [53]. Therefore in terms of efficiency the AC Chopper with auto-transformer hybrid is the suggested architecture.

In terms of power quality, the AC Chopper provides adequate performance with harmonic distortion of linear loads never exceeding 2.5% THD, even when the source voltage is already distorted. However the AC Chopper with auto-transformer hybrid for linear loads a power quality improvement has been observed, with voltage distortion dropping from 1.77% to as low as 0.9%.

For non-linear loads however, the standard AC Chopper offered better performance as the voltage THD equalled 4.9% compared to the ac chopper with auto-transformer hybrid voltage distortion of 9.49%.

As established in Section 2. 1. 4. a voltage THD supplied to the customer of greater than 5% is unacceptable in the UK distribution grid, therefore while the AC Chopper with auto-transformer performs better in terms of power quality with linear loads, due to the fact that it cannot supply a common household non-linear load without breaching distortion limits, it is not suitable for PUVR. However PUVR still remains viable using the original AC Chopper architecture.

6. 8. Chapter Summary

The efficiency and power quality results from the practical experiments with the AC Chopper are in line with predicted values from simulation, reaching a maximum efficiency of 97%. The harmonic distortion was found to never breach any established limits. The AC Chopper with auto-transformer hybrid was found to have a similar level of efficiency but improved the power quality by decreasing the voltage distortion seen by the user for linear loads. However it was found that for non-linear loads, due to the line impedance introduced by the auto-transformer, voltage distortion exceeded the 5% limit described in ENA Engineering Recommendation G5/4 with values of voltage distortion as high as 9.5% being observed. Therefore the AC Chopper with auto-transformer hybrid is not acceptable for use with PUVR and that other methods of increasing efficiency and power quality must be used.

CHAPTER 7

7. Updated Cost-Benefit Analysis

Using the results previously gained in Section 4. 1. 2. 3. and the AC Chopper design from Chapter 6. a new cost benefit analysis can be performed which utilises the AC Chopper design in lieu of off-the-shelf back-to-back converters. This will inform on whether the use of the AC Chopper has made PUVR more or less viable as an alternative to standard network re-enforcement

7. 1. Cost-Benefit with AC Chopper Methodology

It has been established that the AC Chopper is a viable architecture for PUVR in terms of efficiency. However it has yet to be proven viable in terms of cost. Therefore a second cost-benefit analysis has been carried out which evaluates the costing of the practical AC Chopper circuit for use in PUVR compared to network reinforcement.

The costing of the AC Chopper was calculated based on available cost data for the following components:

- one microcontroller [97]
- two filter inductors [83]
- one heatsink [98]
- four drivers [99]
- two transducers [100]
- two filter capacitors [101]
- two varistors [102]
- four IGBTs [103]
- four diodes [104]
- two snubbers [105, 106]

After costing information was gathered, a spreadsheet was produced entitled “Updated CB”, available on provided disc, which calculated the aggregated cost for one AC Chopper unit and two-hundred and twenty AC Chopper units. This is the amount of three bedroom houses in a representative section of the urban UK network, as was used previously in Sections 4. 2. and 4. 1. 2. 3. to establish a comparison between cable reinforcement and PUVR.

The minimum cost takes into account economies of scale and uses the costing information as if two-hundred and twenty units were being manufactured. The maximum cost does not take economies of scale into consideration. It is also worth noting that the cable replacement costing does not take into account any costs incurred due to customer inconvenience e.g. any necessary close of business’s to proceed with works and that the PUVR costing does not take into account any labour, manufacturing, profit margin or maintenance costs.

7. 2. Cost-Benefit with AC Chopper Results

The results of the updated cost-benefit analysis are shown in Table 7-1. It can be observed that the minimum cost favours network reinforcement as the minimum cost of PUVR with the AC Chopper is £54,000 more expensive. However the maximum cost favours PUVR with the AC Chopper as network reinforcement is £162,000 more expensive.

Table 7-1: Updated Cost-Benefit Analysis

Proposed Method	Cost of Transformer Replacement (£1,000)		Cost of Cable Replacement (£1,000)		Cost of Converters (£1,000)		Total Cost (£1,000)	
	Min	Max	Min	Max	Min	Max	Min	Max
PUVR Method with Off-the-Shelf Components	13.8	69.2	-	-	622	1,336	635.8	1,405
PUVR Method with AC Chopper	13.8	69.2	-	-	210	245	223.8	314.2
Cable Replacement Method	-	-	169.7	476.6	-	-	169.7	476.6

7. 3. Cost-Benefit Discussion

From the results shown in Table 7-1 it was found that in terms of cost, network enhancement via the use of AC Chopper circuits is a viable alternative to network reinforcement.

This is an improvement over the previous cost-benefit analysis shown in 4. 2. and Table 4-3. which showed that using off-the-shelf converters based on the back-to-back topology PUVR was not a cost viable compared to network reinforcement.

7. 4. Chapter Summary

An updated cost-benefit analysis was carried out using available costing data from an internet retailer, knowledge of the equipment required from Chapter 6. and data previously collected in Section 4. 1. 2. 3.
From this information it was found that implementing PUVR with an AC Chopper circuit is viable in terms of cost as it is roughly equivalent or cheaper in comparison with standard network reinforcement.

CHAPTER 8

8. Controlled Harmonic Elimination

It has now been established that the AC Chopper circuit is viable for use in PUVR in terms of cost and efficiency but as discussed in Chapter 5. It was also necessary for the AC chopper to improve the power quality in order to be considered a viable alternative to network reinforcement. This was attempted with a new architecture incorporating an auto-transformer that would limit the amount of waveform converted; this was successful with household linear loads however this was found to breach set UK voltage THD limits when energised with household non-linear loads, see Section 6. 6. 3. Therefore other avenues of power quality improvement were explored. It is possible to improve the power quality via an improved control system which dynamically controls the modulation index to eliminate harmonics; this concept will be further explored in this Chapter.

8. 1. Controlled Harmonic Elimination Methodology

A method was considered which adds a second control loop to the PI control. This is shown in Figure 8-1, this second loop compares the input signal to dynamically control the modulation index. This is achieved by first extracting the frequency of the input voltage by use of a Phase-Locked Loop (PLL), therefore even if the input to the circuit has a high voltage THD, a sine wave of unity magnitude and fundamental frequency (50Hz) in sync with V_{GRID} is produced.

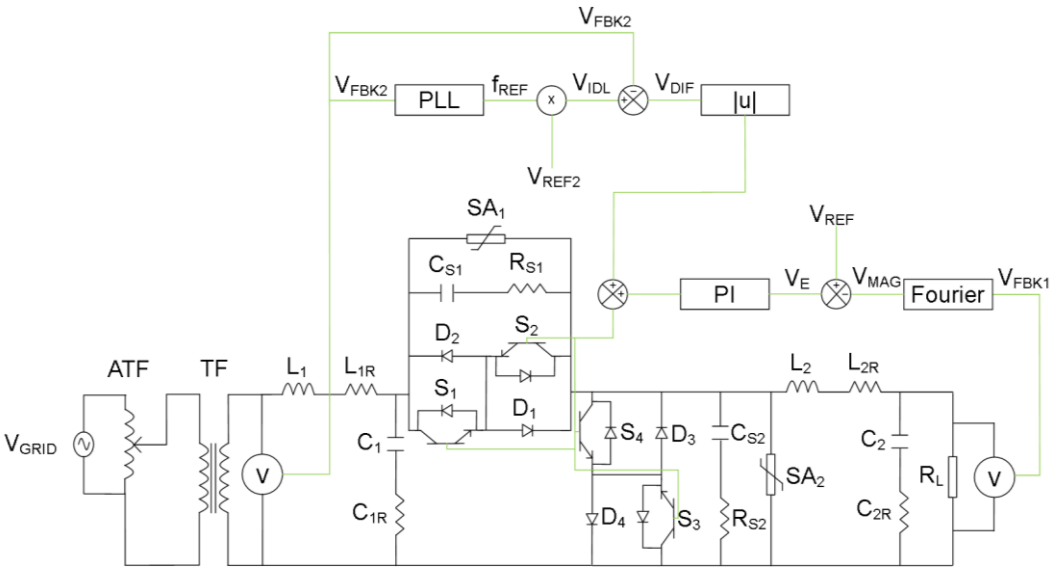

Figure 8-1: AC Chopper Circuit Diagram with Second Control Loop

This signal named f_{REF} in Figure 8-1is then multiplied by the desired amplitude which in this case is 230, now the ideal waveform has been manufactured by the control system, V_{IDL}. This ideal waveform is then compared with the original input waveform and the difference value, V_{DIF} is produced. Therefore any changes from the ideal waveform will be immediately corrected for the end-user via change in modulation index.

The block in Figure 8-1 named |u| produces the absolute value of the input as the output, essentially turning any negative value into the equivalent positive. This is a required step due to the nature of the modulation of a matrix converter, as if the voltage is negative, the change in modulation index must be *positive* to decrease the voltage. The increase in modulation will increase the duty of the negative voltage. More information on the modulation of the matrix converter is available in Section 2. 4.

In order to test and evaluate the harmonic elimination control system, a model was created using Matlab Simulink. This was the same model used in Chapter 5. and Chapter 6. but with the additional control loop shown in Figure 8-1.

To test the effectiveness of the controller in removing harmonics, a source with a high THD must first be created and used with the circuit.

Therefore a diode rectifier was placed in parallel with V_{GRID} in order to produce a voltage source with voltage harmonics of low order (3^{rd}, 5^{th} and 7^{th}) and a magnitude greater than the recommended limit of 5% described in Section 2. 1. 4.

8. 2. Controlled Harmonic Elimination Results

From placing the diode rectifier in parallel to the AC Chopper source (the grid) harmonic distortion was observed in the input current and output voltage of the AC Chopper. The harmonic distortion of input current to the AC Chopper can be observed in Figure 8-2 and Figure 8-3 and the harmonic distortion of output voltage can be observed from Figure 8-4 and Figure 8-5. These figures show that the distorted input voltage to the circuit also provides an equal amount of harmonic current/voltage of approximately 7% THD at steady state.

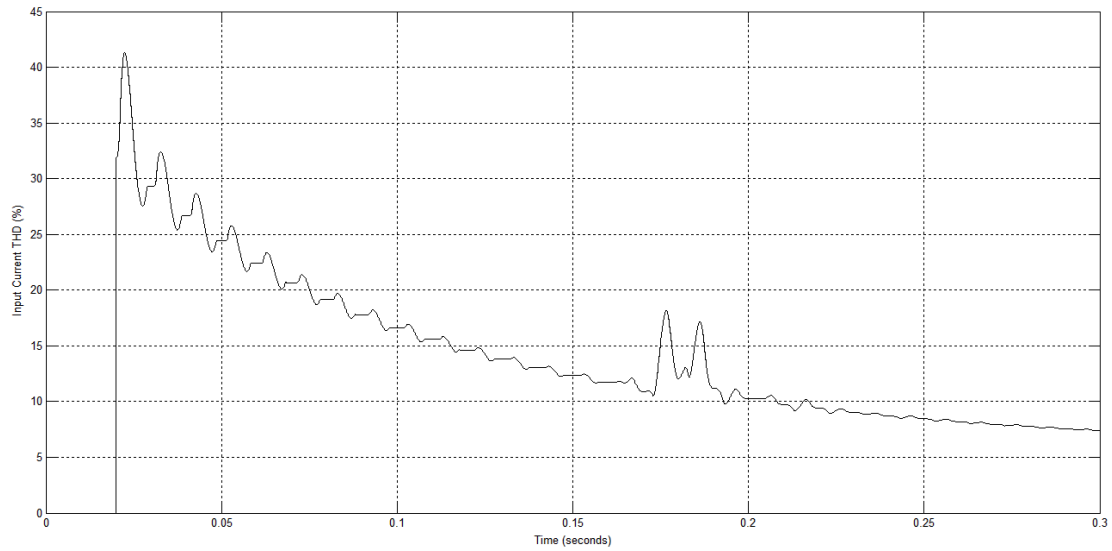

Figure 8-2: AC Chopper without Harmonic Elimination - Input Current THD

It can also be observed that when the input ramps up sufficiently for the PI control to activate the harmonic content is still present in the controlled waveform.

With the second control loop active the observed results are shown in Figure 8-6, Figure 8-7, Figure 8-8and Figure 8-9.

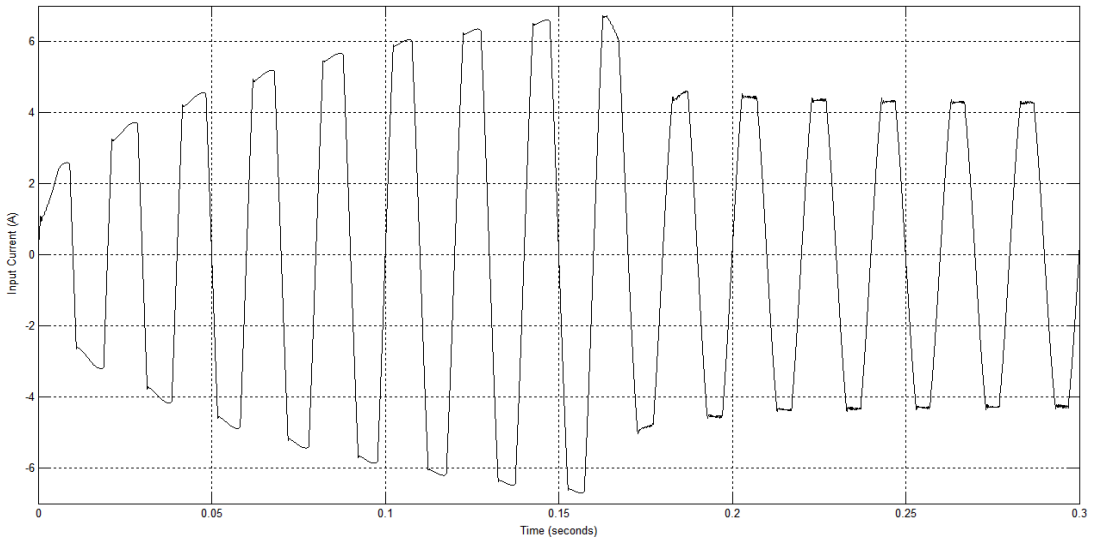

Figure 8-3: AC Chopper without Harmonic Elimination - Input Current

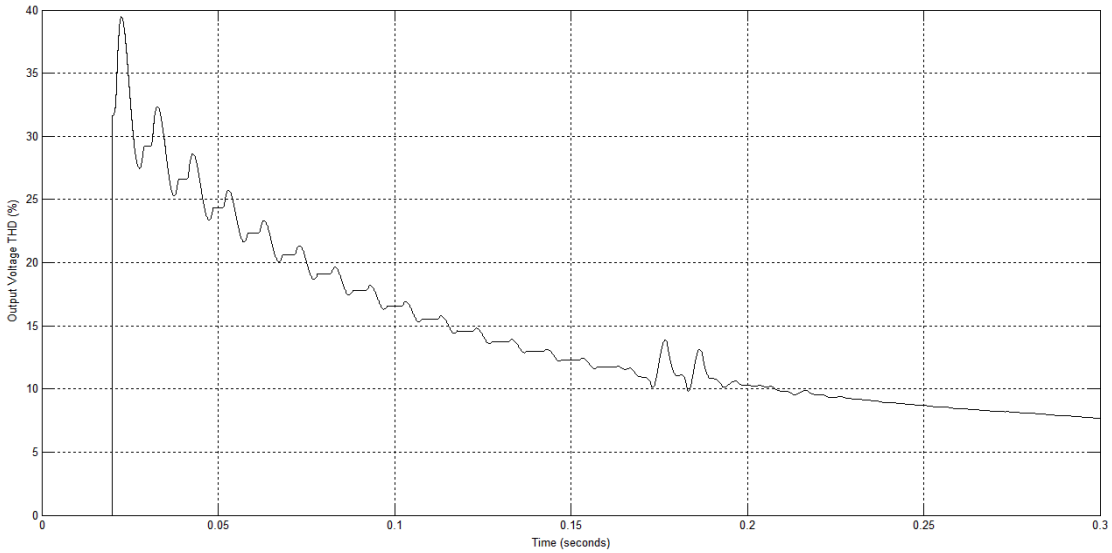

Figure 8-4: AC Chopper without Harmonic Elimination - Output Voltage THD

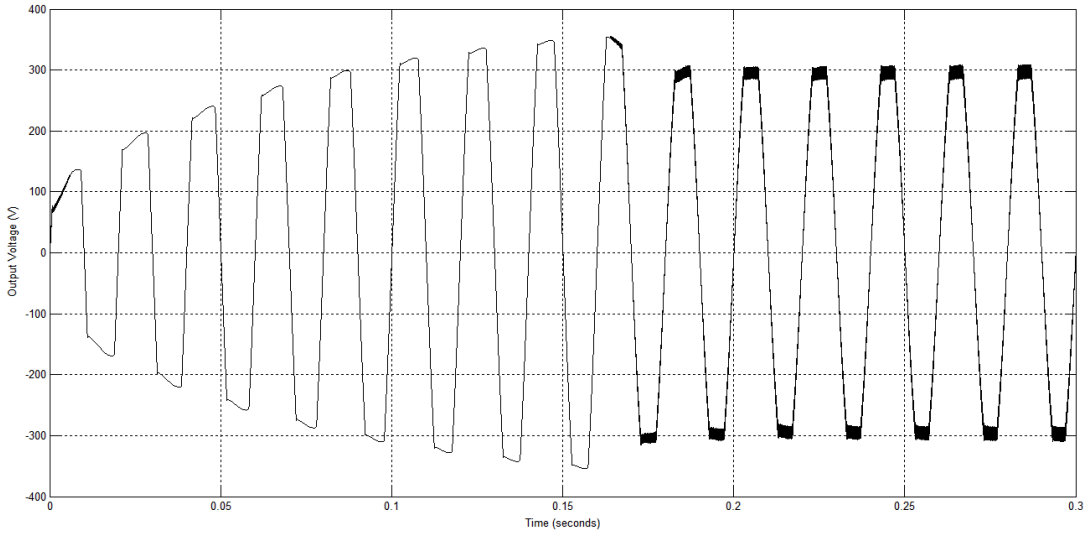

Figure 8-5: AC Chopper without Harmonic Elimination - Output Voltage

It can be seen from Figure 8-6 that the value of input current THD has increased to from 7% to 10% THD and that a corresponding distortion has been added to the input current waveform shown in Figure 8-7.

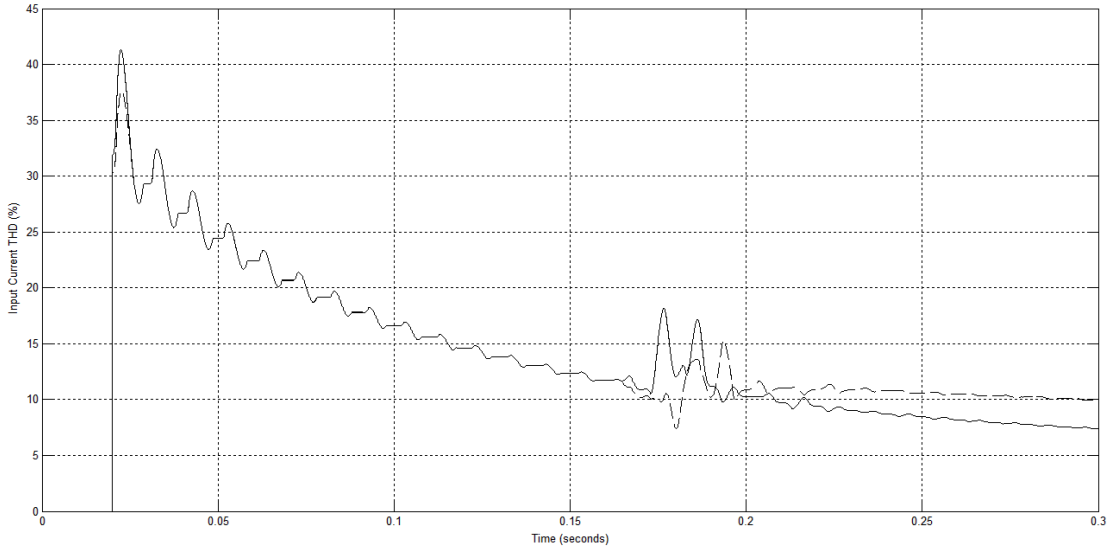

Figure 8-6: AC Chopper with Harmonic Elimination - Input Current THD Solid Line without Second Controller, Dashed Line with Second Controller

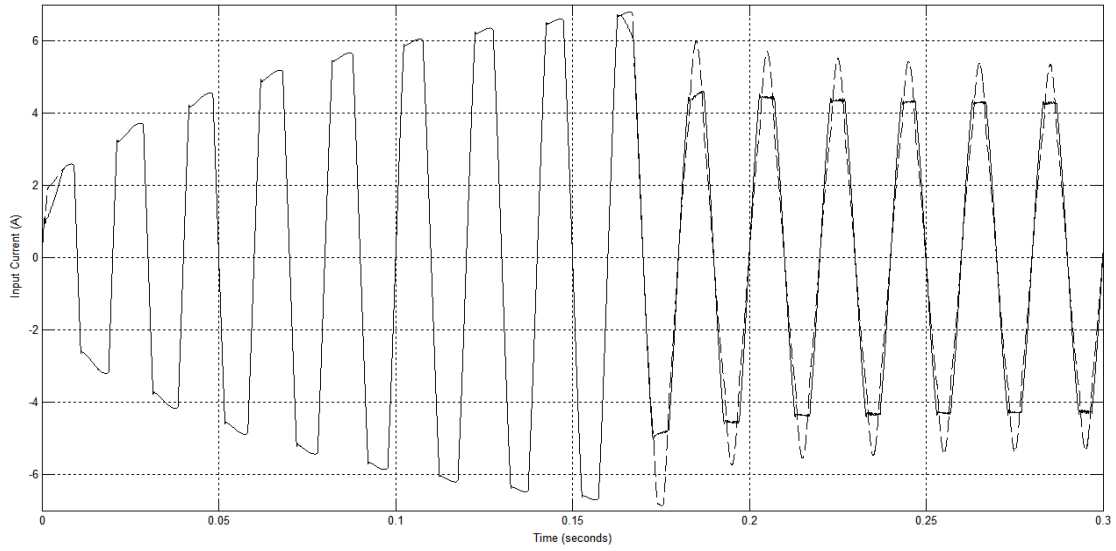

Figure 8-7: AC Chopper with Harmonic Elimination - Input Current - Solid Line without Second Controller, Dashed Line with Second Controller

However it can also be seen from Figure 8-8 that the output voltage distortion has decreased from 7% to 3% and that the corresponding waveform shown in Figure 8-9 is much cleaner than the waveform without the control.

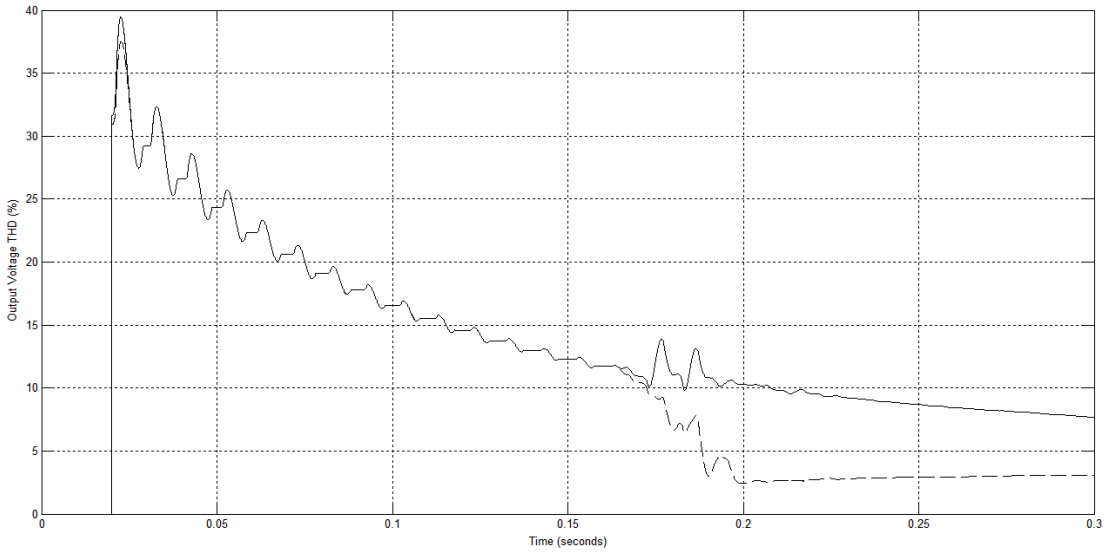

Figure 8-8: AC Chopper with Harmonic Elimination - Output Voltage THD - Solid Line without Second Controller, Dashed Line with Second Controller

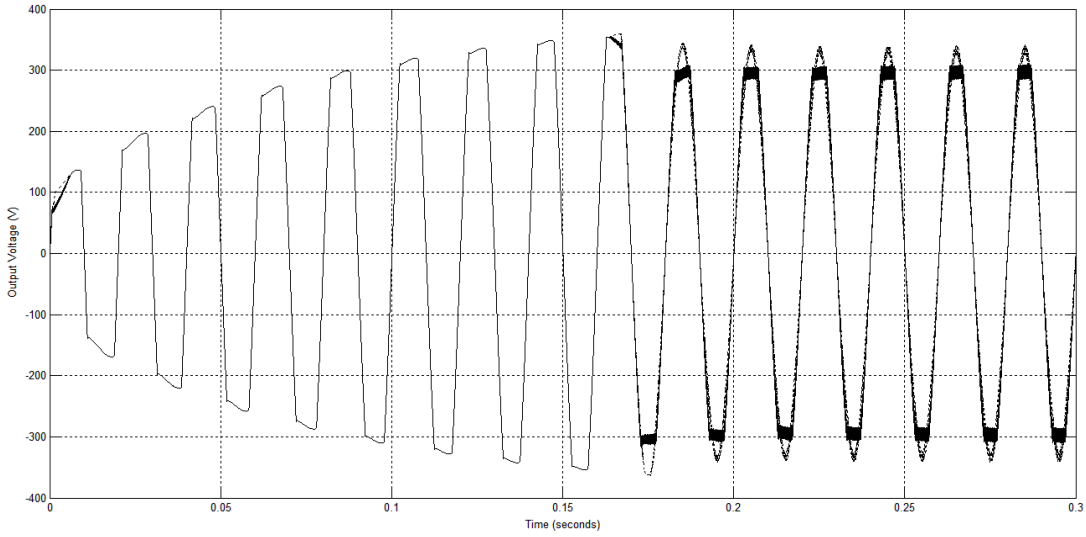

Figure 8-9: AC Chopper with Harmonic Elimination - Output voltage - Solid Line without Second Controller, Dashed Line with Second Controller

8. 3. Controlled Harmonic Elimination Discussion

From the results it is clear that dynamically changing the modulation index with reference to an ideal waveform improves the power quality for the end-user. In this case a decrease of output voltage THD from 7% to 3% was observed which brings the customer to within the recommended harmonic limits of 5% described in Section 2. 1. 4.

This comes at the cost of increasing the harmonic current injected back into the grid; however this is considered to be of less importance due to attenuation of current harmonics upstream of load.

It is also worth noting that these results are only applicable for harmonics of low harmonic order.

8. 4. Chapter Summary

A second control loop was added that compares the input waveform to an idealised version of the same waveform. Any resultant errors were then used to dynamically alter the modulation index of the matrix converter switching. This technique was found to be effective in removing low-frequency harmonics present in the voltage supply to the consumer from the output voltage seen by the consumer. This however comes at the cost of increasing the current harmonics injected back into the grid. However as this is not regulated as the waveform seen by the consumer is, it is considered to be an effective method of increasing the power quality.

CHAPTER 9

9. Conclusion

It was found that the capacity of the network cannot support the predicted increase in load due to current limits on the network. This increase in load would be synonymous with a heat pump boiler or electric vehicle at every household.

To increase the capacity of the network, increasing the voltage level of the system was explored; this is possible as the conductors of the UK LV distribution system were found to have an underutilised insulation limit.

Studies have indicated that increasing the voltage level of the UK LV distribution system will significantly increase the load capacity of urban distribution networks.

The difficulty with this approach is that the end-user receives an unusable voltage supply incompatible with any most household equipment. PUVR was suggested as a possible way of solving this difficulty.

Issues of cost and efficiency were investigated. Results found that for PUVR to be considered viable the efficiency of the converter units in each home must have a maximum lower limit of 93.3% efficiency and the cost per unit must inexpensive and estimated to be between £460-£2100. These limits at the very least provided on-par results with traditional network reinforcement.

With these limits in mind, an evaluation of AC-AC converter architectures was undertaken with these limits as important selection criteria.

Of the two possible system architectures considered, it was made clear that an AC Chopper architecture has several advantages over a back-to-back inverter system. The AC Chopper was found to generate less loss, cost less to build, require smaller filters and have simple control. Cost and efficiency was previously stated as important selection criteria in implementing PUVR.

However, the back-to-back inverter was found to be better in maintaining power quality seen by both the grid and consumer. The AC Chopper is not decoupled from the grid, there is no intermediary buffer, and power quality suffers as a result.

If the AC Chopper could improve the power quality seen by the end-user it would make it comparable to the back-to-back inverter but without the problems found with the back-to-back inverter architecture.

The efficiency and power quality results from the practical experiments with the AC Chopper are in line with predicted values from simulation, reaching a maximum efficiency of 97%. The harmonic distortion was found to never breach any established limits.

The AC Chopper with auto-transformer hybrid was introduced to try and increase power quality and efficiency. Results found a similar level of efficiency but improved the power quality by decreasing the voltage distortion seen by the user for linear loads. However it was found that for non-linear loads due to the line impedance introduced by the auto-transformer, voltage distortion exceeded acceptable standards. Therefore the AC Chopper with auto-transformer hybrid is not acceptable for use with PUVR and that other methods of increasing efficiency and power quality must be used.

An updated cost-benefit analysis was carried out using available costing data from an internet retailer. From this information it was found that implementing PUVR with an AC Chopper circuit is viable in terms of cost as it is roughly equivalent or cheaper in comparison with standard network reinforcement.

To improve the power quality of the AC Chopper a second control loop was added that compares the input waveform to an idealised version of the same waveform. Any resultant errors were then used to dynamically alter the modulation index of the switching. This technique was found to be effective in removing low-frequency harmonics present in the voltage supply to the consumer from the output voltage seen by the consumer. This comes at the cost of increasing the current harmonics injected back into the grid, however as this is not regulated and the waveform seen by the consumer is regulated, it is considered to be an effective method of increasing the power quality.

Therefore it can now be stated that the AC Chopper meets the required cost reduction and high efficiency that was previously stated as required to make PUVR viable. It has also been demonstrated that the AC Chopper can improve the power quality which confirms that the architecture is truly the better choice over the back-to-back inverter for this application.

Therefore PUVR has now been demonstrated as a viable alternative to standard network reinforcement which is required to meet the challenges of future loads and generation placed on the UK LV distribution network.

CHAPTER 10

10. References

1. *Electricity Distribution System Losses: A Non-Technical Overview*. 2009, Sohn Associates Limited.
2. *Powering the Future*. 2010, Parsons Brinckerhoff.
3. Akmal, M., et al. *Impact of High Penetration of Heat Pumps on Low Voltage Distribution Networks*. in *PowerTech, 2011 IEEE Trondheim*. 2011.
4. Yilmaz, M. and P.T. Krein, *Review of the Impact of Vehicle-to-Grid Technologies on Distribution Systems and Utility Interfaces.* Power Electronics, IEEE Transactions on, 2013. **28**(12): p. 5673-5689.
5. *Future Energy Scenarios*. 2014, National Grid. p. 7.

6. *BS EN 7870-3:2011 LV and MV polymeric insulated cables for use by distribution and generation utilities*, in *Part 3: Specification for distribution cables of rated voltage 0.6/1kV Section 3.50: XLPE insulated, copper wire waveform or helical concentric cables with solid aluminium conductors, having low emission of smoke and corrosive gases when affected by fire'* 2011, British Standards Institute.

7. Aziz, T., et al. *Impact of widespread penetrations of renewable generation on distribution system stability*. in *Electrical and Computer Engineering (ICECE), 2010 International Conference on*. 2010.

8. Thomson, M. and D.G. Infield, *Impact of Widespread Photovoltaics Generation on Distribution Systems.* Renewable Power Generation, IET, 2007. **1**(1): p. 33-40.

9. K. Jarrett, J.H., R.Gregory and T.Warham, *"Reverse power flows", Section C.3.32 and C.3.33 in "Distributed generation co-ordinating group technical steering group"*. 2004, Department for trade and industry, Ofgem.

10. Meier, A.V., *Electric Power Systems: A Conceptual Introduction*. 2006, John Wiley and Sons.

11. *Electrical Supply Tolerances and Electrical Appliance Safety*. 2012 [cited 2012 27/11]; Available from: http://www.bis.gov.uk/files/file11548.pdf.

12. A2.50, C.W.G., *Effect of reverse power flows on transformers*, J.C. Riboud, Editor. 2012.

13. Levi, V., M. Kay, and I. Povey. *Reverse power flow capability of tap-changers*. in *Electricity Distribution, 2005. CIRED 2005. 18th International Conference and Exhibition on*. 2005.

14. Hill, G., et al. *Monitoring and Predicting Charging Behaviour for Electric Vehicles*. in *Intelligent Vehicles Symposium (IV), 2012 IEEE*. 2012.

15. Chan, C.C., *The state of the art of electric and hybrid vehicles.* Proceedings of the IEEE, 2002. **90**(2): p. 247-275.

16. Jun, S., C.E. Marmaras, and E.S. Xydas. *Technical and environmental impact of electric vehicles in distribution networks*. in *Green Energy for Sustainable Development (ICUE), 2014 International Conference and Utility Exhibition on*. 2014.

17. Dft, *Transport Statistics Great Britain*. 2012.

18. BERR, *Investigation into the scope for the transport sector to switch to electric vehicle and plug-in hybrid vehicles*. 2008.

19. Kejun, Q., et al., *Modeling of Load Demand Due to EV Battery Charging in Distribution Systems.* Power Systems, IEEE Transactions on, 2011. **26**(2): p. 802-810.

20. So, et al. *Using 1kV Low Voltage Distribution for Connection of Plug-in Vehicles*. in *Innovative Smart Grid Technologies Conference Europe (ISGT Europe), 2010 IEEE PES*. 2010.

21. Harris, A., *Charge of the Electric Car - [Power Electric Vehicles]*. Engineering & Technology, 2009. **4**(10): p. 52-53.

22. Pudjianto, D., et al. *Value of integrating Distributed Energy Resources in the UK electricity system*. in *Power and Energy Society General Meeting, 2010 IEEE*. 2010.

23. Fawcett, T., *The future role of heat pumps in the domestic sector*. 2011, Environmental Change Institute, University of Oxford.

24. *Findings of Pol-PRIMETT research activities*. 2013, Pol-PRIMETT.

25. A. Aizcorbe, S.D.O., D. E. Sichel *Shifting Trends in Semiconductor Prices and the Pace of Technological Progress* in *Finance and Economics Discussion Series*. 2006, Divisions of Research & Statistics and Monetary Affairs, Federal Reserve Board Washington, D.C.

26. Hao, Q., et al. *High-efficiency Bidirectional AC-DC Converter for Energy Storage Systems*. in *Energy Conversion Congress and Exposition (ECCE), 2010 IEEE*. 2010.

27. El Hayek, J. *Transformer Design as a Key for Efficiency Optimization*. in *Electrical Machines (ICEM), 2010 XIX International Conference on*. 2010.

28. *Siemens SINAMICS G110 3.0 kW 1-phase Frequency Inverter*. 2012 [cited 2012 27/11

]; Available from: http://www.conrad-uk.com/ce/en/product/198185/Siemens-SINAMICS-G110-30-kW-1-phase-frequency-inverter-230-VAC-to-6SL3211-0AB23-0AA1/1101123&ref=list.

29. *SQUARE D | Transformer 3kva*. 2012 [cited 2012 27/11]; Available from: http://www.easupplies.com/SQUARE-D-3S4F-Transformer-3K-Watt-1-Phase-600V-P-p/el516e.htm.

30. *Commerical Transformers*. 2010 [cited 2013 07/05]; Available from: http://www.voltageconverters.com/commercial_transformers.html.

31. *Power Electronic Inverters*. 2004 [cited 2013 07/05]; Available from: http://www.dhgate.com/wholesale/store/ff808081365d19ec013670c9d7db2496.html.

32. Yanni, Z., S. Finney, and D. Holliday. *An investigation of high efficiency DC-AC converters for LVDC distribution networks*. in *Power Electronics, Machines and Drives (PEMD 2014), 7th IET International Conference on*. 2014.

33. Hakala, T., P. Jarventausta, and T. Lahdeaho. *The utilization potential of LVDC distribution*. in *Electricity Distribution (CIRED 2013), 22nd International Conference and Exhibition on*. 2013.

34. Nuutinen, P., et al. *Implementing a laboratory development platform for an LVDC distribution system*. in *Smart Grid Communications (SmartGridComm), 2011 IEEE International Conference on*. 2011.

35. Moslehi, K. and R. Kumar, *A Reliability Perspective of the Smart Grid.* Smart Grid, IEEE Transactions on, 2010. **1**(1): p. 57-64.

36. Foote, C., et al. *Second generation active network management on Orkney*. in *Electricity Distribution (CIRED 2013), 22nd International Conference and Exhibition on*. 2013.

37. Wang, J., et al. *Impact of plug-in hybrid electric vehicles on power distribution networks*. in *Electric Utility Deregulation and Restructuring and Power Technologies (DRPT), 2011 4th International Conference on*. 2011.

38. Pieltain, F., et al., *Assessment of the Impact of Plug-in Electric Vehicles on Distribution Networks.* Power Systems, IEEE Transactions on, 2011. **26**(1): p. 206-213.

39. Papadopoulos, P., et al. *Predicting Electric Vehicle impacts on residential distribution networks with Distributed Generation*. in *Vehicle Power and Propulsion Conference (VPPC), 2010 IEEE*. 2010.

40. *Do Storage Heaters still have a place in the home?* 2013 [cited 2014 28/10]; Available from: http://www.thegreenage.co.uk/storage-heaters-still-place-home/.

41. Coote, N., *LCNF Tier 1 Interim Close-Down Report*, in *1MW battery Shetland*. 2013, SSE.

42. Lassila, J., et al., *Methodology to Analyze the Economic Effects of Electric Cars as Energy Storages.* Smart Grid, IEEE Transactions on, 2012. **3**(1): p. 506-516.

43. Tonkoski, R. and L.A.C. Lopes. *Voltage Regulation in Radial Distribution Feeders with High Penetration of Photovoltaic*. in *Energy 2030 Conference, 2008. ENERGY 2008. IEEE*. 2008.

44. Bloemink, J.M. and T.C. Green. *Increasing distributed generation penetration using soft normally-open points*. in *Power and Energy Society General Meeting, 2010 IEEE*. 2010.

45. *G81 - Part 1: Design and Planning* in *Framework for design and planning, materials specification, installation and record for low voltage housing development installations and associated new HV/LV distribution substations.* 2008, Energy Networks Association.

46. *BS EN 7870-1:2011 LV and MV polymeric insulated cables for use by distribution and generation utilities*, in *Part 1: General*. 2011, British Standards Institute.

47. *BS EN 50464-1:2007+A1:2012 Three-phase oil-immersed distribution transformers 50Hz, from 50kVA to 2500kVA with highest voltage for equipment not exceeding 36kV*, in *Part 1: General requirements*. 2012, British Standards Institute.

48. *BS EN 60269-1:2007+A2:2014 BS88-1:2007+A2:2014 Low-voltage fuses*, in *Part 1: General requirements*. 2014, British Standards Institute.

49. *BS EN 60898-1:2003+A13:2012 Electrical accessories - Circuit breakers for overcurrent protection for household and similar installations*, in *Part 1:Circuit-breakers for a.c. operation*. 2012, British Standards Institute.

50. *BS EN 61008-1:2012+A2:2013 Residual current operated circuit-breakers without integral overcurrent protection for household and similar used (RCCBs)*, in *Part 1:General rules*. 2013, British Standards Institute.

51. *G5/4-1 Planning Levels For Harmonic Voltage Distortion And The Connection Of Non-Linear Equipment To Transmission Systems And Distribution Networks In The United Kingdom*. 2005, Energy Networks Association.

52. *BS EN 50160:2010 Voltage characteristics of electricity supplied by public electricity networks*. 2010, British Standards Institute.

53. Ned Mohan, T.M.U., William P. Robbins, *Power Electronics: Converters, Applications, and Design*. 2002: John Wiley & Sons.

54. Kolar, J.W., et al., *Review of Three-Phase PWM AC–AC Converter Topologies.* Industrial Electronics, IEEE Transactions on, 2011. **58**(11): p. 4988-5006.

55. Friedli, T., et al., *Comparative Evaluation of Three-Phase AC–AC Matrix Converter and Voltage DC-Link Back-to-Back Converter Systems.* Industrial Electronics, IEEE Transactions on, 2012. **59**(12): p. 4487-4510.

56. *Rectifier Ripple Demonstration*. [cited 2015 07/05]; Available from: http://web.physics.ucsb.edu/~lecturedemonstrations/Composer/Pages/64.57.html.

57. Singh, B., et al., *A review of single-phase improved power quality AC-DC converters.* Industrial Electronics, IEEE Transactions on, 2003. **50**(5): p. 962-981.

58. M. Petras, A.H.-V. *Tuning Cascade Loops*. 2005 [cited 2013 04/04]; Available from: http://www.controlglobal.com/articles/2005/547.html.

59. Minxia, Z. and D.P. Atherton. *Optimum Cascade PID Controller Design for SISO Systems*. in *Control, 1994. Control '94. International Conference on*. 1994.

60. Yi Zhang, S.S., Rahul Chokhawala, *Snubber Considerations for IGBT applications*. 1995.

61. Wheeler, P.W., et al., *Matrix converters: a technology review.* Industrial Electronics, IEEE Transactions on, 2002. **49**(2): p. 276-288.

62. Empringham, M.L., P.W. Wheeler, and J.C. Clare. *Intelligent commutation of matrix converter bi-directional switch cells using novel gate drive techniques*. in *Power Electronics Specialists Conference, 1998. PESC 98 Record. 29th Annual IEEE*. 1998.

63. Moore, G.F., ed. *Electric Cables Handbook*. 1997, Blackwell Science.

64. Rynone, W., *Power Factor Correction Justified*. 2007, Power Electronics: Annapolis.

65. *Electrical Power System Quality*. 2012: McGraw-Hill Education (India) Pvt Limited.

66. *National Grid: Metered Half-Hourly Electricity Demands* 2012 [cited 2012 27/11]; Available from: http://www.nationalgrid.com/uk/Electricity/Data/Demand+Data/.

67. Berry, R.U., *Possibilities of Heat Pumps for Heating Homes.* American Institute of Electrical Engineers, Transactions of the, 1944. **63**(9): p. 619-622.

68. Baird, P.J., H. Herman, and G.C. Stevens. *Rapid Non-Destructive Condition Assessment of Insulating Materials*. in *Electrical Insulation, 2008. ISEI 2008. Conference Record of the 2008 IEEE International Symposium on*. 2008.

69. Connor, G., C.E. Jones, and S.J. Finney, *End user voltage regulation to ease urban low-voltage distribution congestion.* Generation, Transmission & Distribution, IET, 2014. **8**(8): p. 1453-1465.

70. Connor, G., C.E. Jones, and S.J. Finney (2014) *Easing Future Low Voltage Congestion with an AC Chopper Voltage Regulator*. IET Conference Proceedings, 1.11.01-1.11.01.

71. Triplett, J., S. Rinell, and J. Foote. *Evaluating distribution system losses using data from deployed AMI and GIS systems*. in *Rural Electric Power Conference (REPC), 2010 IEEE*. 2010.

72. Kolar, J.W., et al. *Novel Three-phase AC-DC-AC Sparse Matrix Converter*. in *Applied Power Electronics Conference and Exposition, 2002. APEC 2002. Seventeenth Annual IEEE*. 2002.

73. *Statement of Methodology and Charges for Connection to Scotttish Hydro Electric Power Distribution plc's Electricity Distribution System*. 2013, Scottish and Southern Energy - Power Distribution. p. p130-p140.

74. *Solar Inverters*. 2013 [cited 2013 23/08]; Available from: http://www.pvsupplies.co.uk/5-grid-tie-inverters.

75. *Commander SK SK4402 37kW (45kW) Inverter, 3-phase 480V Input, 3-phase 480V Output*. 2013 [cited 2013 23/08]; Available from: http://www.motorcontrolwarehouse.co.uk/commander-sk-sk4402/prod_289.html.

76. *Productivity and Cyclicality in Semiconductors: Trends, Implications, and Questions -- Report of a Symposium*, ed. D.W. Jorgenson and C.W. Wessner. 2004: The National Academies Press.

77. R. C. Dugan, M.F.M., S. Santoso, H. W. Beaty, *Electrical Power Systems Quality Third Edition*. 2012: Mc Graw-Hill. 417-418.

78. Wheeler, P. and D. Grant, *Optimised input filter design and low-loss switching techniques for a practical matrix converter.* Electric Power Applications, IEE Proceedings -, 1997. **144**(1): p. 53-60.

79. *Insulated Gate Bipolar Transistor with Ultrafast Soft Recovery Diode*. 2004 [cited 2013 01/02]; Available from: http://www.farnell.com/datasheets/34696.pdf.

80. *75A, 1200V Hyperfast Diode*. 2008 [cited 2013 09/04]; Available from: http://www.farnell.com/datasheets/1729228.pdf.

81. Wang, B. and G. Venkataramanan. *Analytical Modeling of Semiconductor Losses in Matrix Converters*. in *Power Electronics and Motion Control Conference, 2006. IPEMC 2006. CES/IEEE 5th International*. 2006.

82. Casanellas, F., *Losses in PWM Inverters using IGBTs.* Electric Power Applications, IEE Proceedings -, 1994. **141**(5): p. 235-239.

83. *ARW - Inductors*. Available from: http://www.arwtransformers.co.uk/listing.htm.

84. *Kemet - C322C473KCR5CA - Capacitor, 47nF, 500V, X7R*. 2013; Available from: http://uk.farnell.com/kemet/c322c473kcr5ca/capacitor-47nf-500v-x7r/dp/1288233?Ntt=1288233.

85. *BHC Components - ALS30A222NP500 - Capacitor, 2200UF, 500V*. 2013; Available from: http://uk.farnell.com/bhc-components/als30a222np500/capacitor-2200uf-500v/dp/536519?Ntt=536519.

86. Haugen, F., *The Good Gain Method for Simple Experimental Tuning of PI Controllers.* Modeling, Identification and Control, 2012. **Vol. 33,** (No. 4,): p. pp. 141-152.

87. *BS88 Fuses*. 2009; Available from: http://fuses.bs88.eu/.

88. Emhemed, A.S., G. Burt, and O. Anaya-Lara. *Impact of High Penetration of Single-Phase Distributed Energy Resources on the Protection of LV Distribution Networks*. in *Universities Power Engineering Conference, 2007. UPEC 2007. 42nd International*. 2007.

89. J. Duncan Glover, M.S.S., Thomas J. Overbye, *Power System Analysis and Design*. Fourth ed. 2010: Cengage Learning.

90. IEE, *Regulations for Electrical Installations*, in *Scope, object and fundamental requirements for safety*. 1981, The Institution of Electrical Engineers, London. p. 2.

91. Srinivasan, R. and R. Oruganti, *A Unity Power Factor Converter using Half-bridge Boost Topology.* Power Electronics, IEEE Transactions on, 1998. **13**(3): p. 487-500.

92. *Insulated Gate Bipolar Transistor IRG7PH50UPbF Datasheet*. 2010, International Rectifier.

93. Littelfuse, *The ABCs of MOVs*. 1999.

94. *TMS320x2833x, 2823x Enhanced Pulse Width Modulator (ePWM) Module Reference Guide*. 2009: Texas Instruments.

95. *Control Systems: Classical and Modern Controls Engineering with Advanced Topics*. 2014: opensource-books.

96. Das, M.K., *Sic mosfet module replaces up to 3x higher current si igbt modules in voltage source inverter application.*

97. *Farnell - Texas-instruments - tmdsdock28335 - tms320f28335*. Available from: http://uk.farnell.com/texas-instruments/tmdsdock28335/tms320f28335-.

98. *Farnell - heat-sink-0-28-c-w*. Available from: http://uk.farnell.com/h-s-marston/96cn-03000-a-200/heat-sink-0-28-c-w/dp/168701.

99. *Farnell - half-bridge-driver-isolated-smd*. Available from: http://uk.farnell.com/analog-devices/adum1233brwz/half-bridge-driver-isolated-smd/dp/1519593?categoryId=700000004235.

100. *Farnell - current-transducer-100a-20-50vdc*. Available from: http://uk.farnell.com/lem/dhr-100-c10/current-transducer-100a-20-50vdc/dp/1002688.

101. *Farnell - cap-film-480uf-1-1kv*. Available from: http://uk.farnell.com/epcos/b25620b1487k101/cap-film-480uf-1-1kv-screw/dp/2219197.

102. *Farnell - varistor-90-0j-420vac*. Available from: http://uk.farnell.com/epcos/b72214s0421k101/varistor-90-0j-420vac/dp/1004368.

103. *Farnell - irg7ph50upbf igbt-1200v-140a-to-247*. Available from: http://uk.farnell.com/international-rectifier/irg7ph50upbf/igbt-1200v-140a-to-247ac/dp/2062048?mckv=s2857eGxz|pcrid|39079000808|kword|irg7ph50upbf|match|p|plid|&CMP=KNC-GUK-FUK-GEN-SKU-MDC.

104. *Farnell - rhrg75120 - diode-hyperfast*. Available from: http://uk.farnell.com/fairchild-semiconductor/rhrg75120/diode-hyperfast/dp/9843736?mckv=scwgMBR3k|pcrid|28495023069|kword|rhrg75120|match|p|plid|&CMP=KNC-GUK-FUK-GEN-SKU-DGA.

105. *Farnell - cap-film-pp-2-2nf-1kv-rad*. Available from: http://uk.farnell.com/wima/fkp2o112201l00jssd/cap-film-pp-2-2nf-1kv-rad/dp/1519284.

106. *Farnell - res-thick-film-4r7-5-50w-to-220*. Available from: http://uk.farnell.com/vishay-sfernice/lto050f4r700jte3/res-thick-film-4r7-5-50w-to-220/dp/9567151.

11. Appendix A - PowerWorld Cable Data

Cable	Cable Resistance (Ohm)	Cable Reactance (jOhm)	Cable Current Limit (MVA)
1	0.006992	0.0031188	0.34431
2	0.00564	0.0021	0.22287
3	0.00188	0.0007	0.22287
4	0.00188	0.0007	0.22287
5	0.012	0.00555	0.26841
6	0.01128	0.0042	0.22287
7	0.049555	0.00646	0.12282
8	0.01222	0.00455	0.22287
9	0.01222	0.00455	0.22287
10	0.00583	0.00076	0.12282
11	0.014575	0.0019	0.12282
12	0.014575	0.0019	0.12282
13	0.0112	0.00518	0.26841
14	0.0188	0.007	0.22287
15	0.0016	0.00074	0.26841
16	0.0016	0.00074	0.26841
17	0.0216	0.00999	0.26841
18	0.0128	0.00592	0.26841
19	0.0192	0.00441	0.18354
20	0.0064	0.00147	0.18354
21	0.00583	0.00076	0.12282
22	0.00752	0.0028	0.22287
23	0.008745	0.00114	0.12282
24	0.008745	0.00114	0.12282
25	0.000376	0.00014	0.22287
26	0.02256	0.0084	0.22287
27	0.024	0.0055125	0.18354
28	0.00846	0.00315	0.22287
29	0.00752	0.0028	0.22287
30	0.016	0.0074	0.26841
31	0.0008	0.00037	0.26841
32	0.00188	0.0007	0.22287
33	0.0216	0.00999	0.26841

34	0.0094	0.0035	0.22287
35	0.00583	0.00076	0.12282
36	0.0047	0.00175	0.22287
37	0.00583	0.00076	0.12282
38	0.01166	0.00152	0.12282
39	0.008745	0.00114	0.12282

12. Appendix B - Non-Linear Power Draw Data from Devices

	DC Power Draw	
	Voltage (V)	Current (A)
Laptop	19	4.74
TV	66.7	1.5
Games Console	12	3.7
PC	12	17
Monitor	66.7	1.5

13. Appendix C - Calculated Value of Controller Gain

	K_{p1}	K_{i1}	K_{p2}	K_{i2}	K_{p3}	K_{i3}
AC Chopper	1	120	-	-	-	-
Back-to-back Inverter	1	120	0.077	0.8	0.85	860

14. Appendix D - Final Manually Tuned Values of Controller Gain

	K_{p1}	K_{i1}	K_{p2}	K_{i2}	K_{p3}	K_{i3}
AC Chopper	1	120	-	-	-	-
Back-to-back Inverter	1	120	0.1	0.8	50	860